WPI

Project ID: 25756

Developing and Validating a Non-Invasive Diagnostic Test for Endometriosis

A Major Qualifying Project Report:

Submitted to the faculty of Worcester Polytechnic Institute

In partial fulfillment of the Degree of Bachelor of Science

Written by:

Burnon Chen

Alexandra Gannon

Lonna Neidig

Kiran Tremblay

04/27/2022

Prof. Zoe Reidinger, Ph.D., WPI

Prof. Destin Heilman, Ph.D., WPI

Table of Contents

THIS PAGE IS BLANK FOR PAGE NUMBERING PURPOSES

THIS PAGE IS BLANK FOR PAGE NUMBERING PURPOSES

Table of Tables

THIS PAGE IS BLANK FOR PAGE NUMBERING PURPOSES

THIS PAGE IS BLANK FOR PAGE NUMBERING PURPOSES

THIS PAGE IS BLANK FOR PAGE NUMBERING PURPOSES

Table of Figures

THIS PAGE IS BLANK FOR PAGE NUMBERING PURPOSES

THIS PAGE IS BLANK FOR PAGE NUMBERING PURPOSES

THIS PAGE IS BLANK FOR PAGE NUMBERING PURPOSES

Table of Appendices

THIS PAGE IS BLANK FOR PAGE NUMBERING PURPOSES

THIS PAGE IS BLANK FOR PAGE NUMBERING PURPOSES

THIS PAGE IS BLANK FOR PAGE NUMBERING PURPOSES

THIS PAGE IS BLANK FOR PAGE NUMBERING PURPOSES

Authorship

All components completed for this Major Qualifying Project at Worcester Polytechnic Institute were contributed equally by all four members of this team. All sections of this report were written, edited, and formatted equally by all four team members.

Acknowledgements

The team would like to acknowledge the contributions of our project advisors Dr. Zoe Reidinger of the Biomedical Engineering Department, and Dr. Destin Heilman of the Biochemistry Department at Worcester Polytechnic Institute. We appreciate your continued support and expertise throughout this project, and could not have made it this far without you. You gave us the power and motivation to keep persevering, and we truly cannot thank you enough. Additionally, we would like to acknowledge Lydia Reidinger (Dr. Reidinger's dog) for her consistent attendance and valuable contribution to the research team's mental well-being.

In addition to our project advisors, we would like to acknowledge the invaluable contributions of Dr. Sakthikumar Ambady, Dr. Marsha Rolle, Will DeMaria and Claire Joswiak from Dr. Rolle's lab from the BME department and Dr. Lou Roberts and Dr. Mike Buckholtz from the BBT department for their contribution of materials and expertise to our project. We would also like to thank Lisa Wall and Robert Kirch, the lab managers for the BME department, and Silvana Reid and Yuting Liu from CBC department for their help in sourcing and ordering materials, their general commitment to the maintaining of lab spaces, and other additional support throughout the duration of our research.

Additionally, we would like to thank Meredith Gauthier and Sean Amberger for their knowledge and support during the project. Their involvement helped ease the work environment throughout the project.

Finally, we would like to thank everyone who worked with us during this project, be it patients, medical professionals, and our peers for their continued enthusiasm and passion for the work we did throughout this academic year. Hearing about the excitement for this device was truly inspiring, and gave us the energy to push through the difficult times. Thank you all for the continued support.

Abstract

Endometriosis is a disorder that affects 10-15% of reproductive aged individuals assigned female at birth (Liu, et al., 2020). Current diagnostic methods are invasive, inaccessible, and subjective. An objective and non-invasive method is crucial toward improving the quality of life of patients. This paper details the creation of a urinalysis device capable of diagnosing endometriosis by quantifying the concentration of sFlt-1 to creatinine. This device is a proof of concept that is capable of changing the diagnostic process for endometriosis.

Chapter 1: Introduction

Endometriosis is a common, complicated, and understudied disease that is difficult to diagnose without expensive and invasive procedures. The disorder affects 10-15% of reproductive age individuals who were assigned female at birth, and is the main cause of over 50% of infertility cases and reported pelvic pain (Liu, et al., 2020). Endometriosis describes the implantation of endometrial tissue in places outside of the uterus. This tissue, which is normally shed during the menstrual period, becomes trapped and leads to inflammation and other disturbances around and on the uterus (Alimi, et al., 2018). Symptoms of the disease can vary from mild and unnoticeable symptoms, to debilitating indications such as chronic pelvic pain, painful bowel movements and urination, and intermenstrual bleeding (Parasar, et al., 2017). As a result, diagnosing the disease is difficult, and due to the limited relevant research, there are very few diagnostic methods. Laparoscopy, the current 'gold standard' diagnostic technique, involves invasive surgical procedures that risk inconclusive results. Invasive physical exams are often utilized but can only detect very specific cases and implant locations indicative of the disease. Imaging-detection of endometriosis also tends to be inconclusive, as the implants are difficult to distinguish from normal tissue. Endometriosis presents a wide variety of issues for patients and diagnosticians. Therefore, a noninvasive, reliable diagnostic technique would not only improve the ability of physicians to assess the disease, but would drastically improve the quality of life of affected individuals undergoing diagnosis.

Endometrial tissue implantation outside of the uterus is the main cause of documented symptoms for individuals with endometriosis. The tissue forms cysts (known as endometriomas) outside of the uterus, typically along the ovaries, fallopian tubes, appendix, bladder, rectum, ureters, pelvic ligaments, rectovaginal septum, and/or other organs located in and along the pelvic region (Alimi, et al., 2018). The abnormal endometrial tissue then responds to hormonal stimulation and grows cyclically, much like normal endometrial tissue. Due to its extrauterine location, the abnormal tissue is unable to leave the body. As a result, endometriomas contribute to several painful symptoms and internal buildup of blood (Alimi, et al., 2018). The aforementioned symptoms can include dysmenorrhea, pelvic pain associated with intercourse, and infertility (Wee-Stekly, et al., 2015).

Although the exact cause of endometriosis is currently unknown, there are three well respected theories that describe the disease's inception. One of these theories is rooted retrograde

menstruation (Alimi, et al., 2018). The most common detractor from this theory is the known number of cases of endometriosis only make up 10% of the number of menstruating individuals (Alimi, et al., 2018). Additional theories address this issue, stating that endometriosis might arise from rarer stem cells moved by retrograde menstruation.

Individuals prone to endometriosis are heavily impacted by the disease. It is estimated that within that population, at least 50% also struggle with infertility (Liu, et al., 2020) and up to 70% experience chronic pelvic pain (Parasar, et al., 2017). On average, it takes 6.7 years for diagnosis, which is detrimental to a patient's health and can severely impact the patient's overall quality of life (Parasar, et al., 2017). Early diagnosis and treatment are key to ensuring the management of pain, prevention of disease progression, and preservation of fertility (Parasar, et al., 2017). The widespread nature of the disease and difficulty of diagnosis emphasize the importance of improving diagnostic tools for endometriosis.

Chapter 2: Literature Review

2.1.0 - Diagnostic Methods

Currently, there are several methods used for diagnosing endometriosis. These include laparoscopic biopsies in conjunction with histologic confirmation, magnetic resonance imaging (MRI), ultrasound imaging, and physical pelvic exams (Mason, et al., 2020). Though many medical professionals view laparoscopy as the best diagnostic technique, it is an extremely invasive, costly, and potentially dangerous process. MRI and ultrasound imaging are useful for diagnosing deep-infiltrating endometriosis while pelvic exams are a tool used to locate endometriomas and other cystic endometrial masses (Mason, et al., 2020). Pelvic exams are also useful for locating areas of tenderness, but this symptom is not exclusive to endometriosis and is often indicative of several other conditions that can be commonly confused with endometriosis if not diagnosed correctly (Parasar, et al., 2017). New blood-based biomarker tests search for critical concentrations of indicator protein CA 125 to diagnose the disease, offering a more accurate diagnostic process. However, this method still requires an invasive blood draw. Additionally, this detection method cannot distinguish between endometriosis and gynecological cancers (UCSF Health, 2021). The American Society for Reproductive Medicine (ASRM) criteria aims to classify the severity of endometriosis as "minimal, mild, moderate, and severe" based on the morphology, number, location, and size of endometriosis lesions (American Society

for Reproductive Medicine, 1997). Although researchers often utilize the ASRM scale to classify the physical severity of endometriosis, it lacks the ability to predict the probability of conception following surgical intervention, which is an important factor to some patients undergoing treatment (Wee-Stekly, et al., 2015). To account for this, the Endometriosis Fertility Index (EFI) can be used in conjunction with the ASRM to predict the probability of successful fertilization following surgery through means excluding in-vitro fertilization (Tanbo & Fedorcsak, 2017).

During laparoscopy, doctors anesthetize the patient before inserting fiber-optic imaging devices known as laparoscopes via the navel to search for ectopic endometrial tissue, as seen in Figure 1. This is the most precise method for determining the location, size, and severity of implants associated with endometriosis (Mayo Clinic, 2021). This method allows for the removal of these implants for a potential biopsy to confirm the diagnosis. In specific cases, all implants can be successfully removed during a single operation (Mayo Clinic, 2021).

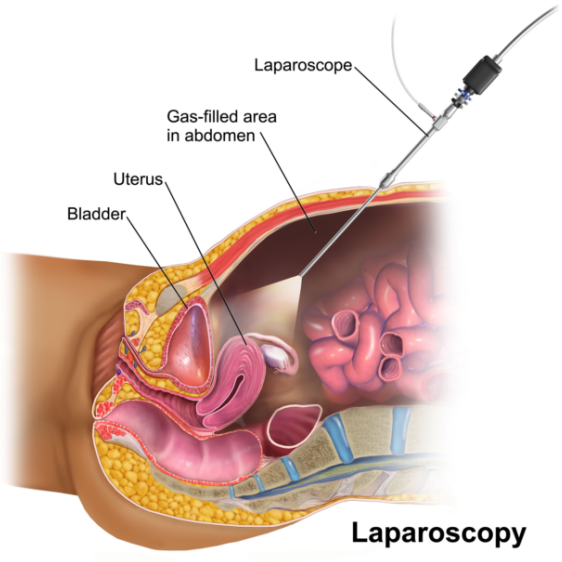

Figure 1 - A diagram demonstrating laparoscopic surgery. (*"Laparoscopy Diagram",* Pelvic Rehabilitation Medicine, 2022)

Ultrasound imaging utilizes high-frequency sound waves to view reproductive organs. When diagnosing endometriosis, a doctor will insert a transducer into the vagina to produce images, as seen in Figure 2 (Mayo Clinic, 2021). Similarly, MRI utilizes a magnetic field and radio waves to render detailed images of internal organs and tissues. MRI and ultrasound are the preferred methods for producing precise details and information about the location and sizes of

ectopic tissues in the body (Mayo Clinic, 2021). However, these methods are unreliable in detecting all implants as they can be easily confused for other innocuous tissue, and much like pelvic exams, are physically invasive.

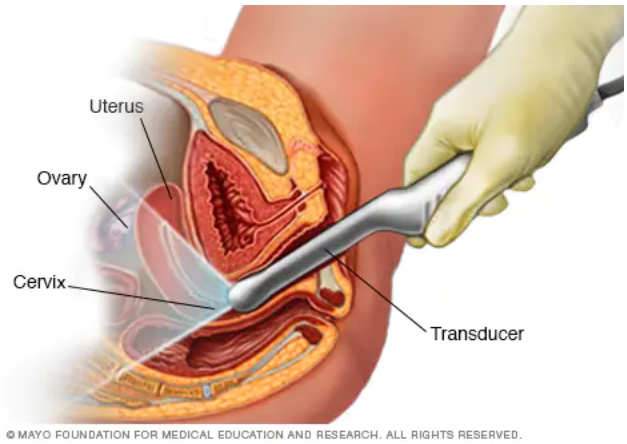

Figure 2 - A diagram demonstrating a transvaginal ultrasound using a transducer. ("*Transvaginal Ultrasound Diagram"*, Mayo Clinic, 2022)

Pelvic exams are typically utilized to physically detect cysts and or scar tissue within the vaginal canal (Mayo Clinic, 2021). As shown below in Figure 3, the procedure involves inserting two fingers into the vagina and then manually palpating to locate any abnormalities. This method is particularly useful for detecting more advanced cases of endometriosis, in which cysts or other abnormalities have formed. (Mayo Clinic, 2021). The quickness and effectiveness of the procedure make it a desirable method. In addition to this, and its low false positive rates. Pelvic exams rarely yield a false positive, but are more likely to produce false negatives due to the subjectivity of the method itself. This method is physically invasive and ineffective when used to detect less advanced cases of endometriosis, especially when the ectopic tissue isn't located directly within or near the vaginal canal.

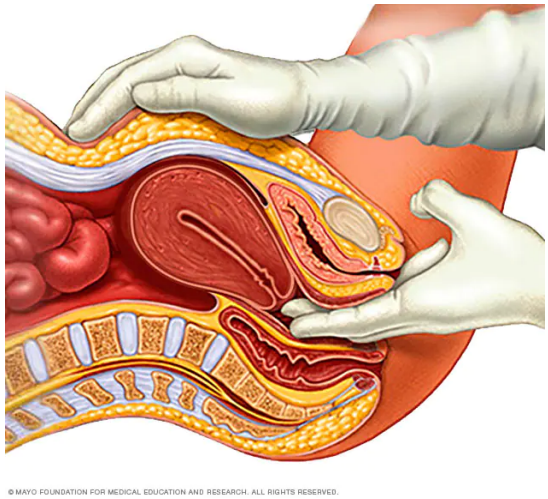

Figure 3 - A diagram demonstrating a pelvic exam. ("*Pelvic Exam Diagram"*, Mayo Clinic, 2022)

A more radical approach to treatment is a hysterectomy. This procedure involves the surgical removal of the uterus, the cervix, and/or ovaries. This can be an effective form of treatment for patients where endometriomas develop on the outside of the uterus, along the fallopian tubes, or on the ovaries. Hysterectomies are used to significantly reduce pain and other symptoms in patients with endometriosis with long lasting effects, but is not a permanent solution as symptoms may return after surgery (Sandström, et al., 2020).

The most widely available options for diagnosing endometriosis, as discussed above, are all physically invasive. As of 2021, there are no widely available methods to diagnose endometriosis in a non-invasive way. Research suggests that there could be a way to non-invasively diagnose endometriosis utilizing various biomarkers, however, the research lacks "definitive and consistent biomarkers" (Parasar, et al., 2017). Studies have identified several biomarkers potentially indicative of endometriosis, but require further research to obtain reliable results (Parasar, et al., 2017). Recent work completed at Worcester Polytechnic Institute in a BME3300 class conceptualized the ability to non-invasively diagnose endometriosis through means of urinalysis. This project is a continuation of a proof of concept that arose from a BME3300 course. The team in question based their work off of Cho, et al., 2007, and conducted preliminary research on standard curves of sFlt-1 and MMP-9 and utilized an enzyme-linked immunosorbent assay (ELISA) for MMP-9, an ELISA for MMP-9 in sFlt-1 concentrations, and an absorbance assay for creatinine. These tests were never used on urine samples, but could

successfully detect concentrations of the MMP-9, sFlt-1, and creatinine. This team's future work built off the biomarker detection idea and worked towards developing a device to detect certain proteins within urine as a means to diagnose endometriosis (Tremblay, et al., 2019). This paper was not published, but can be read in its entirety in Appendix A.

Medication is a last resort in diagnosing and eventually treating symptoms of endometriosis. A doctor may prescribe hormonal therapy as a means to mitigate symptoms if they are unable to locate cysts and or scarring. If the patient sees a decrease in symptoms they are then typically diagnosed with the condition.

2.2.0 - Treatment and Management of Symptoms

Currently, there is no cure for endometriosis. Both the condition and treatments for it span the entire lifetime of the patient. Hormonal therapy, usually in the form of birth control, regulates estrogen in the body, which can help reduce pain (Mayo Clinic, 2021). Similarly, Gn-RH agonists and antagonists aid in limiting the production of hormones that stimulate the ovaries (Mayo Clinic, 2021), which contributes to this reduction of pain. Hormonal therapy works to lower estrogen levels and prevent the monthly menstrual cycle, which can cause endometrial tissue to shrink. The chemicals induce menopause-like symptoms in the patient with the intention of reducing pain during treatment. Progestin (delivered via intrauterine device) combined with levonorgestrel hormonal medication in the form of an implant, pills, or injection, can stop the menstrual cycle and reduce symptoms (Mayo Clinic, 2021). However, data on the prescription and dosing of these drugs are limited to qualitative data. Once patients stop using the medication, symptoms return, making this a lifelong treatment and relief only temporary (Mayo Clinic, 2021). If a patient undergoes a laparoscopic surgery for diagnosis and the presence of endometriomas are confirmed and of a known location, the lesions are usually removed as well (Mayo Clinic, 2021). A last resort in symptom management is for patients to undergo a hysterectomy. This method significantly decreased symptoms in patients with severe endometriosis, but symptoms may return after an extended period of time (Sandström, et al., 2020). This method is viewed as a radical approach to treatment, and due to its invasive nature is typically only used in extreme cases.

2.3.0 - Biomarkers for Endometriosis

Biomarkers offer a promising step in the direction of beginning to non-invasively diagnose endometriosis. Aromatase is an enzyme used in the production of estrogen, and plays a critical role in angiogenesis (creation of new tissue, especially in reference to endometrial tissue). Aromatase increases levels of estrogen and estradiol hormones, which increases inflammation. This enzyme is found in endometrial tissues at higher concentrations than elsewhere in the body (Bulun, et al., 2004). Prostaglandin-E2, which is also present in endometrial tissues at elevated concentrations, mediates pain but also increases aromatase production (Agrawal, et al., 2018). Aromatase is easiest to detect in the blood of endometrial tissues, but expresses at highly variable levels, making it unreliable for testing. Endometriosis produces aromatase via a chain pathway beginning with microRNA (miRNA), as seen in Figure 4. Decreases in the expression of miR-20a and miR-199a initiate angiogenesis and indicate endometriosis, but the precise pathways affecting miRNAs are unknown (Bjorkman & Taylor, 2019). None of the biomarkers associated with angiogenesis are expressed in urine at consistent and/or high enough levels to be used reliably in a urine test. Hypoxia-inducible factor 1-alpha (HIF1-a) and Vascular Endothelial Growth Factor-A (VEGF-A), among other biomarker proteins, can be found in significant levels in the blood, but blood draws are invasive and defeat the purpose of pursuing a non-invasive test.

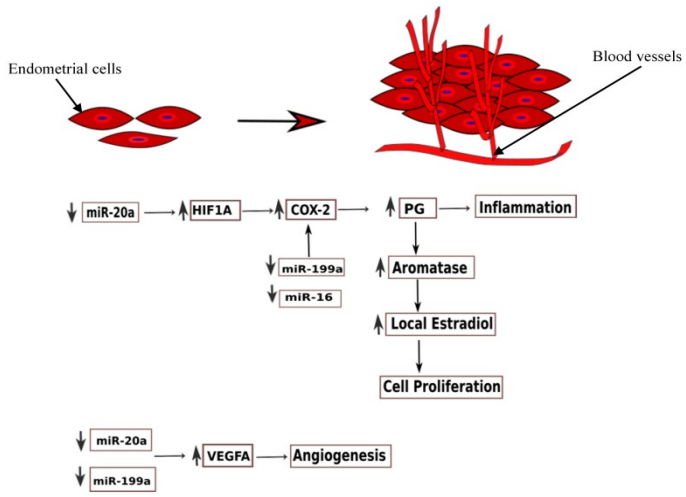

Figure 4 - The chemical pathway leading to angiogenesis. (*"Angiogenesis Diagram",* Agrawal, et al., 2018)

Angiogenesis is likely to be a critical factor in the development and progression of endometriosis, as well as establishing blood supply to endometriomas. Many studies center on the relationship of vascular endothelial growth factor (VEGF) in serum and peritoneal fluid in endometrial patients. Soluble fms-like tyrosine kinase (sFlt-1) is a VEGF receptor, and most likely regulates vascular endothelial growth activity. Studies link elevated concentrations of sFlt-1 to tumor development in leukemia,l and lung and colorectal cancer, and it has recently been linked to issues with preeclampsia. A study found that sFlt-1 expresses higher concentrations in endometriosis' early stages, demonstrating that kinases are an inhibitor of angiogenesis (Cho et al., 2007). Following corrections for creatinine in urine, Cho, et al., found that endometrial patients expressed sFlt-1 at much higher concentrations when compared to their control group (Cho et al., 2007). This study also found that Vitamin D Binding Protein (VDBP) can be used as an additional indicator of endometriosis.

2.3.1 - sFlt-1 as a Biomarker for Endometriosis

sFlt-1, also known as Soluble VEGFR-1 Isoform 2, is a protein isoform of Vascular Endothelial Growth Factor Receptor-1 (VEGFR-1). VEGFR-1 is also known as hFlt-1, or human fms-like tyrosine kinase. hFlt-1, also known as Flt-1, is a highly specific kinase and receptor for VEGF-A. More specifically, VEGF-A Isoform 4 (UniProtKB: P15692), also known as VEGF165 or simply VEGF (Markovic-Mueller, et al., 2017). VEGFR-1 consists of three main domains: an intracellular domain, a transmembrane domain, and an extracellular domain. Soluble VEGFR-1 Isoform 2 (VEGFR-1-I2, sFlt-1) lacks the intracellular domain and transmembrane domain (amino acids 657-1338) of VEGFR-1 (Markovic-Mueller, et al., 2017). These two domains are replaced by a 31 amino-acid sequence (amino acids 657-687). This difference can be seen in Appendix B (hFlt-1 sequence) and Appendix C (sFlt-1 sequence). This change prevents sFlt-1 from binding to the membrane of the cell, allowing it to be soluble. However, since the functional receptor for VEGF does not change between the two proteins, both VEGFR-1 and sFlt-1 bind to VEGF. The extracellular domain consists of seven immunoglobulin-homologous domains, referred to as IG domains 1-7. sFlt-1 is expressed and secreted from cells, mainly human endothelial tissues. The focus for this device is endometrial endothelial tissue. It is currently unknown why sFlt-1 can be found in urine, as the renal excretion pathways have not been extensively researched (Hagmann, et al., 2014). As Cho, et al.,

2007 states, sFlt-1 can be used as a biomarker indicative of endometriosis when corrected for creatinine in urine. Creatinine is a waste product generated through protein metabolism and the supply of energy to the body's muscles. It is removed from the blood by the kidneys and a common test to run when evaluating kidney function. Normal creatinine levels in individuals prone to endometriosis range from 20 – 275 mg/dL (Eng, 2021).

2.3.2 - MMP-9 and VDBP as Biomarkers for Endometriosis

Matrix metalloproteinases (MMPs) are a family of zinc-dependent endopeptidases (enzymes that break peptide bonds). They consist of 39 different matrices divided into groups based on their cellular localization, which includes gelatinases. MMPs play a major role in the degradation and remodeling of the extracellular matrix. MMP-9, also known as gelatinase B, is crucial in angiogenesis, cell migration, and wound healing. During menstruation, the concentration of MMP-9 increases significantly to help break down the endometrium. Abnormal concentrations of MMP-9 typically present as dysfunctional uterine bleeding, infertility, leiomyoma, and or endometriosis. A study written by Becker, et al., found that concentrations of MMP-9 in urine samples could be a potential non-invasive diagnostic method for endometriosis and concluded that higher concentrations of MMP-9 can indicate endometriosis (Becker, et al., 2010).

Vitamin D binding protein (VDBP) is the dominant carrier of vitamin D in the body (Fernando, et al., 2020). VDBP is mainly synthesized in the liver and carries vitamin D throughout the body. VDBP is also shown to aid the immune system by recruiting white blood cells and acting as a precursor to a macrophage activating factor (SiHyun et al., 2012). Protein analysis of urine samples from patients with and without endometriosis show that the urinary concentration of VDBP significantly increases in individuals with endometriosis compared to individuals without endometriosis. A western blot analysis of the two tissue groups showed a significant increase in the relative density of VDBP in tissues with endometriosis (Hwang, et al., 2013). In a patient study, VDBP levels in patients with endometriosis increased 80% based on an ELISA quantification of VDBP concentration compared to patients without endometriosis (SiHyun, et al., 2012). In a 2D protein gel analysis, VDBP % volume in urine increased by 200% (SiHyun, et al., 2012). In both tissue and patient studies, VDBP concentration increased greatly. Despite the potential as a biomarker, a urinary VDBP test does not perform as well as the serum

CA-125 test, a blood based test for endometriosis. In a receiver operating characteristic (ROC) curve, a VDBP based test has lower sensitivity and specificity compared to the serum CA-125 (SiHyun, et al., 2012).

In summary, preliminary research by Cho, et al., in 2007 denoted several proteins expressed in urine and in serum as potential biomarkers for endometriosis in patients. Work done by Tremblay, et al., focused specifically on the potential for MMP-9 in relation to creatinine and sFlt-1 in relation to creatinine expressed in urine as potential biomarkers for use in a non-invasive diagnostic test for endometriosis due to their roles in the degradation of the extracellular matrix and in regulating angiogenesis, respectively. Due to their presence in elevated levels in urine in endometriosis positive patients, MMP-9 and sFlt-1 are attractive biomarkers for non-invasive diagnosis, however they must also be corrected for creatinine.

2.4.0 - The Function and Use of Colorimetric Assays

Colorimetric tests, which include devices like pH strips, can be used to visually or spectrophotometrically determine the process of a reaction, the concentration of an analyte, and much more. Colorimetric assays, such as a Jaffe reaction assay to detect creatinine, or an ELISA assay, produce a color indicative of a property, such as the concentration of a molecule in solution. These assays use a chemical or physical reaction to produce a visible result. This section will briefly explore certain aspects of colorimetric assays and how they can be leveraged to detect biomarker ratios by comparing colors.

2.4.1 - Enzyme Linked Assays

ELISA (enzyme-linked immunosorbent assay) assays are likely the most common way to detect specific biological analytes and their concentration in solution. This option was explored for detecting low concentrations in a previous unpublished paper. It was determined that this option would be difficult to pursue due to low sensitivity and high cost (Tremblay, et al., 2019). One type of ELISA is called a sandwich ELISA, which can be seen in Figure 5.

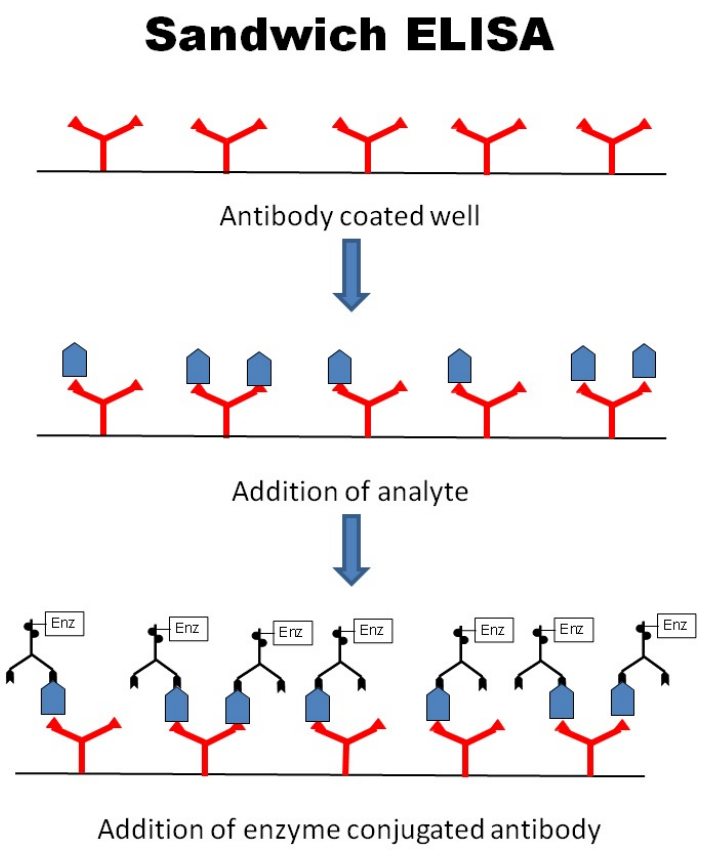

Figure 5: Diagram detailing operation of a Sandwich ELISA Assay. ("*Sandwich ELISA Diagram",* NCBI, n.d.)

Sandwich ELISAs work by "sandwiching" an analyte between two sets of antibodies. One set of antibodies anchors the analyte to a well plate, and a second antibody conjugated to an enzyme such as alkaline phosphatase (AP) then binds to that analyte. When exposed to a specific substrate, the enzyme can produce a detectable signal (ex. color, fluorescence) to determine the concentration of the analyte.

2.4.2 - BCIP-AP Reaction and Its Applications in Colorimetric Assays

Alkaline Phosphatase (EC 3.1.3.1) is a common enzyme that catalyzes the hydrolysis of phosphates in alkaline (pH > 7) solutions (Posen, 1967). AP can nonspecifically hydrolyze many different types of phosphate esters such as para-nitrophenyl phosphate (PNPP) (Posen, 1967). AP is commonly used for colorimetric assays because of the reaction between AP and phosphate groups on certain molecules, like PNPP (Reichardt, et al., 1967) or 5-Bromo-4-chloro-3-indolyl phosphate (BCIP), which further reacts with nitro blue tetrazolium (NBT) (Kundu, 2014). The

PNPP and BCIP/NBT reactions cause a shift from an initial colorless solution into a colored solution. PNPP turns the solution yellow, while BCIP/NBT turns the solution into a blue color. This reaction can be seen in Figure 6. Both reactions can be stopped at a certain time point and are readable on a colorimeter. In addition to taking part in color changing reactions, AP can also be coupled to proteins and antibodies (AB) using the one-step glutaraldehyde method (Stratis, 1969). The one-step glutaraldehyde method is meant for conjugation of enzymes to proteins using glutaraldehyde. The glutaraldehyde acts as a coupling agent, which allows for proteins, like an AB, to link to an enzyme like AP (Stratis, 1969). Because of its ability to cause a color changing reaction and be coupled to proteins, AP is an enzyme with large potential for use in a color-metric detection assay. If AP can couple to an AB or other molecules that have a high specificity towards a biomarker related to a certain disease, that disease can be monitored through AP's reaction with one if its color changing substrates.

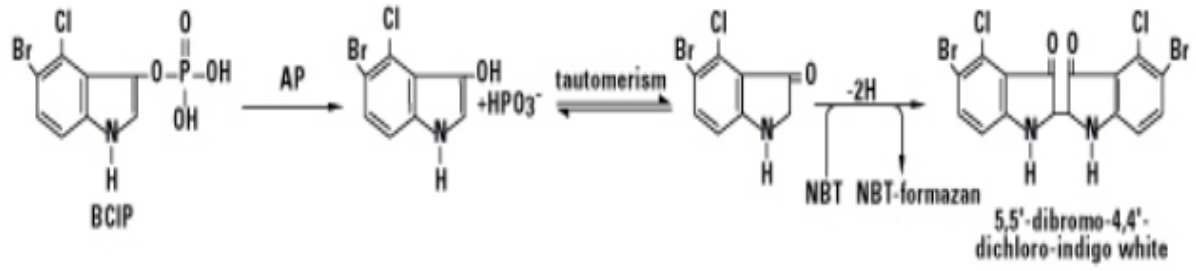

Figure 6 - A diagram showing the chemical reaction of BCIP with Alkaline Phosphate to produce a blue pigment. (*"BCIP-AP Diagram",* Kundu, 2014)

2.4.3 - Jaffe Reaction and Its Applications in Colorimetric Assays

Another colorimetric reaction is the Jaffe reaction, seen in Figure 7, which detects the amount of creatinine in a solution such as urine. The Jaffe reaction occurs in alkaline conditions and refers to the conversion of picric acid to alkaline picrate, which then reacts with creatinine to form a complex known as the Janovsky complex (Delanghe & Speeckaert, 2011). This complex is a soluble crystal with a red-orange hue in alkaline conditions. In a Jaffe reaction using 1% (wt) picric acid and 0.75N NaOH at room temperature, the reaction is measurable on a spectrophotometer (A520) after 15 minutes. A reaction using a minimum of 0.25N NAOH provides the maximum color in urine (Toora & Rajagopal, 2002). The red color produced by the Janovsky complex in an alkaline solution provides a color-metric method of determining

creatinine amounts in urine. This method would require the comparison to an already known creatinine standard curve relating the concentration of creatinine to the color of the reaction after a set amount of time.

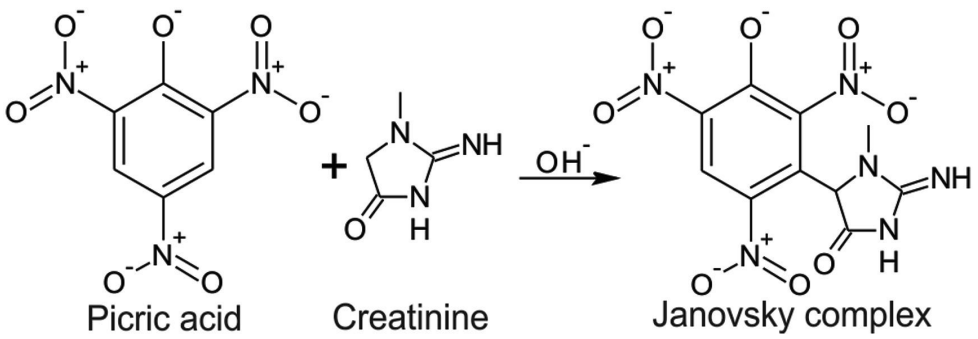

Figure 7 - A diagram of the chemical reaction between picric acid and creatinine to form a Janovsky complex, otherwise referred to as a 'Jaffe Reaction'. (*"Jaffe Reaction Diagram",* Rossini, et al., 2018)

2.4.4 - Combining Colorimetric Assays and Their Purpose

These colors (blue pigments from alkaline phosphatase reactions and orange/yellow pigments formed due to the Jaffe reaction) can be compared against one another and analyzed to determine the ratios they exist in. The overlapping of two separate colors can visibly produce one new unified hue to the viewer. This can be done by either physically mixing two separate colors, or by viewing colors in tandem to each other. This type of color mixing is broken down into two methods: additive and subtractive color mixing. Additive mixing is seen as combining colors (generally red, green, and blue) together to create additional colors (Matsushiro & Ohta, 2003). Additive mixing is generally used for digital displays (Ibraheem, et al., 2012). Subtractive mixing is seen as superimposing layers of colors (generally cyan, magenta, yellow) over a certain background (Matsushiro & Ohta, 2003), generally white (Simonot & Hébert, 2014). This allows for each color to act as a filter for the color of the background and form different colors. Subtractive mixing is used for printed paper (Ibraheem, et al., 2012) and can be described by color transparency. Color transparency is the phenomenon that while viewing a color, the color of the background can also be seen (Simonot & Hébert, 2014). This effect can be coupled by viewing multiple colors through one another to create a new color. Color transparency is commonly used on either a white or black background but can be applied to other colors. With a color-metric detection assay, subtractive mixing can be used to view both color changing

reactions (AP and Jaffe) together to create a new color that is readable on a predetermined scale. Subtractive mixing is more appealing because additive mixing generally uses a red, green, blue model, which makes specific color recognition difficult (Ibraheem, et al., 2012). By using the subtractive model, colors can be easily recognized. Additionally, additive mixing is generally reserved for digital displays, while subtractive mixing is used for printed color (Ibraheem, et al., 2012), which can help create a simpler color mixing system because it does not require the use of a digital display.

2.4.5 - Wavelength Filtering

Wavelength filters can be used to aid in the analysis of these colors. Optical filters are used to select for certain wavelengths of light. This can be used to allow only a certain color of light to continue through the light path past the filter. These filters work by transmitting only a certain set of wavelengths as light passes through them (Anjali, et al., 2020). Filters can be split into two filtering methods: absorptive and dichroic. Absorptive filters work by blocking light by absorbing unwanted light, while dichroic filters work by using interference to block unwanted light (Anjali, et al., 2020). There are three common filter types for blocking wavelengths. They are high pass, low pass, and band pass. High pass filters only allow light above a certain wavelength to pass through the device. Low pass filters only allow light below a certain wavelength to pass through the device. Band pass filters only allow a certain wavelength (and some surrounding wavelengths) to pass through the device (ThorLabs, 2022). Wavelength filters can be used to select for certain colors of light from certain objects. For example, using a low pass filter that allows light below 450 nm on an AP reaction can ensure that only blue and violet light is seen. Additionally, using a high pass filter that allows light above 600 nm on the Jaffe reaction can ensure that only red light is seen. Customizing these filters can allow for selective transmission of wavelengths.

Chapter 3: Project Strategy

3.1.0 - Client Statement

Prior to the formation of this project, there were no widely available methods of noninvasive endometriosis detection. The aim of this project was to design and validate a new method to accurately and non-invasively diagnose endometriosis in individuals who are

experiencing endometriosis-like symptoms. This method focused on being non-invasive, inexpensive, providing quick diagnostic turnaround times, and having a significant impact on the medical field. Endometriosis is a disease with symptoms similar to many other conditions, which further complicates the diagnostic process and can delay proper diagnosis for many years on average. Formulating a cheaper, non-invasive, and accessible method of diagnosis is critical in reducing the time period between patient symptom inquiry and eventual treatment.

3.2.0 - Design Requirements

This project was a continuation of work completed in Worcester Polytechnic Institute's Biomedical Engineering Design course. Previously conducted research and experimentation laid the foundation for deciding how to best proceed. Work on this project centered on creating a tool that analyzes urine samples and would be easily implemented into doctor's offices. Analysis concentrated on detecting and analyzing specific biomarkers associated with endometriosis. This test, once completed, would utilize VDBP, sFlt-1, and MMP-9, whilst also accounting and correcting for concentrations of creatinine. In addition to the previously described criteria, this test was to be accurate, yielding ideally no false positives and false negatives.

3.3.0 - Engineering Standards

This device would be classified as a Class I Medical Device. It is non-invasive and only requires a urine sample from a patient, and as a result poses little to no risk to the patient. This device was planned to follow ISO standards 20916 and 23118, which outline testing procedures critical for the development of in-vitro diagnostic tests and sample procurement respectively. Since the device is meant for use outside the body and the fluids tested are never reintroduced to the body, this device is much easier to develop in terms of standards; the two standards previously mentioned only control how samples are collected, handled, and used for testing rather than control how the device is developed.

ISO 20916 refers to a set of guidelines established to ensure that sample collection does not harm the patient and ensures that the diagnostic test results are not used to harm the patient in any way. Sample collection for urine is easier than most other fluids, as it is naturally expelled from the body and does not require invasive measures to obtain. Since this device is meant for a doctor's office, the sample collection will likely be handled by that office. Urine samples can

then be taken from a collection cup to be tested in the device in a sterile environment with proper safety equipment. ISO 23118, or the "Specifications for pre-examination processes in metabolomics in urine, venous blood serum and plasma," outlines the standards for urine sample collection and handling (International Organization for Standardization, 2021). This team developed the device to use only urine samples, which allows for easier collection that fully fits under both ISO 23118 and ISO 20916 guidelines. The main issue this device poses is in regards to the ISO 20916 clause that states the device cannot "directly or indirectly harm the patient…[including through] false negatives and positives" (International Organization for Standardization, 2019). Although the team has developed the device to the best of their ability to prevent false results, the possibility is always present, especially with these kinds of biomarker tests. Research indicates that possible false results may occur if the patient has kidney cancer, preeclampsia, and potentially other diseases that affect biomarker ratios in the patient's urine. These standards will be maintained as the team develops the device further.

3.4.0 - Project Management Strategy

After weighing individual strengths and weaknesses, the current team discussed work delegation. Individual strengths and weaknesses included writing, editing, project management, communication, big picture thinking, detailed work, and other skills. The team was well-equipped under the guidance of one of the team's advisors, Dr. Reidinger. To utilize the skills of each individual most efficiently, team roles were assigned as follows: Kiran Tremblay as the Team Lead, Burnon Chen as the Project Manager, Lonna Neidig as the Lead Writer, and Alexandra Gannon as the Lead Editor and Product Design Lead.

3.5.0 - Time-Ordered Development Plan

There were many steps within the project that required chronological completion. In efforts to visually organize each step of the project, the team developed a flowchart, as seen in its entirety in Appendix D. Figure 8 below shows an example layout of the flowchart for the end of A-term.

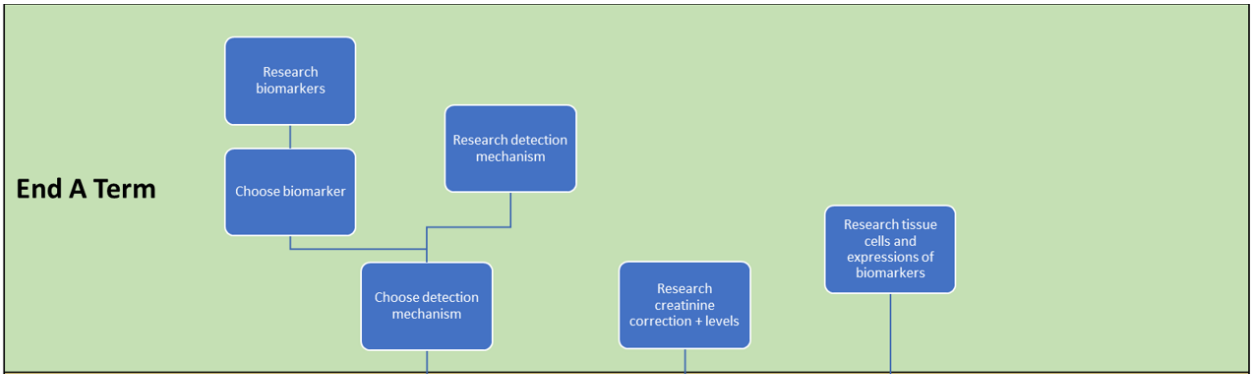

Figure 8 - A clip of the planned flow chart for the team to work on for the end of A-term.

The flowchart is divided into 4 separate 7-week 'terms', reflective of WPI's academic calendar. Planned work in the first term, A-term, consisted of biomarker and detection method research as well as biomarker selection, which allowed for detection method process selection. Additionally, the team researched creatinine levels and corrective methods, while also researching tissue cells and how they express the selected biomarkers.

Planned work for B-term included the development of a method to correct for creatinine and development and testing of the detection mechanism. Additionally, the team deliberated over the physical form of the test, integrated the finalized detection method into the design, and assembled a fully working prototype. The team also obtained the desired tissues and genes. The team edited these genes, transfected the genes into the cells, cultured, froze, and isolated cells and proteins while maintaining a running stock. Finally, the team conducted outreach to procure urine samples from research groups.

The planned focus of C-term was to test the device with standardized synthetic urine before finally testing with proper urine samples, which left work in D-term to finalize the team's presentation and final reports to remain in compliance with Worcester Polytechnic Institute's requirements for the Major Qualifying Project.

This flowchart was developed with an ideal schedule in mind, but the execution of the project was fluid and continually adjusted throughout the year. Testing did not occur until D-term due to complications with reaction kinetics and other logistic and objective based challenges.

3.6.0 - Team Interactions and Weekly Meetings

To ensure that the team remained on track, and that work was being completed properly, the team conducted weekly meetings with their advisors, Dr. Reidinger and Dr. Heilman. Additionally, weekly meetings were conducted with only the students in attendance. All meetings were structured with pre-prepared agendas and recorded with meeting minutes to serve as documentation for plans and discussions within the project.

Chapter 4: Design Process

4.1.0 - Previous Research

As previously stated, this project is a continuation of work from WPI's Biomedical Engineering Design course. The previous team developed a proof of concept for a device capable of non-invasively diagnosing endometriosis by analyzing a urine sample from a patient. This team was able to detect levels of sFlt-1 and creatinine in the ranges expected for a patient with endometriosis. Work also included research into utilizing MMP-9 and VDBP as biomarkers in addition to sFlt-1.

Research conducted by Cho, et al., in 2007 served as the foundational research for work completed in the design course. This paper detailed biomarkers in serum and in urine for endometriosis as well as their numerical concentrations when corrected for creatinine. The previous team selected biomarkers as points of interest from this list and worked to develop a theoretical proof of concept that exploited those biomarkers.

4.2.0 - Needs Analysis

Current methods for diagnosing endometriosis include laparoscopic surgery (the current gold standard), MRI, ultrasound imaging, blood draws, and/or physical pelvic exams. These methods lack precision (pelvic exams and imaging), are invasive (laparoscopy and blood draws), lack accessibility, and are expensive. These issues provided the basis for criteria with which the team used to design the novel device.

4.2.1 - Design Criteria

Existing limitations and anticipated patient and stakeholder needs must be carefully considered when developing a new and alternative diagnostic method. The criteria deemed crucial in guiding the development of an alternative diagnostic method are as follows:

1. Non-Invasive

   The current gold standard to medically diagnose endometriosis is a laparoscopic surgery, which confirms the physical presence of endometriotic lesions, known as endometriomas. This process is invasive, painful, and expensive, and risks potential damage to arteries during the procedure. Other diagnostic methods, such as pelvic exams and transvaginal ultrasounds, are physically invasive and uncomfortable. An ideal alternative method to diagnose endometriosis would be able to provide a sample and diagnosis non-invasively, while still ensuring a reliable and accurate diagnosis.

2. Consistent and Quantifiable Results

   Methods such as a pelvic exam and ultrasound imaging pose a risk of misdiagnosis or prolonged diagnosis times due to their subjective nature and their inability to detect endometriomas outside of the area being examined. An ideal method should be able to produce results objectively that can reliably provide insight into the severity of the disorder through quantifiable data. In the case of this device, the detection will be based on relative protein biomarker levels found in urine, which is noninvasive, quantifiable, and replicable.

3. Unobtrusive

   Unobtrusive methods are capable of diagnosing endometriosis without invading the emotional security or personal space of the patient. This metric can only be measured by user experience, but should be achieved by meeting the criteria of the method being non-invasive. By designing a non-invasive diagnostic method, it can be more accommodating and inviting to a patient as it can be less mentally and physically taxing while also hopefully being a faster procedure.

4. Painless

   Laparoscopy or physical examinations can be painful to patients, especially those with endometriosis. Laparoscopic surgery also requires bed rest following the procedure. Creating a device that is painless in both the sample collecting and testing phases provides an added benefit for the patient/user, which is a pivotal expectation in this product's design.

5. Simple and Easy to Use

   The end product should minimize the possibility of user error on both the patient and professional side. Minimizing user error ensures an accurate result and a less aggressive experience for the patient.

Additional anticipated constraints included: device use only when a patient suspects endometriosis (i.e. exhibiting symptoms) and limiting access to only healthcare professionals.

4.2.2 - Criteria Comparison

To prioritize, visualize, and condense the criteria for the device, the team created a Pugh selection matrix. Pugh selection matrices can aid with the comparison of proposed device criteria by ranking them in accordance to their value. Based on the existing diagnostic methods and literature review, it was determined that the most critical qualities for the device to have are as follows: non-invasive, consistent and quantifiable results, unobtrusive, painless, simple, and easy to use. These qualities were then evaluated from a market standpoint and were assigned an associated "cost" from 1-4, where a lower cost corresponds to a higher overall priority. The market-based classifications included monetary cost, feasibility, research cost, return on investment, intellectual property, and market need. Once evaluated at each of these standards, each quality was given an overall development cost, which would identify which need would be the highest priority and which would follow. The matrix determined that a non-invasive device was highest in priority, with a development cost of nine. This was closely followed by consistency and quantifiable results, unobtrusive, painless, and with simplicity and ease of use becoming the lowest principle priority, as seen in Figure 9.

	Monetary Cost	Feasibility	Research Cost	Return on Investment	Intellectual Property	Market Need	Development Cost
Non-Invasive	2	2	2	1	1	1	9
Consistent & Quantifiable Results	2	3	2	1	1	1	10
Unobtrusive	1	2	3	2	1	2	11
Painless	2	2	1	2	2	2	11
Simplicity & Ease of Use	3	3	4	1	1	1	13

Figure 9 - Pugh selection matrix of proposed device criteria.

These qualities allowed the team to conceptualize several possible detection techniques, which were then compared using a risk evaluation matrix. A risk evaluation matrix compares multiple proposed solutions directly against the criteria determined in the Pugh selection matrix. Due to its widespread use in the industry, laparoscopy was used as a baseline standard to compare all of the theoretical methods. The final four diagnostic methods were algorithmic, urinalysis, a peritoneal fluid test, and a menstrual fluid test, as seen below in Figure 10.

	Weight	Laproscopy	Alogrithm	Urine Test	Peritoneal Fluid Test	Menstrual Fluid Test
Non-Invasive	5	0	1	1	0	1
Consistency & Accuracy	4	0	0	1	1	0
Unobtrusive	3	0	1	1	0	0
Painless	3	0	1	1	0	1
Simplicity	2	0	1	1	0	1
Low Production Cost	2	0	1	1	1	1
Total		0	15	19	6	12

Figure 10 - Risk evaluation matrix of proposed device criteria.

The proposed algorithmic diagnostic method processes a given list of symptoms associated with endometriosis and compares the given symptoms to those actively displayed in a patient. From this comparison, the algorithm gives a predicted diagnosis based on symptom compatibility. This algorithm would utilize user-surveys outlining general and gynecological health issues of endometriosis-positive and endometriosis-negative individuals, which would compile the information into a neural network. This method was discarded due to its lack of ability to produce reproducible and quantifiable results. Additionally, the scale of information needed to effectively and accurately develop said algorithm was deemed too far out of the scope of this project.

The peritoneal fluid and menstrual fluid were evaluated as potential fluids for biomarker analysis. According to Cho, et al., these solutions contain indicative biomarkers such as HIF1-a and VEGF-A. A peritoneal fluid test utilizes a needle for sample collection, which makes it invasive, obtrusive, and painful, thus disqualifying its ability to be used for the device. A menstrual fluid test, which is not invasive, costly, or complex, is obtrusive and only tests for VEGF-A. However, the concentration of this biomarker varies in level from person to person. Additionally, a patient with endometriosis may experience irregular menstrual cycles, which makes menstrual fluid collection unreliable.

Finally, the team determined that urinalysis met all given criteria. The process is non-invasive, simple, cost-effective, unobtrusive, and painless. The biomarkers present in a patient's urine allow for the test to be quantifiable, reliable, and accurate.

4.2.3 - Alternative Solutions

Designing a non-invasive diagnostic test for endometriosis can be broken into exploring and implementing several parts: selecting a biomarker, selecting a detection strategy, selecting an appropriate display, selecting appropriate testing of the device, and developing and implementing a user interface. The team designed and assessed a urine test that can reliably produce consistent and quantifiable results for diagnosing endometriosis. These methods were not only thoroughly tested and evaluated on their ability to produce consistent and quantifiable data, but also on their cost-effectiveness and ease of use.

The team had three initial ideas for developing and testing a biomarker detection mechanism and a device to house this mechanism. Cho, et al., determined in 2007 that endometriosis could be detected by measuring the relative concentration of sFlt-1 compared to that of creatinine. Individuals with endometriosis exhibited 0.54 ± 0.09 pg/mg of sFlt-1 to creatinine while a healthy individual's urine only contains 0.26 ± 0.06 pg/mg of sFlt-1 to creatinine. As such, the detection methods for the biomarkers needed to test for the quantitative levels of both biomarkers and compare the levels to check the ratio of sFlt-1 to creatinine.

The first idea for a dual biomarker detection method involved fluorescence. The team determined that finding a way to bind the solubilized biomarkers to a molecule that initiates fluorescence would provide an easy way to visualize biomarker concentrations. However, photodiodes or other wavelength detection methods would be necessary in order to quantitatively

analyze the fluorescence expression of both biomarkers. A second idea involved colorimetric reactions for both biomarkers, with each reaction producing an amount of colored substrate representative of the concentration of the biomarker. The creatinine test would utilize the Jaffe reaction, and the sFlt-1 colorimetric test would utilize a biochemical chain that binds an AP to each sFlt-1 molecule; this AP converts a colorless substrate to a blue-colored substrate over time. As such, the amount of substrate converted (and therefore the depth of the blue coloring in the vial) would indicate the concentration of sFlt-1 in the original sample. The overlaid colors of the two separate reactions would then be compared to a chart of shades of green that correspond to varying ratios of creatinine to sFlt-1, where certain levels would be indicative of sFlt-1. The third and final design builds upon the third and aims to reduce the subjectivity of the test to further standardize the results, allowing for more consistent results. This third idea utilized wavelength filters to concretely compare the final shade produced by the test to known wavelengths that correspond to the likelihood of endometriosis, which would remove human opinion and error from the process.

The team proceeded with the second design, a colorimetric test with a color chart. The first design with fluorescence was deemed not feasible due to the difficulties of effectively binding to the selected biomarker and then causing them to fluoresce in a detectable and quantifiable manner. The third design was deemed not feasible due to time constraints and the difficulty in sourcing wavelength filters for the final design, but could potentially prove as a significant improvement in standardizing the test to further ensure consistent and quantifiable data while improving upon the ease of use of the final device.

4.3.0 - Goals for Expansion of Research

The original proof of concept from the founding team in BME3300 helped the current team develop a more in-depth project. Research goals included developing a method for detecting sFlt-1 corrected for creatinine in a quantitative manner. This method had to be housed in a small, disposable, and relatively inexpensive device for a medical professional's use. Originally, the team wanted to utilize fluorescence for the detection and quantification of sFlt-1, but following several reiterations of the project, settled on utilizing two colorimetric reactions for detecting ratios of sFlt-1 concentrations to creatinine concentrations. The group determined which hues of green are associated with endometriosis based on known values and ratios of

sFlt-1 to creatinine in urine. MMP-9 and VDBP were no longer the focus of the project, as the research team decided to focus on sFlt-1 and creatinine to create a more attainable goal.

4.4.0 - Objectives of Current Project

Several objectives were established in order to complete the project. The team needed to obtain a usable stock of protein (sFlt-1 and creatinine), obtain urine samples, develop the detection mechanism and necessary ligand binding, develop a device to house the detection mechanism, and combine all previously completed work to test the final product. Additional objectives included making the device easy to use and results easy to obtain.

4.4.1 - Modeling of the Device

The BME3300 team intended to model the final device after over the counter pregnancy tests. Due to concerns of user-error in this format, the current team decided to stray from this model. Since the initial conceptualization of the device, the team has explored the idea of fluorescence as a tool for diagnosis, but was ultimately ruled out due to cost-restraints. One of the primary issues surrounding the pregnancy-test model was proper diagnosis, as the team did not want the device to be improperly used, which could potentially result in false positives or false negatives. Similarly, designing the test with the intent for use by only medical professionals further streamlines the diagnosis process as well as subsequent treatment timelines. Additionally, this model would not be able to accommodate the two necessary chambers for the two colorimetric reactions as well as the proper viewing window to determine a diagnosis. The team instead opted to create a device with two separate internal compartments to accommodate the separate detections of sFlt-1 and creatinine. Each internal compartment houses a colorimetric reaction which produces a unique color for each biomarker. sFlt-1 detection produces a blue color, while creatinine detection produces a yellow-orange. A darker color indicates higher amounts of the specific biomarker. When viewed in tandem, the two reactions would produce a green hue which could be used to determine whether or not the patient had endometriosis. The standardization of this process was made possible with backlighting from a white LED, which provides the necessary lighting to view the color of both reactions.

The first prototype following this model can be seen in a cross-sectional view below in Figure 11, labeled ‘1.’ This prototype took heavy inspiration from urine specimen jars, featuring

a screw-top lid and two separate vials which would be filled by direct urination into the jar. This protype relied on a numeric reading of the ratio of the two reactions, and was intended to digitally display the diagnostic results to the user. Due to time, budget, and feasibility constraints, the numeric display was later removed to instead result in a visual diagnostic method through colorimetric interpretation. The second prototype, labeled '2,' kept most of the same characteristics of the previous model like that of the screw-top lid and housing of two cuvettes, but this time instead including a viewing port with which both of the vials could be viewed in tandem.

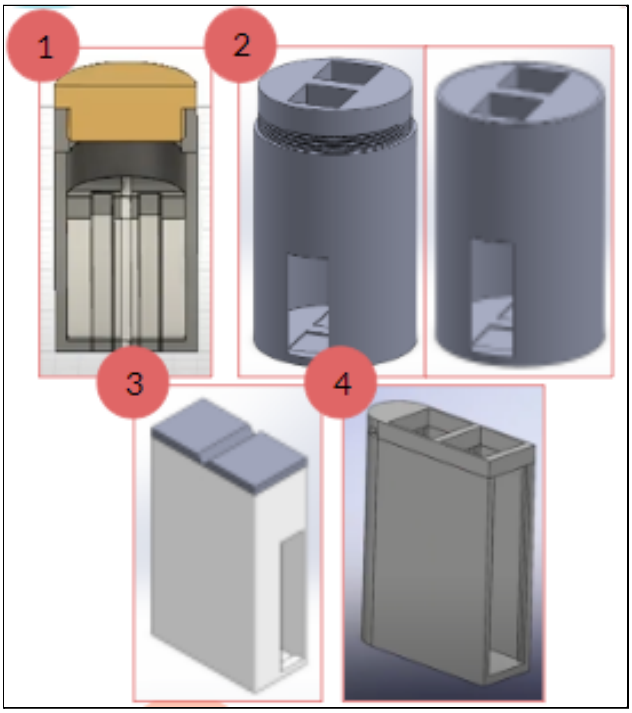

Figure 11 - The progression of the first prototype through the fourth, labeled as such.

The third prototype was created in an effort to reduce the unused and unnecessary space surrounding the dual-cuvettes. This model featured only enough room for the cuvettes, a flip-top lid, and a viewing port that was intended to have a colorimetric diagram on the side for reference and diagnostic purposes. The fourth prototype seen in Figure 11 was similar to that of the third, but contained enough room to house an LED strip which would help to standardize the future testing results. The lid for this model was left open for ease of operations during lab testing. Each

of these prototypes helped to lay the foundation for the most recent prototype which can be seen in the CAD model Figure 12, below.

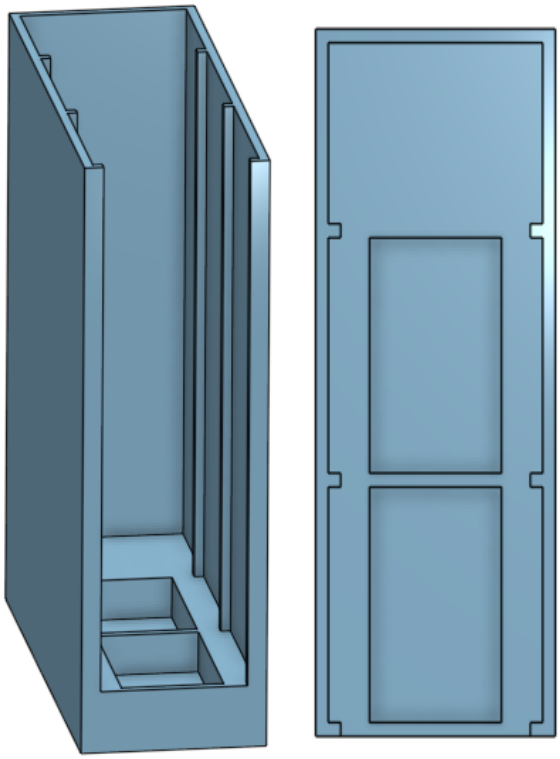

Figure 12 - CAD of the most recent prototype. A dimetric view (left) next to an overhead view (right) highlighting the built-in magnet holders. The device stands with dimensions of 51mm x 39mm x 14.5mm

The final prototype houses two cuvettes with a viewing port, responsible for generating the colorimetric result indicative of endometriosis, enough room for an LED, which will standardize the results of each test, and two grooves to hold neodymium magnets, which will ensure the A/G coated magnetic beads will not be expelled from the cuvette upon disposal of liquid. The A/G coated magnetic beads function as an intermediate to bind the means in which sFlt-1 is detected within the cuvettes. Their purpose will be explored and discussed further in section 4.4.3. A progression of the most-recent prototype with each discussed component can be seen below in Figure 13.

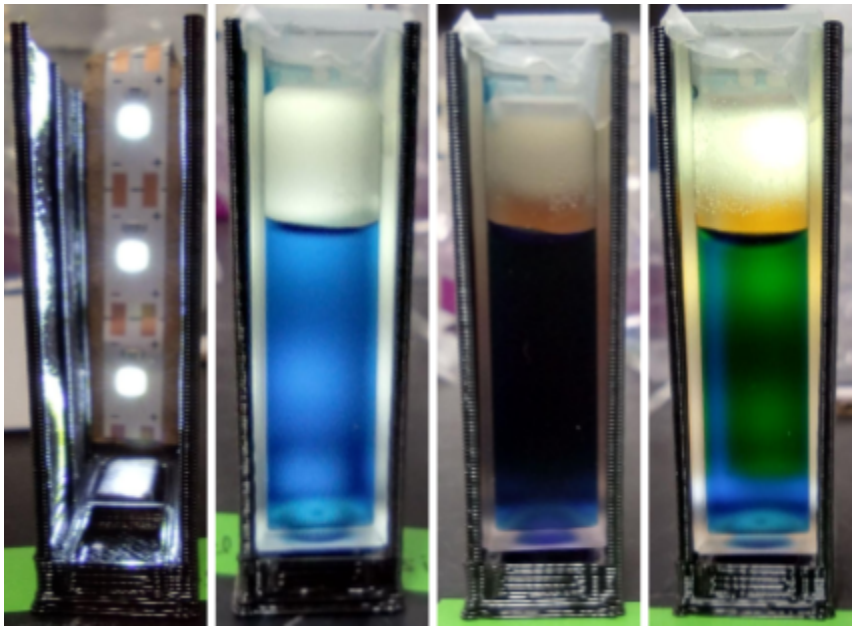

Figure 13 - Progression of front-view photos of the most recent prototype version. From left to right: The prototype without cuvettes showing backlit LEDs, the prototype with a sFlt-1 cuvette only and LEDs on, the prototype with both the sFlt-1 cuvette and the Jaffe reaction cuvette with no LED, and the prototype with both the sFlt-1 cuvette and the Jaffe reaction cuvette and LED.

Looking ahead, future prototypes of the device may include visual aids such as bandpass or wavelength features which only let through specific wavelengths of light, or would only let light through based on a specific diagnosis.

4.4.2 - Creatinine Detection

Creatinine detection is based on the Jaffe reaction, where creatinine and picric acid react to form the Janovsky complex: a molecule with a red color. One Janovsky complex molecule is created for every creatinine and picric acid in the reaction. This reaction is catalyzed by an alkaline environment (pH > 7). NaOH is needed to speed up the reaction kinetics to lower the time needed to determine the amount of creatinine. Both creatinine and picric acid on their own are colorless, but when combined, form a colored molecule. In an environment with excess picric acid, the amount of Janovsky complex created is limited by the amount of creatinine in the reaction. Creatinine is the limiting reagent in the reaction. This is crucial for the indirect quantification of creatinine. This is because the color intensity is based on the amount of

Janovsky complex, which is based on the amount of creatinine. A greater intensity indicates a higher amount of creatinine and a lower intensity indicates a lower amount of creatinine.

The team plans to add excess picric acid and NaOH to the sample to determine the amount of creatinine. Excess picric acid is needed to ensure that creatinine is the limiting reactant. This is important for the indirect quantification of creatinine based on the color intensity caused by the amount of Janovsky complex.

4.4.3 - sFlt-1 Detection

sFlt-1 detection (see Figure 14) is based on a sandwich ELISA analytical assay platform. The concept relies on two complexes: a stabilization complex (Complex 1) and a detector complex (Complex 2). The stabilization complex links sFlt-1 to the device. The detector complex allows for indirect quantification of sFlt-1. sFlt-1 acts as a linker between the two complexes.

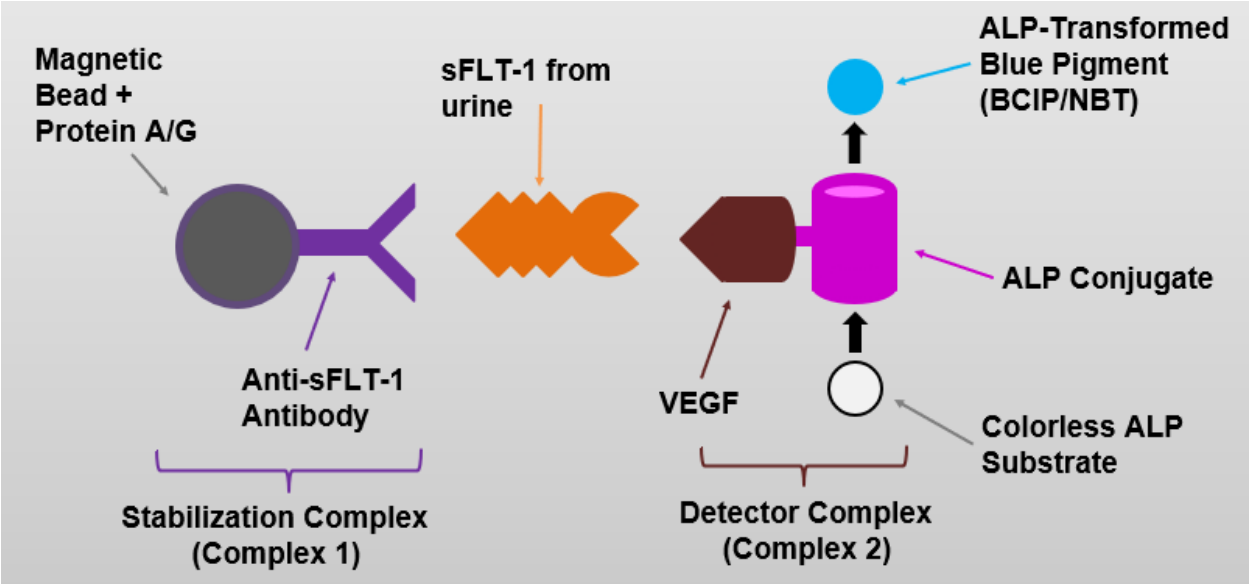

Figure 14 - The planned sFlt-1 detection method. Full detection chain unlinked to indicate individual sections of the chain.

The stabilization complex consists of two pieces: a sFlt-1 binder and device binder. The sFlt-1 binder is an anti-sFlt-1 antibody. The variable region (light chain) of the antibody will bind to sFlt-1 rapidly with high specificity. The device binder is multiple Protein A/G molecules

conjugated to a magnetic bead. Protein A/G is known for its ability to readily bind to the constant region (heavy chain) of antibodies. This ability is depicted below in Figure 15.

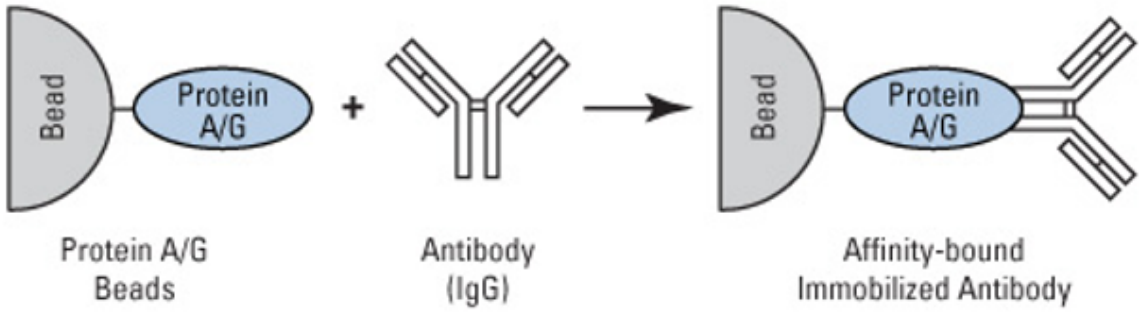

Figure 15 - A diagram depicting Protein A/G coated beads and their ability to bind to antibodies (*"A/G Coated Bead Diagram",* CD Bioparticles, 2022)

This interaction between Protein A/G and the antibody allows both pieces of the stabilization complex to link together. The magnetic bead is used to help attach the stabilization complex to the device. If the device is fitted with a strong magnet, the magnetic beads will gravitate towards the magnet and stay in the device. When both pieces of the stabilization complex are bound together, they can be magnetically linked to the device.

The detector complex consists of two pieces: a sFlt-1 binder and detector. The sFl-1 binder is VEGF165. This receptor/ligand interaction is very competitive and binding happens rapidly. The detector is an AP enzyme. AP is an enzyme which catalyzes the removal (hydrolysis) of phosphate groups. This is combined with BCIP/NBT, which is a naturally colorless molecule prior to adding a phosphatase. After reacting with phosphatases, the colorless molecule undergoes a chemical change and becomes a blue/purple color over time. When reacting with excess BCIP/NBT, the amount of color generated over time is based on the amount of AP available. Because of the AP and BCIP/NBT reaction (previously shown in Chapter 2, Figure 6), the detector complex can be used to indirectly quantify the amount of sFlt-1 in the sample. The sFlt-1 binder and detector will be conjugated together. This can be achieved through a method called one-step glutaraldehyde coupling. One-step glutaraldehyde coupling is typically used for antibody to protein conjugation, but can also work for protein to protein conjugation.

When combined together, the stabilization complex and detector complex are linked by an sFlt-1 molecule. After binding, the device can be washed out to remove excess detector

complex before adding excess BCIP/NBT. sFlt-1 is needed to link the detector complex to the stabilization complex, and the detector complex is needed to determine the relative amount of sFlt-1 in the sample. Because of this linking, the amount of color generated (due to the AP BCIP/NBT reaction) is related to the amount of sFlt-1 in the sample. A darker shade of blue indicates a greater amount of sFlt-1 in the sample. Like other ELISA assays, this method allows for the indirect quantification of a biomarker. In the case of the new device, this is sFlt-1.

4.4.4 - Protein Stock Process

Stocks of creatinine and sFlt-1 were needed to test the device in an artificial environment. Artificial environment testing is a necessary initial testing step to determine the device's feasibility for endometriosis diagnosis. While creatinine was readily available for purchase, sFlt-1 was not. The sFlt-1 protein and physical gene were unavailable for purchase. Because of the sourcing issue, the team planned on genetically engineering sFlt-1 for synthetic testing through a modified Gibson assembly approach (see Figure 16). Once the team engineered the sFlt-1 gene, protein production would become possible. This involved modifying a human Flt1 delta CTD (hFlt-1) gene, before transforming the gene into Human Umbilical Vein Endothelial Cells (HUVECs), the appropriate cells for sFlt-1 protein production. This process will be further detailed later in Chapter 6.

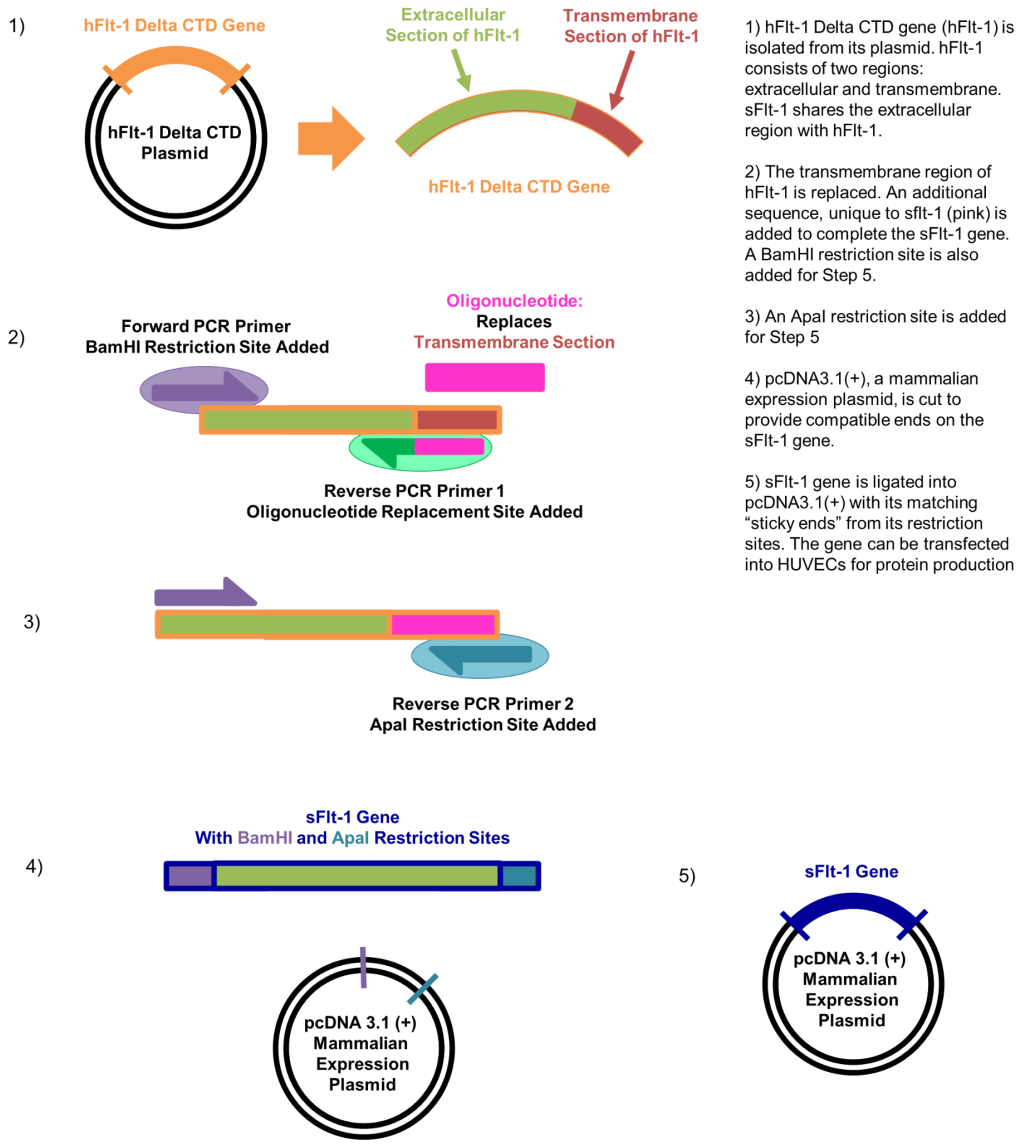

Figure 16 - Overall plan to genetically engineer sFlt-1 gene from hFlt-1 plasmid.

4.4.5 - Testing with Synthetic Controls

Before beginning testing, the team devised four synthetic testing environments to determine the accuracy and feasibility of the device for determining the concentration of sFlt-1. These tests involved:

1. Testing only AP.
2. Testing only Complex 2 (VEGF-AP).
3. Testing Complex 2 (VEGF-AP) linked to sFlt-1 (synthetic biomarker).
4. Testing Complex 1 (magnetic bead with Protein A/G linked to anti-sFlt-1 antibody) linked to sFlt-1 (synthetic biomarker) linked to Complex 2 (VEGF-AP).

The first test involved AP at concentrations similar to sFlt-1. Testing AP independently of all other parts of the detection method allowed for the determination of the time scale needed to ensure that AP was producing a noticeable color. The AP was mixed with excess BCIP/NBT, the substrate necessary to produce a blue color. Because the BCIP/NBT was in excess, the only factor contributing to the color produced was the amount of AP within the reaction. In this case, higher AP concentration simulated a higher sFlt-1 concentration and vice versa. This test also helped identify any revisions needed to the detection method. If a 1:1 molar ratio of AP to sFlt-1 was not enough to produce a visible difference in a set amount of time, then subcomplex 2 could be modified to include more than one AP molecule, which would in turn, speed up the colorimetric reaction.

The second test involved subcomplex 2 (VEGF-AP) at concentrations similar to sFlt-1. Testing subcomplex 2 independently of all other parts of the detection method confirmed that the protein coupling worked between VEGF and AP. Because the means by which these specific proteins couple to each other are still unknown, VEGF-AP needed testing to ensure that AP could still function as a phosphorylase after conjugation. Like the first test, subcomplex 2 was mixed with excess BCIP/NBT. With the BCIP/NBT in excess, the only factor contributing to the color produced was the amount of AP available. In this case, higher AP concentration simulated a higher sFlt-1concentration and vice versa.

The third test involved subcomplex 2 (VEGF-AP) and synthetic sFlt-1. Testing subcomplex 2 linked to the synthetic sFlt-1 confirmed that sFlt-1/VEGF binding did not interrupt AP activity. This was crucial because AP allows for the determination of sFlt-1 concentration therefore it was necessary to ensure that AP function was not blocked throughout the whole detection process.

The fourth test involved the full detection pathway: Subcomplex 1 (magnetic bead with Protein A/G linked to anti-sFlt-1 antibody), sFlt-1 (synthetic biomarker), and Subcomplex 2 (VEGF-AP). Testing the full detection pathway would confirm or deny that sFlt-1 AB/sFlt-1 binding does not interrupt AP activity. This was crucial because AP allows for the determination of sFlt-1 concentration. It was necessary to ensure that AP function was not blocked throughout the detection process. This would also confirm if the sFlt-1 AB and VEGF can both bind to sFlt-1 and work as a linking molecule.

Once each test was complete, the test could include the introduction of creatinine colorimetric tests. Coupling the creatinine detection tests with the sFlt-1 detection tests would confirm whether the device can produce green hues distinguishable from each other for different concentrations of sFlt-1 and in turn, the presence and varying levels of endometriosis in patients.

4.5.0 - Design Process Summary

The team determined the need for a non-invasive, unobtrusive device that analyzed urine samples for the ratio of sFlt-1 to creatinine expressed in urine via a novel dual colorimetric assay approach. Development began on the described device and several methods of testing its ability to diagnose endometriosis were used. In order to validate this device, the team considered previous research, determined the needs of the client and how criteria and objectives may meet those needs. Using this workflow, a device was researched, developed, and prototyped, along with the detection methods of specific biomarkers. These methods were tested and used by the team to evaluate the device.

Chapter 5: Materials and Methods

The current device design underwent many revisions. Below are the materials and methods used in the most recent iteration of the device, its detection methods, and testing.

5.1.0 - Physical Device Design and Printing

The final prototype was designed using the modeling software SolidWorks. It contains housing for two cuvettes, slots for neodymium magnets, space for an LED strip, and an open viewing face. The device was prepared for printing using the software 3DPrinterOS, and was printed out of PLA filament using a LUA TAZ06 3D printer.

5.2.0 - Preliminary Assay Testing

Preliminary testing of the assays tested the feasibility of using AP and Jaffe detection methods at urine biomarker concentrations commonly found in individuals prone to endometriosis. Levels of sFlt-1 in urine range from 0.20-0.63 pg sFlt-1/mg creatinine (Cho et al., 2007). Levels of creatinine in urine range from 20-275 mg creatinine/dL urine (Eng, 2021). Absorbance values were taken using a Thermo Scientific™ GENESYS™ 20 Visible Spectrophotometer.

5.2.1 - Jaffe Reaction for Creatinine Detection

Creatinine detection was tested by mixing 1mL creatinine, 1mL picric acid, and 2mL 1N NaOH. Creatinine was serially diluted (2 fold) to create a concentration gradient within the typical creatinine levels found in urine. Creatinine (anhydrous, 98%) and Picric Acid (0.9-1.1%, alkalimetric) were sourced from MilliporeSigma (Sigma-Aldrich, St. Louis, MO). Reactions were incubated for at least 72 hours before beginning qualitative analysis, and 96 hours before beginning quantitative analysis (A483). Creatinine reactions were diluted 1:8 in dH2O before beginning quantitative analysis.

5.2.2 - Determination of Supplied AP concentration

AP concentration was determined by a Bradford Assay (A595). Concentration was calculated using a standard curve of 6 step 2 fold serially diluted BSA starting at 0.5 mg/mL. Used 3mL of Bradford Reagent per sample. Tested 50uL of 1:100 AP diluted in 1x TE buffer. AP (*E. coli* C90 bacterial AP) was sourced from Thermo Fisher (Thermo Fisher Scientific, Waltham, MA).

5.2.3 - Isolated AP testing for sFlt-1 Detection

AP detection at concentrations similar to sFlt-1 levels found in urine of individuals prone to endometriosis was tested by mixing 1mL AP and 1mL BCIP/NBT tablet solution. BCIP/NBT tablet solution was created by dissolving 1 SIGMAFAST™ BCIP®/NBT tablet in 10mL of dH2O. SIGMAFAST™ BCIP®/NBT tablets were sourced from MilliporeSigma (Sigma-Aldrich, St. Louis, MO). AP was serially diluted (2 fold) to create a concentration gradient within the typical sFlt-1 levels found in urine. Samples were split between urinary sFlt-1 levels found in endometriosis positive and negative patients. An additional sample was run at 100x the urinary sFlt-1 levels found in endometriosis negative patients. Reactions were incubated for at least 72 hours before qualitative analysis, and 96 hours before quantitative analysis (A490).

5.3.0 - Synthetic sFlt-1 production

The enzymes and other reagents used were purchased from New England Biolabs (NEB, Ipswich, MA) unless otherwise specified. Primers and oligonucleotide were synthesized by Integrated DNA Technologies (IDT, Coralville, Iowa). The MW ladder (1kB) was sourced from Promega (Promega, Madison, WI). Plasmid concentration was determined with a NanoDrop Lite (Thermo Fisher Scientific, Waltham, MA). All PCR reactions used a BioRAD MyCycler Thermocycler (BioRAD, Hercules, CA).

5.3.1 - Isolation of hFlt-1

hFlt-1 delta CTD (hFlt-1) was streaked onto a 1x Kanamycin plate and incubated overnight (37C, 5% CO2) to isolate a monoclonal colony. hFlt-1 delta CTD (Addgene Plasmid #86036) was sourced from the Christie Thomas lab (Addgene, Watertown, MA). A single colony was picked and incubated in liquid culture (5x Kanamycin LB media) overnight (37C, 5% CO2, 200 RPM) before plasmid purification. Plasmids were purified using the Promega PureYield Plasmid Miniprep kit (Promega, Madison, WI) according to the centrifugation method (see Appendix E).

5.3.2 - Synthesis of Primers and Oligonucleotide

The primers and the oligo were designed using SnapGene6.0. The oligo was synthesized to reflect the 31 amino-acid sequence found on sFlt-1. Three primers were synthesized. One

primer was responsible for creating an overhang between the shared Flt-1 sequence and the oligo. The other two primers were responsible for adding restriction-sites compatible with the pcDNA plasmid (BamHI, ApaI).

5.3.3 - Preparation of hFlt-1 for oligo annealing

hFlt-1 was prepared for oligo annealing by PCR amplification of the shared sequence between hFlt-1 and sFlt-1. The isolated hFlt-1 gene was PCR amplified in a 50uL reaction mixture of 2uL hFlt-1 template DNA, 2.5uL of each primer (BamHI site adder, Oligo overhang adder), 25ul Q5 High-Fidelity 2x MasterMix (NEB, Ipswich, MA), and filled to 50uL with autoclaved dH2O. PCR cycling parameters were: one 30 second cycle at 98C, followed by 30 cycles of 30 seconds at 98C, 30 seconds at 55C, and 2 minutes at 72C, finished with a 2 minute extension at 72C. Raw PCR product was purified using the Promega Wizard PCR and Gel Cleaning Kit (Promega, Madison, WI) according to the centrifugation method (see Appendix F). Purified PCR product and hFlt-1 were run on a 1% agarose gel with ethidium bromide at 90V for 90 minutes and analyzed under short-wave UV to confirm modification.

5.3.4 - Completion of sFlt-1 gene

sFlt-1 gene completion began by gel purifying purified PCR product and hFlt-1 on a 1% agarose gel with ethidium bromide at 90V for 90 minutes and analyzed under short-wave UV to confirm modification. Oligo annealing happened in an 8uL reaction mixture of 2uL oligo and 6uL purified PCR product incubated at 95C for 1 hour. The reaction used 1:1 mass ratio of purified PCR product and oligo. Relative amount of hFlt-1 plasmid was determined using ImageJ compared known amounts of DNA in the MW ladder.

The sFlt-1 gene was completed by PCR amplifying annealed oligo product in a 50uL reaction mixture of 4uL oligo annealed construct template DNA, 2.5uL of each primer (BamHI site adder, ApaI site adder), 25ul Q5 High-Fidelity 2x MasterMix (NEB, Ipswich, MA), and filled to 50uL with autoclaved dH2O. PCR cycling parameters were: one 30 second cycle at 98C, followed by 30 cycles of 30 seconds at 98C, 30 seconds at 55C, and 2 minutes at 72C, finished with a 2 minute extension at 72C. Raw PCR product was purified using the Promega Wizard PCR and Gel Cleaning Kit (Promega, Madison, WI) according to the centrifugation method (see Appendix F).

The sFlt-1 gene was also digested by restriction enzymes in preparation for a ligation. Digestion happened in 20uL reaction mixtures of 2uL complete sFlt-1, 2uL Buffer E (Promega, Madison, WI), 1uL of BamHI, 1uL of ApaI, and filled to 20uL with autoclaved dH2O.

5.4.0 - Restriction Profiling of pcDNA

pcDNA was analyzed for restriction sites within its multiple cloning site (MCS). Two restriction sites, BamHI and ApaI were chosen for use in the ligation of a complete sFlt-1 gene into a plasmid. A restriction profile using BamHI and ApaI restriction enzymes was run to confirm the presence of the restriction sites. pcDNA was digested with either BamHI, ApaI, or both BamHI and ApaI. The digestion mixture contained 2uL pcDNA, 2uL Buffer E (Promega, Madison, WI), 1uL of specific restriction enzyme (either 1uL BamHI, 1uL ApaI, or 1uL of BamHI and 1 uL ApaI), and filled to 20uL with nuclease free water. Reactions were incubated at 37C for 1 hour before running on a 1% agarose gel with ethidium bromide at 90V for 90 minutes and analyzed under short-wave UV to confirm digestions.

5.5.0 - DNA Sequencing

PCR products were sampled throughout the sFlt-1 design process. Raw hFlt-1 delta CTD and pcDNA were sequenced by Psomagen (Psomagen, Rockville, MD). Sequences were analyzed using SnapGene6.0.

Chapter 6: Design Verification

6.1.0 - The Need for Protein Stocks

In order to determine if the device could detect endometriosis, it needed to be tested against synthetic biomarker standards. Creatinine is a common chemical, and 10 grams of 98% anhydrous creatinine were easily procured from Millipore Sigma. sFlt-1, the other biomarker in contention, was more difficult to find as this protein was unavailable for sale at the time this project started in late 2021. The next option was to purchase the physical gene responsible for producing sFlt-1. Much like the protein, the gene was also unavailable for purchase. However, a similar gene to sFlt-1, hFlt-1 delta CTD, was able to be purchased from AddGene, which would enable the team to synthesize the sFlt-1 gene by altering the hFlt-1 sequence.

sFlt-1, the end product, is a soluble protein. hFlt-1, the starting product, is a transmembrane protein. While they have similar roles (bind to VEGF), their structure differs. Because of this, hFlt-1 must be modified to remove its transmembrane region and replace it with a unique tail end cap. This can happen via Gibson assembly, which is a method used for annealing two pieces of DNA together. PCR, or polymerase chain reactions, use enzymes to replicate DNA given "templates" such as plasmid DNA, constructs, and primers. Gibson assembly involves introducing longer pieces of DNA that attach to these templates and are integrated into the gene by the DNA synthase during the PCR.

Verification of the purchased plasmids and the restriction profile of pcDNA established a jumping-off point for the rest of the project. The next step in the process was to edit the hFlt-1 delta CTD into sFlt-1. In order to complete this process, the transmembrane portion of the hFlt-1 delta CTD needed to be replaced by a 31 amino acid sequence unique to sFlt-1, the gene needed to be linearized out of the plasmid, needed to be bookended by restriction enzyme sites present in pcDNA, and amplified to a working concentration. This genetic engineering required a Gibson-assembly-like PCR amplification, a synthesized oligonucleotide 31 amino acid sequence, and primers to assemble the construct.

The Gibson assembly provides the means for replacing the transmembrane section of hFlt-1 delta CTD with an oligonucleotide. This substitution was arranged with the help of a primer. The procedure that prepares the replacement of the transmembrane sequence with the oligonucleotide would occur during PCR. Ideally, the steps would occur as follows. First, the hFLt-1 delta CTD plasmid would be combined with a forward DNA primer that would add an BamHI restriction site to the 5' end of the hFlt-1 delta CTD gene and a reverse primer that would bind to 25 bases of the pre-transmembrane section at the 3' end of the construct and would have a loose end with the first 18 bases of the oligonucleotide. The amplification of PCR would occur when the plasmid is denatured and binds to the forward primer and the reverse replacer primer. This amplification would produce a linear segment of DNA with an BamHI site on the 5' end and a 15 base pair portion of the oligonucleotide that has replaced the transmembrane portion of hFlt-1 delta CTD on the 3' end. This linear sequence contains a restriction site on the 5' end and the means to anneal an oligo to the construct on the 3' end. The second step of the process involved denaturing this double-stranded construct and annealing it to the synthesized oligonucleotide. Once this annealing had occurred, it could be placed into a PCR machine along

with the original forward primer and an additional reverse primer that contains an XbaI restriction site at the 3' end. The PCR would produce a linear construct of sFlt-1 bounded by two restriction enzymes, BamHI and XbaI.

6.2.0 - sFlt-1 Protein Stock Production

Several challenges arose surrounding the procurement of sFlt-1 stock, as it was not available for purchase in either protein or gene format. This section outlines the process used to synthesize, verify, and harvest sFlt-1 protein through genetic altering of hFlt-1 and ligation.

6.2.1 - hFlt-1 Starting Material

The hFlt-1 delta CTD (Plasmid #86036) purchased from AddGene was supplied by the Christie Thomas lab, where it was created in order to study the protein (Raikwar, et al., 2014). The plasmid was transported as an agar stab, and was transformed into pCMV6 Entry *E. coli*. The plasmid carried a gene for Kanamycin resistance, and was otherwise a standard cloning vector. A full vector map can be found in Appendix G. The gene was tagged with an HA tag at the N terminus and was preceded by a CMV promoter. The gene had a length of 2567 base pairs. hFlt-1 delta CTD is an isoform of hFlt-1 (Flt-1) with the intracellular portion of the protein excised, leaving the transmembrane portion and the extracellular portion of hFlt-1. This gene was ideal for the purposes of this project, since sFlt-1 is an isoform of hFlt-1 with both the intracellular portion and the transmembrane portion replaced by a novel 31 amino acid sequence. This hFlt-1 delta CTD gene could be genetically edited to create a gene for sFlt-1, which in turn could be transfected into human endothelial cells to express and secrete sFlt-1. This secreted sFlt-1 could be purified out of solution to create a stock of protein that the device could be tested with.

Since the hFlt-1 delta CTD arrived as an agar stab, it needed to be streaked onto a plate to isolate monoclonal colonies. This process, performed on Kanamycin-agar plates, would allow for colonies expressing the hFlt-1 delta CTD and the appropriate resistance gene to develop and be picked to propagate. A "KAN" (1X Kanamycin) plate was brought to room temperature upside-down to prevent condensation drips. The bottom of the plate was marked into four quadrants, labeled Q1 through Q4. Bacteria was transferred from the agar stab to Q1 using a P-200 pipette tip, and was streaked across the quadrants according to Figure 17 below. Each

streak was performed with a clean pipette tip. This plate was incubated upside-down for 16 hours at 37C in a bacterial incubator, and the stab was returned to a 4C freezer. After 16 hours, there was little growth outside of quarter 1 (Q1), as shown in Figure 18.

Figure 17 - Diagram of KAN plate 1 (04 NOV 2021) bacteria streaking. Colors indicate streaking pattern per P-200 pipette tip. Red = 1st streak, Blue = 2nd streak, Orange = 3rd streak, Green = 4th streak.

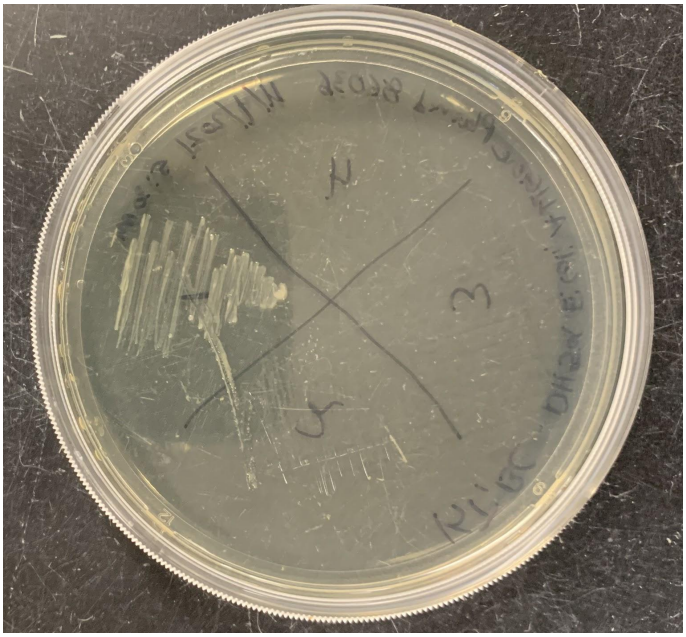

Figure 18 - Picture of KAN plate 1 (04 NOV 2021) after 16 hour incubation at 37C. Image taken on 5 NOV 2021 at 9:35 AM

This slow growth was unusual, as healthy colonies usually form in at least Q2 and Q3 after 12 hours of incubation. A colony from Q2 was selected from the plate and streaked onto a second plate and was returned to the incubator along with the original plate. After 16 hours, the original plate showed little growth past further than the 16 hour mark. After 25 hours after initial streaking, the plate streaked with a colony from the original plate had produced colonies, but they were difficult to distinguish from one another, as can be seen in the Figure 19 below.

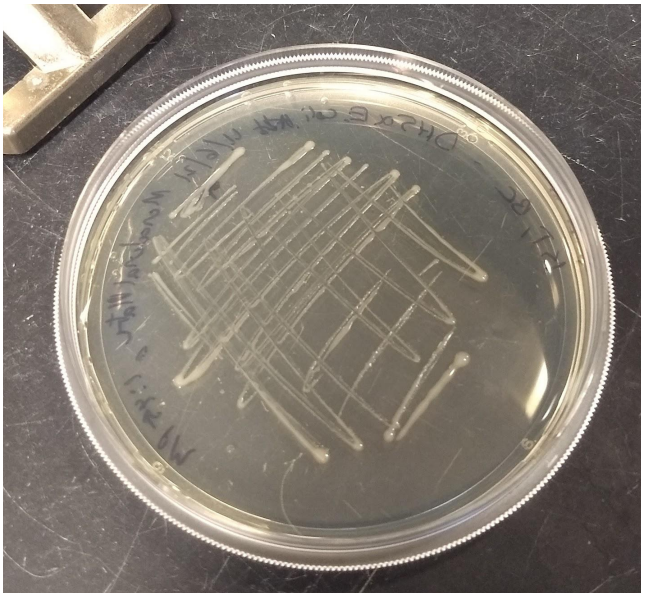

Figure 19 - Picture of KAN plate 2 (06 NOV 2021) after 25 hour incubation at 37C. Image taken on 7 NOV 2021 at 3:30 PM.

Although these plates were left in the incubator for longer times and periodically observed, the results of the experiment had to be discarded because *E. coli* left to grow for that long may acquire mutations that would affect the experiment. At this point, a new plate was streaked with similar results.

6.2.2 - Determining Antibiotic Concentration for hFlt-1 Gene Amplification

A new strategy to propagate the plasmids was developed due to the lack of monoclonal colonies produced using the plate streaking method. This strategy involved inoculating the bacteria from the stab into liquid cultures of varying antibiotic concentrations. Liquid cultures with the highest optical density and highest antibiotic concentration would be chosen to prepare plasmids from. This method produces monoclonal colonies through the use of high amounts of antibiotic; the point of this method is to use enough antibiotic to kill any

non-plasmid-transformed *E. coli* while allowing the transfected *E. coli* to slowly propagate and react to higher concentrations of antibiotic. Kanamycin tubes were used for the hFlt-1 delta CTD plasmid. Tubes were prepared according to Table 1 below for the antibiotic experiment. These tubes were prepared with LB media and 1000x antibiotic stocks.

Table 1 - Amounts of LB media, antibiotic, and cells added to form a liquid culture for the propagation of *E. coli* containing hFlt-1 delta CTD plasmid.

Sample ID	Tube #	LB Media (mL)	Cells	Antibiotic Strength (x)	KAN (uL of 1000x)
LB Media Control	0	4	NONE	0	-
KAN Cell Control	K0	4	KAN Resist	0	0
KAN 1x	K1	4	KAN Resist	1	4
KAN 2x	K2	4	KAN Resist	2	8
KAN 3x	K3	4	KAN Resist	3	12
KAN 5x	K5	4	KAN Resist	5	20
KAN 10x	K10	4	KAN Resist	10	40
KAN 20x	K20	4	KAN Resist	20	80

The Kanamycin tubes were inoculated using pipettes inserted into the hFlt-1 delta CTD agar stab. 4uL of the transformed *E. coli* containing pcDNA were added to each of the Ampicillin tubes. These tubes were then transferred to an incubator-shaker set to 37C and a shake rate of 200 RPM, which is standard for *E. coli*. The tubes were checked after 20 hours and were observed to have low turbidity. The tubes were left to incubate for 21 more hours for a total of 41 hours before they were removed from the incubator and placed in a 4C fridge.

Tubes containing 5x antibiotic were chosen to be prepped for plasmids due to their high antibiotic concentration and relatively high turbidity.

6.2.3 - hFlt-1 Gene Stock Production

The plasmid preparation was carried out using a Promega PureYield Plasmid Miniprep kit and system. The protocol for this kit can be found in Appendix F. Three ml of each 5x antibiotic culture tube was prepped, and the only exception to the protocol was that the hFlt-1 delta CTD plasmid was resuspended in 15uL instead of 30uL on accident. The concentration of the hFlt-1 delta CTD plasmid was measured at 203.5 nanograms of DNA/uL using a nanodrop. The nanodrop was turned on and blanked using 1uL of pure DIH2O. uL of the elution was added to the dried device and run.

6.2.4 - hFlt-1 Gene Sequencing

These plasmids were sent for sequencing with Psomagen; these sequencing results revealed that the prepared plasmids contained the proper sequences when analyzed against known sequences.

6.2.5 - *In Silico* Primer and Oligo Design for hFlt-1 Modification

The first step towards building an sFlt-1 gene was to analyze the hFlt-1 and compare its nucleotide sequence to the nucleotide sequence for sFlt-1. Once the sequences were aligned, the hFlt-1 sequence could be analyzed for the area where the two genes have different nucleotides. This area is the location in which the first primer can be designed. The primer was designed to attach to the shared hFlt-1/sFlt-1 sequence and create an overhang for annealing of the tail end sequence. This overhang was necessary for Gibson assembly. In addition, the team needed to design the tail end of the sequence, otherwise known as the oligo. This oligo matches the 31 amino-acid sequence that is only found on sFlt-1, and necessary for its binding to the anti-sFlt-1 antibody in the sFlt-1 detection method's stabilization complex. Once the oligo was added, the sFlt-1 gene was complete.

Two additional primers were also needed to amplify and clone the PCR product into a mammalian-expression plasmid, pcDNA3.1(+) (pcDNA). This plasmid is a self-contained loop of DNA that allows for the introduction of new genes into cells, to be transduced and translated by the cell's machinery. Once the plasmid housed the sFlt-1 gene, it could be replicated in *E. coli* and then transfected into HUVECs, where the plasmid would induce the formation of sFlt-1

protein. Mammalian expression vectors such as pcDNA (shown in Appendix G) come equipped with additional replication tools that aid in protein production in mammalian cells. These tools include the CMV promoter region, which increases gene expression in mammalian cells. pcDNA contains other necessary tools for gene development, replication, and expression: like an F1 origin site, CMV promoter, and AMP resistance gene. To insert the gene into the plasmid, the team designed complementary restriction sites on the complete gene. When inserting a gene into a plasmid (a process called a 'ligation'), there must be complementary ends to have a kinetically favorable rejoining of the gene (insert) and plasmid (vector). These two additional primers would add complementary restriction sites onto the complete sFlt-1 gene to enable ligation into the pcDNA plasmid.

After designing and synthesizing the primer and oligo, the modification of the hFlt-1 gene could begin. The construct eventually needed to be a linear sequence; however, PCR produces linear segments bounded by primers, requiring the entire plasmid to be used as the template in the PCR reaction and the linear construct produced was later purified out. This PCR reaction was carried out with the Oligo-adding primer and one of the restriction-site adding primers, which added restriction sites onto the 3' and 5' end of the construct. This accomplished three goals:

1. Amplified the shared hFlt-1/sFlt-1 sequence out of the plasmid.
2. Added the overlap necessary for Gibson assembly of the Oligo.
3. Added one of the restriction sites necessary for the future ligation back into a plasmid.

Primer design constituted a large portion of the setup for this experiment. The primers could only be designed after the restriction profile had been completed, in order for the proper restriction sites to be added. Primer design for PCR also needs to follow certain rules: the GC content of the primer should be around 40-60%, the melting temperatures should be relatively consistent and between 50C and 70C, and the primers should be around 20 base pairs long. With three primers to contend with, fulfilling these objectives was difficult. Thankfully, the primers were developed using SnapGene, a program that visualizes DNA and aids in primer design.

SnapGene allows for real-time estimation of melting temperature and provides GC content percentages.

6.2.6 - Initial Primer Design (BamHI & Xbal)

The first primer developed was the forward primer, which added a BamHI site to the 5' end of the start sequence of the hFlt-1 delta CTD gene. The primer and the starting sequence of the gene can be seen in Figure 20 below.

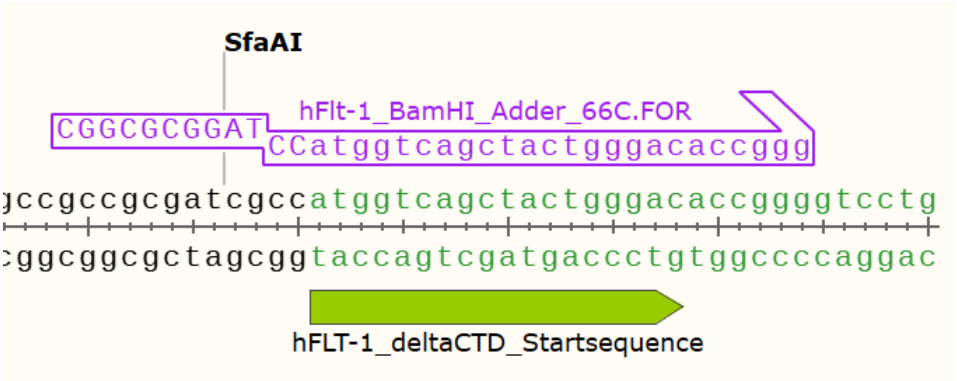

Figure 20 - hFlt-1 delta CTD in plasmid backbone with forward BamHI-adding primer.

The BamHI site sequence added was GGATCC, and is preceded in the primer by a CGGCGC sequence. This extension sequence gives the BamHI restriction enzyme enough bases to connect to in order to begin digestion. This primer had a melting temperature of 66C, a GC content of 69%, and was 36 units long. This was a long primer, but was within most bounds.

The second primer to be designed was the middle primer, the primer meant to replace the transmembrane portion of the hFlt-1 delta CTD gene with the initial 18 bases of the oligonucleotide. This primer caused difficulty, since most of the sequence it bound to consisted of adenosine and thymine, which have weaker interactions than guanine and cytosine. This meant that the primer had to be longer in order to come close to the 66C melting temperature of the forward primer. Primer 2, shown in Figure 21, was instead designed to have reasonable length despite its low melting temperature. In Figure 21, the portion of the DNA similar between sFlt-1 and hFlt-1 delta CTD is shown in green, and the transmembrane portion of hFlt-1 delta CTD is highlighted in red. Primer 2 had a melting temperature of 55C, was 43 units long, and

had a GC content of 37%. Although this primer was different from Primer 1 in terms of length, GC content, and melting temperature, it was good enough to continue PCR with.

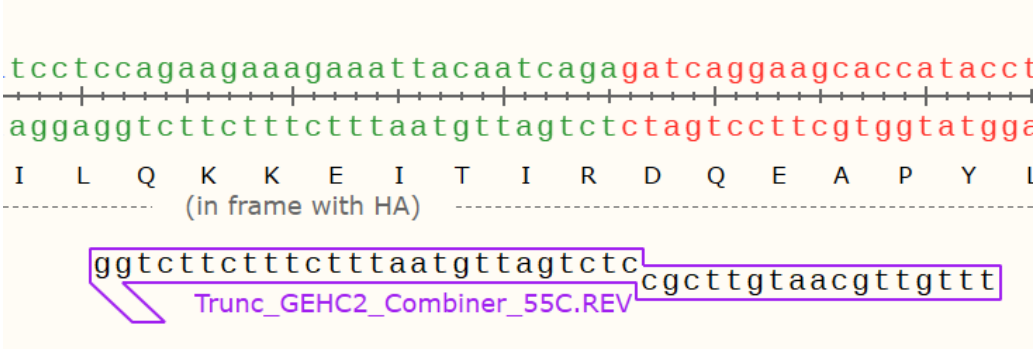

Figure 21 - Primer 2 shown with hFlt-1 delta CTD gene.

The third primer, another reverse primer meant to add an XbaI restriction site to the sFlt-1 construct, was developed shortly after. This primer was long, consisting of 44 base pairs with a GC content of 50% and a melting temperature of 65 C. The primer can be seen in Figure 22. The XbaI site can be seen directly after the end of the GEHC sequence in Figure 22, with a restriction sequence of AGATCT. The CGCCG segment following the restriction sequence provides enough room for the XbaI restriction enzyme to grab onto the DNA and cut.

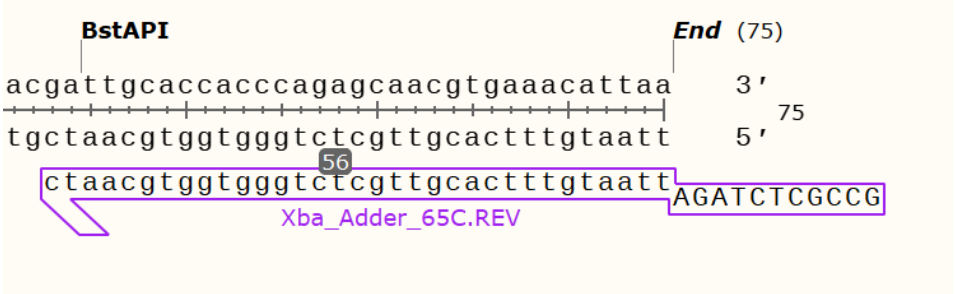

Figure 22 - The 3' end of the GEHC sequence and primer 3.

After the initial PCR, the oligo was mixed with the PCR product to anneal the two pieces of DNA together. This produced a complete sFlt-1 gene, without the second restriction site. This was confirmed by running the resulting annealed product on a DNA agarose gel against the raw hFlt-1 isolated gene. An annealed product lower in molecular weight (MW) than the isolated raw hFTl-1 indicates that the annealed product was made correctly. A second PCR was run to add the second restriction site. This run only utilized the restriction-site adding primers. After this PCR,

the team checked the final product against the annealed product and raw isolated hFlt-1. A final product with slightly higher MW than the annealed product meant that the final product was made correctly.

Once the primers had been designed, they were sent to IDT to be synthesized. The primers were returned as lyophilized DNA, meaning they needed to be reconstituted prior to use. Each primer was resuspended in enough TE buffer to produce a 50uM stock, based on the number of moles of DNA present in the lyophilized sample (indicated on the receipt). These primers were then diluted 10x in TE buffer to form 5 pmol/uL working stocks. The PCR reaction mixture included 18uL of autoclaved DIH2O, 25uL of NEB Q5 High-Fidelity 2x MasterMix (which contained the bases and enzymes necessary for PCR), 2uL of 0.5 ng/uL template DNA (which in this case was the hFlt-1 delta CTD plasmid DNA prepared earlier), and 2.5uL each of Primer 1 and Primer 2, diluted down to their 5 uM working concentrations. This mixture was transferred to a PCR tube and placed in a thermocycler set to the following program: a 30 second single cycle at 98C, followed by 30 cycles of 30 seconds at 98C, 30 seconds at 55C, and 2 minutes at 72C, finished with a 2 minute extension at 72C. The sample was then transferred to a 4C fridge and then to a -20C freezer for longer-term storage.

This sample was then run on a gel to determine if the PCR product was the proper size. 5uL of the PCR product was added to 1uL 6x NEB Purple Gel Loading Dye (6x) and was loaded into a 1% agarose gel. 10uL of a Promega 1 kB DNA ladder was combined with 2uL dye and added to the same gel. This gel was run for 90 minutes at 90 V and viewed on a UV table. This gel can be seen in Figure 23.

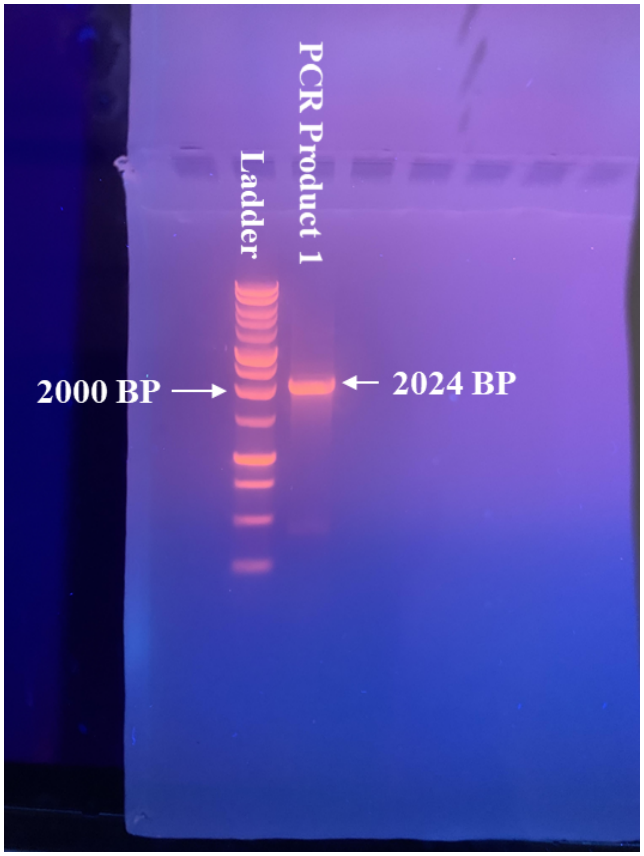

Figure 23 - Gel with PCR product 1 run against 1kB molecular ladder.

Once confirmed, the PCR product 1 was cleaned using a Promega Wizard PCR and Gel Cleaning Kit. The centrifuge method was employed, and the full protocol can be found in Appendix F.

6.2.7 - Final Primer Design (BamHI & ApaI)

The next step was to digest the sFlt-1 construct with BamHI and XbaI (restriction sites on pcDNA). This forms sticky ends on the ends of the sFlt-1 gene to prepare for amplification inside a cell. 14 ul autoclaved DIH2O was added to each, along with 2uL Promega Buffer E and 2uL DNA (sFlt-1). 1uL of BamHI and 1uL of XbaI were added to the tube. This mixture was then placed in a 37C water bath for 1 hour, and then frozen at -20C.

The digestion of the construct produced with the BamHI and XbaI sites produced inconsistent results when run on a 1% agarose gel (see Figure 24). Namely, the digestion resulted in very low percent yield, leading to faint or nonexistent bands on the gel. This unexpected outcome led to the construct being reexamined in silico.

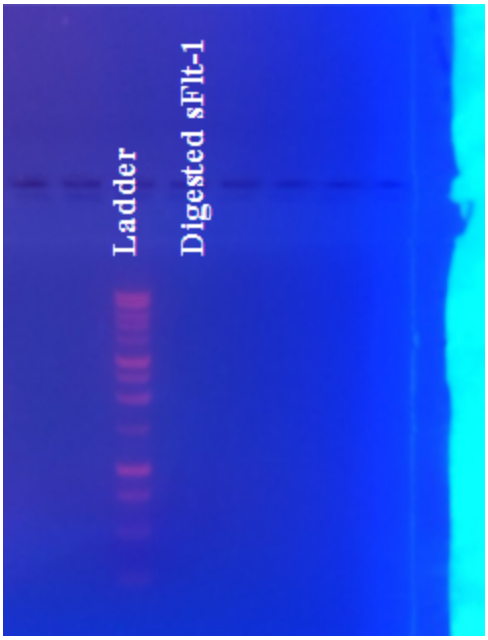

Figure 24 - Digested complete sFlt-1 product ran against a 1 kB MW ladder. The digested sFlt-1 product does not show up on the gel.

Upon review, it was found that there was a second XbaI site present in the construct, 1612 base pairs into the sequence. As it stood, the construct produced had two XbaI sites, which digested the product too much, instead of producing a double digested sFlt-1 that could be inserted into the pcDNA vector. This needed to be remedied, and the restriction profile of pcDNA was studied again, along with the vector map of pcDNA. The restriction enzyme compatibilities were also compared using the Promega restriction enzyme compatibility site (promega.com/resources/tools/retool/). ApaI was chosen as the proper restriction enzyme to replace the XbaI site, and the construct was checked again to ensure that there were no other extra BamHI or ApaI restriction sites. A primer was synthesized in exactly the same way as the XbaI reverse primer, except the restriction site was changed to an ApaI site. The primer can be seen in Figure 25.

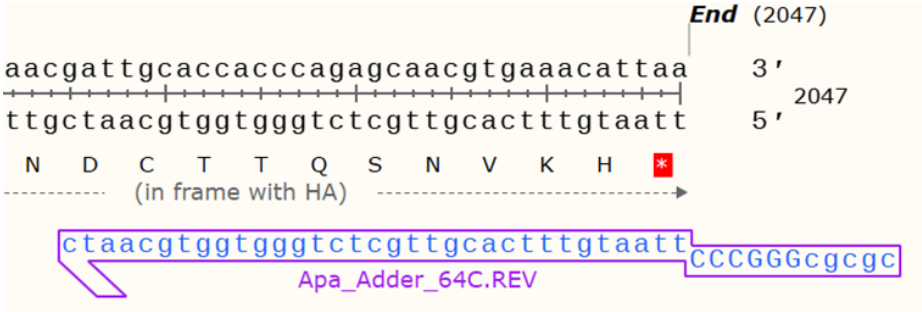

Figure 25 - Primer 3.5, or ApaI restriction site adder, shown with 3' end of sFlt-1 construct.

The primer had a similar composition to the XbaI site adder (Primer 3), and was 44 units long with a GC content of 59% and a melting temperature of 64 C. Once ordered and resuspended in a working concentration (5uM), this primer was combined with an oligo-annealed PCR 1 product and placed in a thermocycler with the same program as previously described.

6.2.9 - Oligo Design

The next sequence to be developed was the oligonucleotide. The oligonucleotide was to be used as a reverse primer to reduce the number of PCR steps necessary, and had to be the reverse complement of the 31 amino acid sequence unique to sFlt-1. This sequence is composed of the amino acid string GEHCNKKAVFSRISKFKSTRNDCTTQSNVKH plus a stop codon at the end. This sequence was converted to bases, as can be seen in Figure 26.

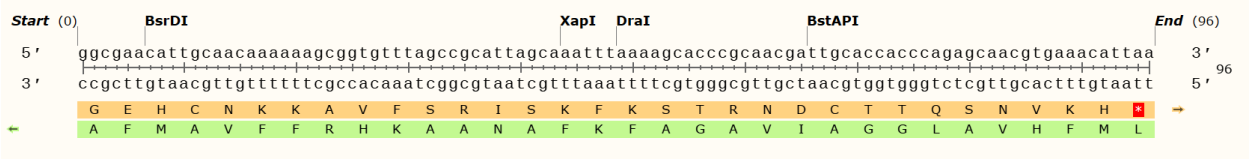

Figure 26 - The 31 amino acid sequence novel to sFlt-1 plus stop codon, translated.

All together, this sequence (referenced in this paper as the GEHC sequence due to the first four amino acids of the sequence) shown in Figure 26 was 96 base pairs long. The reverse complement of the GEHC will henceforth be referred to as the oligonucleotide. The

oligonucleotide was synthesized by an external company, IDT (Integrated DNA Technologies) on December 10, 2021.

In order to fully convert this truncated construct into sFlt-1, the oligonucleotide needed to be annealed to the first PCR product. Since the oligonucleotide needed to be added in a 1:1 mass ratio of PCR product to oligonucleotide, the amount of DNA in the purified product needed to be determined. This was done by running 5uL of the purified product on a gel with a 1kB ladder and imaging the gel, then comparing the brightness of the ladder bands to the brightness of the PCR product band. Knowing the concentration of the DNA ladder band allowed for a relationship between the concentration and the brightness to be developed. The analysis can be seen in Figure 27 and Table 2 below.

Figure 27 - Brightness of gel with ladder and PCR product 1, Analyzed in ImageJ for brightness.

Table 2 - Intensity density of measured bands, analyzed in ImageJ.

Sample ID	Intensity Density (units)	Amount (ng)
Ladder (1.5kB)	1533463	57
Purified PCR Product 1 Sample	1116201	54.19

ImageJ was used to determine the relative amount of DNA in the purified gel. First, the total intensity was calculated for all bands in the MW ladder. Then, the amount of intensity density per ng of DNA was calculated using the ladder as a reference. This calculated the ratio for intensity density/ng of DNA. Using this ratio, the intensity density of the purified PCR product was measured and converted into estimated ng of the DNA.

ImageJ analysis determined that there were 54.19 nanograms of DNA in the purified PCR product, producing a concentration of 10.8 ng/uL. Diluting 1uL of the 50uM oligonucleotide stock in 82uL of TE buffer produced a concentration of 36.13 ng/uL. 2uL of this working stock contained 72ng of oligonucleotide DNA. Since 72 cannot be evenly divided by 10.8, it was decided that 6uL of 10.8 ng/uL PCR product (64.8ng total) would be combined with 72ng oligonucleotide.

This annealing was carried out by combining the 6uL PCR product and 2uL oligonucleotide in a PCR tube. A heat block was set to 95C, however the highest temperature reached was 91.8C. This was acceptable, as the temperature was still high enough to denature the DNA. The tube was placed in this block for 5 minutes, and then the entire block was removed from the heating apparatus and left to passively cool on a benchtop. This process initially denatures the double stranded target (the PCR product), opening up the bases for the oligonucleotide to anneal to. The annealing occured as the block slowly cooled. Once the block reached 40C, the tube was removed and placed in a 4C fridge. Once annealed, the PCR product and the oligo formed the complete sFlt-1 construct.

The final step in the process involved amplifying the sFlt-1 construct while adding an XbaI site to the 3' end. This was achieved through PCR. First, 16uL autoclaved DIH2O and 25uL Q5 MasterMix were combined in a PCR tube. 4uL of the oligo-annealed construct were added to this mixture along with 2.5uL of Primer 1 and 2.5uL of Primer 3, each diluted to 5uM working stock. This tube was then placed in a BioRAD MyCycler Thermocycler for the same program as described earlier. Once the reaction had finished, the tube was tested on a nanodrop, which indicated that the reaction mixture contained 222.4 ng/uL sFlt-1 DNA.

The next step was to digest the sFlt-1 construct with BamHI and ApaI (restriction sites on pcDNA). This forms sticky ends on the ends of the sFlt-1 gene to prepare for amplification inside a cell. 14 ul autoclaved DIH2O was added to each, along with 2uL Promega Buffer E and

2uL DNA (sFlt-1). 1uL of BamHI and 1uL of ApaI were added to the tube. This mixture was then placed in a 37C water bath for 1 hour, and then frozen at -20C.

6.3.0 - pcDNA Preparation for sFLt-1 Amplification

During sFlt-1 production, a stock of a separate plasmid was procured in order to have a vector to clone the constructed sFlt-1 into. This new vector, an edited pcDNA plasmid, was chosen since it was available in the lab, contained the proper cassettes for mammalian expression, and it contained a luciferase gene that could be used to determine if the cloning region of the plasmid was intact. A complete vector map of pcDNA can be found in Appendix E.

Similar to hFlt-1 propagation, a new strategy to propagate the plasmids was developed due to the lack of monoclonal colonies produced using the plate streaking method. This strategy involved inoculating the bacteria from the pcDNA stock into liquid cultures of varying antibiotic concentrations. Liquid cultures with the highest optical density and highest antibiotic concentration would be chosen to prepare plasmids from. This method produces monoclonal colonies through the use of high amounts of antibiotic; the point of this method is to use enough antibiotic to kill any non-plasmid-transformed *E. coli* while allowing the transfected *E. coli* to slowly propagate and react to higher concentrations of antibiotic. Since pcDNA contains an Ampicillin resistance gene, Ampicillin tubes were used for pcDNA cultures. Before the tubes could be prepared, the pcDNA needed to be transformed into available cells and plated. A set of 1X Ampicillin plates (AMP) were prepared for use in propagating pcDNA. One tube of 50 uL L200B JM109 *E. coli* and one tube of plasmid (pcDNA 3.1) were thawed on ice. 2uL of the plasmid was added to the thawed cells and this mixture was incubated on ice for 15 minutes. The tube was then heat-shocked in a water bath set to 42C for exactly 1 minute. This step causes the cell walls of the *E. coli* to break apart, allowing plasmids and other DNA to enter the cells. Following heat shock, the bacteria were returned to ice for 2 minutes. 450uL LB media were added to the bacteria to help the cells recover, and this mixture was placed on a rotator in an incubator at 37C for 1.5 hours. At the same time, an AMP plate was warmed in an incubator upside-down. A pasteur pipette was sterilized, sealed, and bent using a Bunsen burner. After the 1.5 hour recovery, 150uL of the pcDNA transformed JM109 cells were pipetted onto the plate and spread with the pasteur pipette. The remaining 350uL of transformed *E. coli* were moved to

a 4C fridge. This plate was then incubated for 16 hours, at which time it showed few monoclonal colonies of transformed *E. coli*.

Tubes were prepared according to Table 3 below for the antibiotic experiment. These tubes were prepared with LB media and 1000x antibiotic stocks.

Table 3 - Amounts of LB media, antibiotic, and cells added to form a liquid culture for the propagation of *E. coli* containing pcDNA plasmids.

Sample ID	Tube #	LB Media (mL)	Cells	Antibiotic Strength (x)	AMP (uL of 1000x)
LB Media Control	0	4	NONE	0	-
AMP Cell Control	A0	4	AMP Resist	0	0
AMP 1x	A1	4	AMP Resist	1	4
AMP 2x	A2	4	AMP Resist	2	8
AMP 3x	A3	4	AMP Resist	3	12
AMP 5x	A5	4	AMP Resist	5	20
AMP 10x	A10	4	AMP Resist	10	40
AMP 20x	A20	4	AMP Resist	20	80

4uL of the transformed *E. coli* containing pcDNA were added to each of the Ampicillin tubes. These tubes were then transferred to an incubator-shaker set to 37C and a shake rate of 200 RPM, which is standard for *E. coli*. The tubes were checked after 20 hours and were observed to have low turbidity. The tubes were left to incubate for 21 more hours for a total of 41 hours before they were removed from the incubator and placed in a 4C fridge.

Tubes containing 5x antibiotic were chosen to be prepped for plasmids due to their high antibiotic concentration and relatively high turbidity.

The plasmid preparation was carried out using a Promega PureYield Plasmid Miniprep kit and system. The protocol for this kit can be found in Appendix E. Three ml of each 5x antibiotic culture tube was prepped. The pcDNA plasmid elution was measured at a concentration of 106.1 ng/uL using a nanodrop. The nanodrop was turned on and blanked using 1uL of pure DIH2O. uL of the elution was added to the dried device and run.

Before the pcDNA could be used for any restriction, it needed to be tested to see which restriction enzymes had been cut out during the insertion of luciferase. A range of restriction enzymes at different points in the multiple cloning region (MCR) of pcDNA were chosen to analyze. The sites chosen were BamHI, EcoRI, EcoRV, NotI, XhoI, XbaI, and ApaI. BamHI in particular was chosen as the enzyme to compare reaction efficiency to, since the sequencing results revealed an intact BamHI upstream of the luciferase gene. This way, the only enzymes that needed to be tested were the enzymes that followed BamHI on the MCR. These enzymes were checked on the Promega restriction enzyme tool site to determine their best buffers and to see if the enzymes had star activity. The results of this analysis can be seen in Table 4 below.

Table 4 - Restriction enzymes and their reaction efficiency in various buffers.

		RE Buffer:							
		A	**B**	**C**	**D**	**E**	**Multicore**	**Best Buffer To Use:**	
Enzyme:	**BamHI**	X	75-100	75-100	50-75	100	75-100		
	EcoRI	25-50	50-75	50-75	50-75	100	100	**E**	
	EcoRV	10-25	25-50	50-75	100	X	100	**Multicore**	
	NotI	<10	10-25	25-50	100	X	25-50	**D**	Slowest
	XhoI	25-50	75-100	75-100	100	X	10-25	**B or C**	
	XbaI	50-75	75-100	75-100	100	X	100	**Multicore**	
	ApaI	100	50-75	50-75	X	X	75-100	**Multicore**	

Restriction digests were carried out in 20 uL reactions, consisting of 14 uL autoclaved DIH2O, 2 uL of the appropriate buffer, 2uL of pcDNA, and 1uL of each restriction enzyme. Once combined, each reaction tube was cooked in a 37C water bath for 60 minutes. Once digested, each tube was run on a 1% agarose gel for 90 minutes at a constant 90 volts along with a molecular weight ladder. Reaction tubes that dropped out bands indicated that those two enzymes (BamHI and the tested enzyme) flanked the luciferase gene and could be used to clone in sFlt-1. The planned reactions are summarized in Table 5 below.

Table 5 - Reaction volumes for restriction profiling of pcDNA.

Table 1: Enzyme Reaction Summary							
Sample ID		EcoRI	EcoRV**	NotI*	XbaI	XhoI**	ApaI
Trusty dH2O		14	14	14	14	14	14
Buffer	B					2	
	C					2	
	E	2			2		
	Multicore		2				2
	D			2			
	H			2			
pcDNA 3.1		2	2	2	2	2	2
Restriction Enzyme	BamHI	1	1	1	1	1	1
	EcoRI	1					
	EcoRV		1				
	NotI			1			
	XhoI				1		
	XbaI					1	
	ApaI						1
Incubation Time (37C Water Bath)		60 min					
Buffer Coactivity (BamHI/RE)		100/75	75/100	50/100	100/100	75/75	75/75

*RE buffer combo has low (below 75%) coacvitiy
**RE buffer combo is better w/ NEB buffers (see Table 2)

Notes:
Used this (https://www.promega.com/resources/tools/retool/) to find buffer coability
If there's two buffers listed, that's just because you can use either, they have the same coacitivity
So, BamHI and NotI don't really have great compatability. The best option is Buffer D or Buffer H (50/100 Coactivity)
Most numbers are in uL - excel gets upset when I try to do some fancy stuff so we can still do math + keep units

Table 2: NEB Buffer Compatability						
Sample ID	EcoRI	EcoRV	NotI	XbaI	XhoI	ApaI
NEB Buffer	n/a	r3.1	r3.1	r3.1	r3.1	n/a
Buffer Coactivity (BamHI/RE)	n/a	100/100	100/100	100/75	100/100	n/a

*Only listed ones that are "better" than the promega buffers

Due to the low reaction efficiency of NotI and the lack of available EcoRV, the only restriction digests run with BamHI were EcoRI, XbaI, XhoI, and ApaI. The restriction profiling results, which can be seen in Figure 28 below, revealed that all of the enzymes dropped out similar-sized bands, indicating that they all were downstream of the enzyme used to insert luciferase into the vector and as such were available for cloning. However, the EcoRI digest resulted in a few more digestion bands, and as such it was ruled out as a useful cloning enzyme. XbaI, therefore, was chosen as the 3’ restriction site in addition to the BamHI 5’ restriction site.

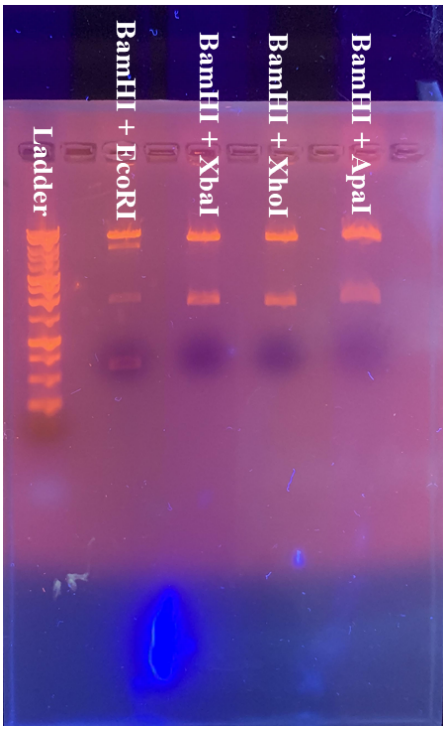

Figure 28 - Restriction profile of pcDNA.

pcDNA was digested with both BamHI and ApaI to both ensure that both sites were active and available, and also to prepare for insertion and ligation. The plasmid was digested three ways- once with just BamHI, once with just ApaI, and a third time with both enzymes. Ideally, the two single-enzyme digestions would create the same-length band (due to pcDNA being broken in only one place) and the double digest would drop out the luciferase gene. Each reaction was run in 20uL volumes, with either 15uL water, 2uL Buffer E, 2uL pcDNA, and 1uL enzyme for the single-enzyme digestions or 14uL water, 2uL Buffer E, 2uL DNA, and 1uL each ApaI and BamHI for the double digest. These vials were incubated at 37C for 1 hour before being run on a standard 1% agarose gel to determine if the sites were active. Upon determination that the sites were available, the vector was transformed into JM109 E. coli for propagation, and inoculated overnight at 37C in 1x Ampicillin LB media. These transformations and inoculations were plasmid-prepped and nano dropped to check their concentrations, which can be found in Table 6. These tubes were then used for all future pcDNA digestions.

Table 6 - A table of concentrations of several vials of plasmid-prepped pcDNA.

Vial Number, pcDNA Plasmid	Concentration (ng/ul)
1	34.8
2	35.1
3	126.2
4	118.9
5	91.8
6	84.5
7	31.1
8	102.7

Due to the small fragments that contain sticky ends produced during restriction digestion, the digestion products could not just be cleaned using a PCR clean-up kit. The digestion product first had to be run through a 1% agarose gel to separate out the sticky-ended digestion product. These bands had to then be excised from the gel and dissolved and cleaned to finally extract the digestion product. All gel cleanings were carried out using a Promega Wizard PCR and Gel Clean-Up Kit. Both the pcDNA and sFlt-1 vector and insert were cleaned using the kit following digestion. The protocol for the cleaning can be found in Appendix G.

6.3.1 - Preparing sFlt-1 for Amplification of sFlt-1 Production

Following the formation of a complete sFlt-1 gene, the team needed to ligate the gene into the pcDNA plasmid. This involved cutting both plasmid (pcDNA3.1) and the insert (complete sFlt-1 gene) with their respective restriction enzymes. These enzymes were specifically cut (also known as digest) at their restriction sites. Once both insert and vector were digested, they could be ligated together in a ligation. This involved using an enzyme called a ligase, which helps anneals two pieces of DNA together. After ligation, the complete sFlt-1 gene was a plasmid, henceforth referred to as the sFlt-1 plasmid, and ready to replicate inside HUVECs, the appropriate cell for sFlt-1 protein production.

Before the sFlt-1 plasmid can be transformed into HUVECs, the amount of plasmid needed to be duplicated. This is because transformations (the insertion of DNA into mammalian cells) are very inefficient and need a large amount of plasmid to work. To create replicates of the plasmid, the sFlt-1 plasmid needed to be transformed (have their DNA inserted into bacterial cells) into chemically competent *E. coli* cells (ex. JM-109, DH5alpha) that are specifically designed to replicate plasmid DNA at high copy numbers. The first step in a transfection is to insert the plasmid DNA into the cells. Then, one can select for cells that have taken in the plasmid by growing the cells in environments with Ampicillin, an antibiotic. Since the sFlt-1 plasmid had an Ampicillin resistance gene, cells that take in the DNA would grow in the presence of Ampicillin. A cell colony grown in the presence of Ampicillin suggests that the cell colony was positive for the sFlt-1 DNA. These colonies needed to be verified using sequencing since random mutants can form that are resistant to the target antibiotic that do not contain the proper plasmids or constructs. This colony was isolated and allowed to grow in liquid culture until turbid. After reaching a high enough turbidity, the plasmid DNA was purified from the cells through plasmid purification kits. This left the team with a greater amount of purified sFlt-1 plasmid DNA.

Once the proper linear construct of sFlt-1 was created and it was verified that the pcDNA contained the proper restriction enzyme sites, the next step was ligation. This ligation would involve the introduction of the two cleaned double-digested fragments (sFlt-1 insert and pcDNA vector) to one another along with a T4 DNA ligase in a ligation buffer. Ideally, this would insert the linear sFlt-1 sequence into the vector and connect the two enabling the vector to carry the construct. This setup was attempted multiple times, and each time the ligation failed. A new setup was then employed, this time using a strategy known as in-gel ligation. In-gel ligation refers to ligations performed by excising and combining double-digested inserts and vectors run on low-melt agarose gels. In-gel ligations are generally more effective for difficult ligations, since the gel forces the DNA to interact, according to A. Furtado, 2014. The sFlt-1 and pcDNA were subsequently digested with ApaI and BamHI and run on a low-melt agarose gel. The bands were excised and combined in a microcentrifuge tube with the proper amount of ligase and buffer.

Once the ligations had run their course, the products were transformed into JM109 *E. coli* and plated on AMP plates. Several controls were also transformed and plated to diagnose any

issues with the ligation. Positive controls included undigested, unligated pcDNA, which was expected to form a lawn once transformed. This test was performed to ensure that the plates could safely grow Ampicillin-resistant bacteria. A second test involved ligating the luciferase band cut out of pcDNA during the digestion back into the pcDNA backbone. This test was carried out to see if the ligase worked at all and if the restriction sites could support re-ligation. A third control, which was a negative control, involved ligating cut pcDNA into JM109s. This control should not have produced any colonies, and served as an indicator of contamination or unexpected products. Finally, the test cases were ligated, transformed and plated; these test cases consisted of digested sFlt-1 ligated with digested pcDNA. Ideally, this test plate would produce pickable colonies that could be inoculated into liquid cultures and plasmid prepped. After plating, it was observed that the uncut pcDNA control did indeed produce a lawn, and the negative control produced no colonies, but both the relegation of luciferase control and the ligation of sFlt-1 into pcDNA produced no colonies. This indicated that the ligase was either degraded or the ATP in the buffer necessary for ligation had degraded. This test was attempted multiple times, with varying ligases and buffers. Colonies were never able to be produced for the ligation. However, it is important to mention that no ligase was used that was not past its expiration date.

6.3.2 - Final Steps in Producing an sFlt-1 Protein Stock

Unfortunately, due to various complications and time constraints, the team was not able to continue with the production of a stock of sFlt-1. As a result, this subsection will instead detail the planned next steps in establishing a reliable stock of this protein. Following the generation of a stock of sFlt-1 plasmid DNA, the team would transfect HUVECs. The HUVECs would need to be prepared to the correct confluency before undergoing a transfection. After transfection, the HUVECs would start to produce synthetic sFlt-1 in the cell media. This is because sFlt-1 is a soluble protein and is known to be secreted by endothelial cells, although the secretion pathway is poorly understood (Jung, et al., 2012). After protein production, purifications and quantifications of sFlt-1 would quantify the concentration of sFlt-1 in stock solutions, allowing for artificial environment testing to begin.

Early on, it was established that sFlt-1 was only expressed and secreted by specific endothelial tissues. Zhai, et al., determined in 2020 that sFlt-1 could be expressed by human

endometrial tissue or by human umbilical vein endothelial cells (HUVECs). While neither cell line was cheap to purchase, Will DeMaria and Claire Joswiak from the Rolle lab at WPI were able to supply a frozen stock of passage 4 HUVECs. A growth and media kit (ATCC, Manassas, VA) was purchased for the propagation of the HUVECs, and bovine brain extract was chosen as a growth accelerator instead of VEGF to prevent VEGF binding to any produced sFlt-1. Once the media had been assembled and aliquoted, one 1 million cell vial of the frozen HUVECs (1mL) was reconstituted in an additional 5mL of complete HUVEC media in a T25 flask. After 1 day, the flask was rinsed with 5mL dPBS (-) and 6mL fresh media was added. The cells were left until 80% confluent, which took 3 days, in a 37C incubator. At this point, the cells were trypsinized and passaged into three flasks, with two flasks seeded with 1/6th of the cells each and the final flask being seeded at ⅔. These cells were fed every 2 days and passaged at 1/6th when they reached 80% confluency, usually every five or six days. Although the cells were never used for transfection, as a construct was never developed, these cells were kept healthy and fed in the eventuality they were required.

6.4.0 - Detection Method - Subcomplex 1

The detection of sFlt-1 in solution depends on a two-stage biochemical complex assembly that creates a stack of proteins that couple sFlt-1 molecules to both the device and to an alkaline phosphatase (ALP) enzyme. The first complex in this stack of molecules focuses on binding to both the device itself and to sFlt-1. Complex 1 consists of a magnetic bead (Dynabeads, as purchased from Thermofisher) coated in protein A/G. Protein A/G binds non-selectively to the heavy chains of antibodies, allowing for diverse antibody coupling. An anti-sFlt-1 antibody, purchased from US Bio, was then conjugated to this protein-coated bead. This antibody was a polyclonal antibody produced in rabbits that targeted the C terminus region of sFlt-1 (the novel 31 amino acid sequence).

6.4.1 - Detection Method - Subcomplex 2

The second complex is used to conjugate an alkaline phosphatase molecule to each sFlt-1 molecule. This complex is composed of VEGF conjugated to ALP. Ideally, these two proteins can be combined through a one-step glutaraldehyde coupling. One-step glutaraldehyde is a method used to conjugate (or “stick”) proteins and antibodies together, but can be extended

towards conjugating antibodies and other proteins to AP (Warren, 2005). Although the exact mechanism is unknown, when glutaraldehyde reacts with amino and thiol groups found on proteins, they become very reactive and prone to chemical bonding with other functional groups (Migneault, et al., 2004). This reactivity and chemical bonding eventually leads to proteins chemically "sticking" together. In preparation for protein coupling, the team made several buffers and reagents necessary for the reaction. These reagents included: modified PBS (20 mM sodium phosphate buffer, pH 7.2, containing 0.15M NaCl), 50mM Tris-HCl buffer (pH 7.5, containing 1mM MgCl2, 0.02% w/v NaN3, 2% w/v bovine serum albumin), and a 1% v/v glutaraldehyde solution. Despite having the materials ready, the team was not able to complete the coupling reaction to test the validity of a VEGF-AP detector complex for sFlt-1 detection. This is due to scheduling conflicts and results from the isolated AP test.

6.5.0 - Device Testing

In order to determine if alkaline phosphatase could be used to detect sFlt-1 in a 1:1 molar ratio at the low concentrations it is present in urine in, a preliminary test was run. This test involved diluting isolated AP to the concentrations found in endometriosis-positive and endometriosis-negative patients, corrected for creatinine in the 20-300 mg/dL range. This AP was tested without coupling it to any proteins or antibodies. The standard levels of creatinine were also tested with the Jaffe reaction and run on a spectrophotometer to determine their absorbances.

6.5.1 - Device Testing - Jaffe Reaction

First, a standard curve of creatinine was created, with concentrations of 300 mg/dl, 150 mg/dL, 75 mg/dL, 37.5 mg/dL, and 18.75 mg/dL. This standard curve contained the standard range of creatinine found in urine of individuals prone to endometriosis, which is 20 to 275 mg/dL (Eng, 2021).

The creatinine reaction tubes were prepared by combining 1 ml creatinine solution, 1 ml 1% w/v picric acid, and 2mL 0.5N NaOH in a 15mL centrifuge tube. These solutions were left to incubate at room temperature. Figure 29 shows the results of a 72 hour incubation at room temperature.

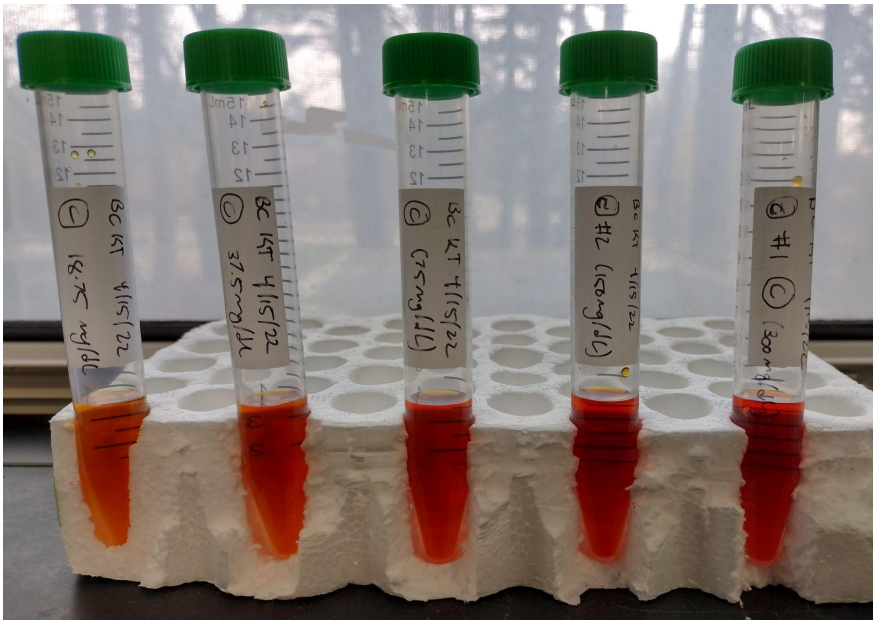

Figure 29 - The Jaffe reaction at varying concentrations of creatinine after 72 hours incubation.

Following incubation, the reaction tubes were run on a spectrophotometer to determine absorbance. The Janovsky complex vials were too concentrated to be measured on the spectrophotometer as they were. In efforts to address this, the samples were diluted 8x in dH2O before being measured at 483nm. The results can be seen in Table 7 below.

Table 7 - A table of absorbance values of 1:8 dilutions of sample tubes after a 72 hour incubation. at 483 nm.

Creatinine (diluted 1:8)	
Sample ID	**ABS (483 nm)**
300.00 mg/dL	0.545
150.00 mg/dL	0.424
75.00 mg/dL	0.322
37.50 mg/dL	0.269
18.75 mg/dL	0.18
Blank (NaOH, Picric Acid)	0

These absorbance readings were graphed in Figure 30, and the curve indicates that the absorbance readily changes with concentration.

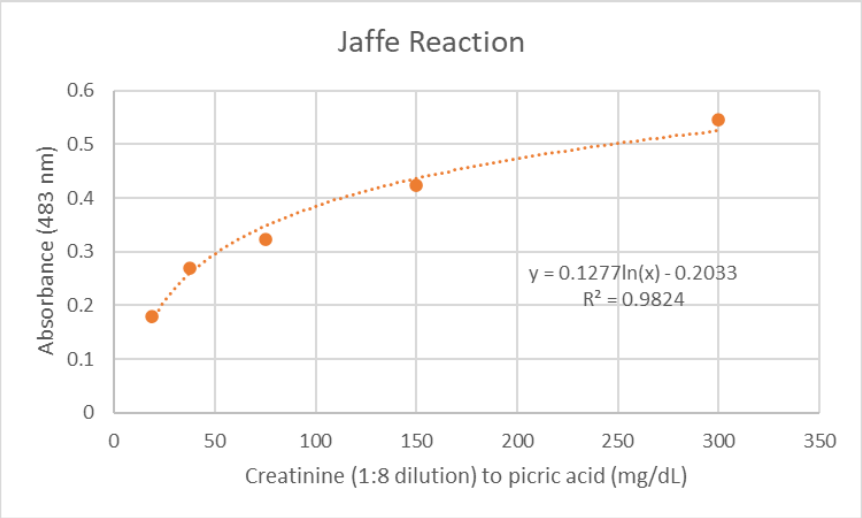

Figure 30 - Absorbance values of the Janovsky complex at 483nm vs. varying concentrations of creatinine.

Figure 30 shows that the absorbance levels relative to the amount of creatinine within the samples are distinguishable for a quantitative reading. Even after a 1:8 dilution, the absorbance values read relatively high.

6.5.2 - Device Testing - sFlt-1 Reaction

The amount of sFlt-1 indicative of endometriosis positive and negative cases was calculated based on the Cho, et al., finding. This was converted to moles and then used to determine the mass of alkaline phosphatase necessary to mimic a 1:1 molar ratio of sFlt-1 to AP for each case. Mass of AP needed was calculated using a Bradford Assay to determine the concentration of AP supplied. The calculations can be found in Table 8 below.

Table 8 - A table containing the standard curve of creatinine, amount of sFlt-1 (indicative of positive and negative individuals), and mass of AP necessary to mimic the moles of sFlt-1 in a sample.

Creatinine concentration (mg/100 mL)	sFlt-1 negative cases, average (pg/100 mL)	sFlt-1 positive cases, average (pg/100 mL)	sFlt-1 negative cases, average (pg AP/100 mL), using AP as sFlt-1 analog	sFlt-1 positive cases, average (pg AP/100 mL), using AP as sFlt-1 analog
300	78	162	95.6	198.65
150	39	81	47.8	99.32
75	19.5	40.5	23.9	49.66
37.5	9.75	20.25	12.0	24.83
18.75	4.875	10.125	6.0	12.42

These calculations were based off the knowledge that sFlt-1 concentrations in negative cases are between .2 and .32 pg/mg creatinine, and sFlt-1 concentrations in positive cases are between .45 and .63 pg/mg creatinine, as indicated by Cho, et al., 2007. 1mL of each of these concentrations of AP were combined with 1mL of BCIP/NBT substrate, where 1 tablet of BCIP/NBT had been dissolved in 10mL DIH2O. A final tube of AP was prepared at a 1:100 ratio, with a concentration of AP of 7 E11 pg/uL. This tube was combined with BCIP/NBT in the same way. These solutions were left to incubate for 72 hours. As can be seen, only the 1:100 AP tube produced any noticeable blue coloring, even after this long time. Figure 31 shows the reaction vessels after a 72 hour incubation.

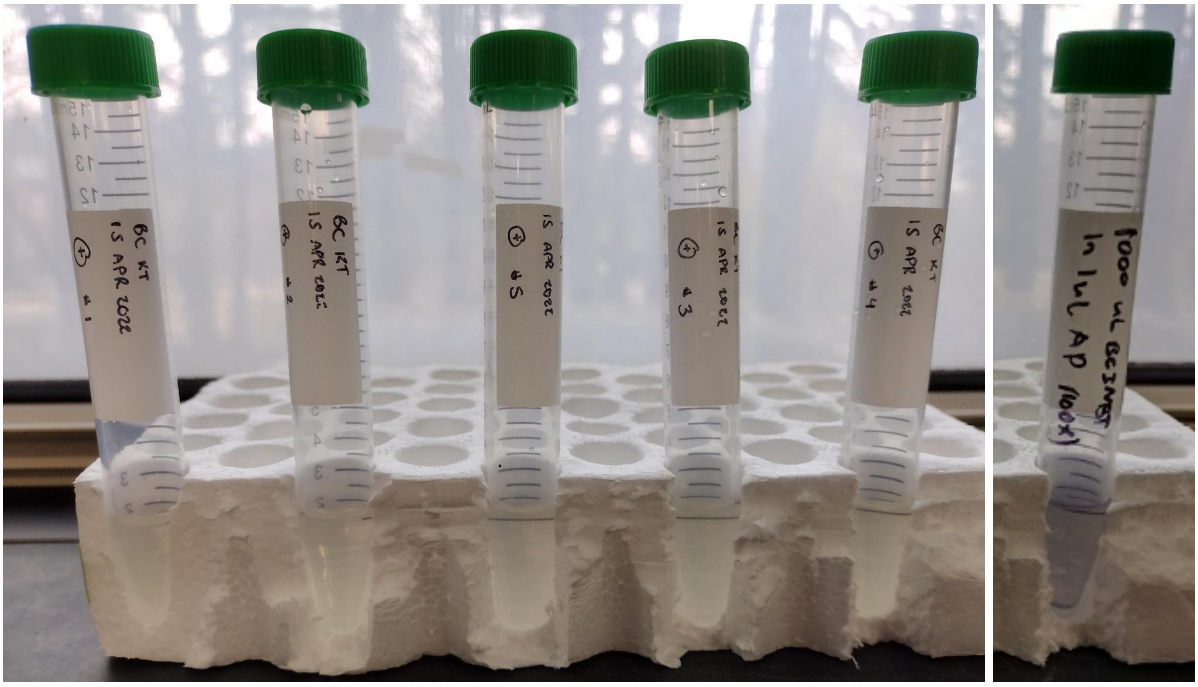

Figure 31 - Varying concentrations of AP mixed with BCIP/NBT, after 72 hours incubation.

The AP reaction was run at both 490 and 590 nanometers wavelength in a spectrophotometer to cover the range of BCIP/NBT absorbance wavelengths (Sigma-Aldrich, 2014).The absorbance values can be seen below in Table 9.

Table 9 - A table of absorbances of each AP tube at 490nm and 590nm.

Alkaline Phosphatase		
Sample ID	**ABS (490 nm)**	**ABS (590 nm)**
162.00 pg/mL	0.007	0.006
81.00 pg/mL	0.005	0.003
40.50 pg/mL	0.003	0.002
20.25 pg/mL	0.003	0.001
10.13 pg/mL	0.004	0.002
78.00 pg/mL	0.006	0.003
39.00 pg/mL	0.003	0.003
19.50 pg/mL	0.003	0.003
09.75 pg/mL	0.002	0.001
04.88 pg/mL	0.011	0.009
100x (16,200.00 pg/mL)	0.037	0.052
Blank (BCIP/NBT)	0	0

Since the limit of detection of this spectrophotometer is ±0.003 A from 0.0 to 0.3A, it can be stated that almost none of the readings were above the limit of detection, and therefore were unusable. However, since the 100x tube produced both spectrophotometric and visual readings, it was determined that the molar ratio of sFlt-1:AP had to be increased before the test could accurately pick up endometriosis. These values were plotted with absorbance at each wavelength vs. the concentration of AP in each vial for the 490 nanometer wavelength. This plot can be seen in Figure 32 below.

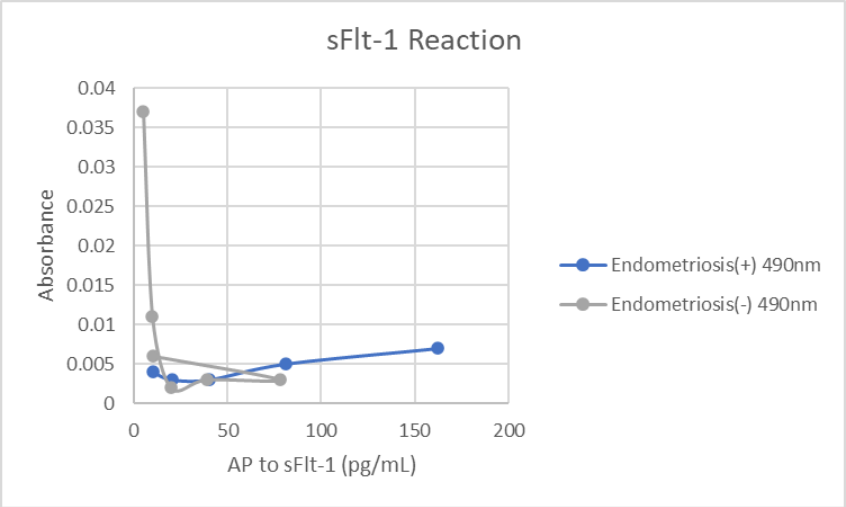

Figure 32 - Absorbance values of AP-reacted BCIP/NBT after 72 hour incubation vs. concentration of AP at 490 nm.

Figure 32 shows that the absorbance levels relative to the amount of AP within the samples are very small even for a quantitative reading. It is very difficult to distinguish the absorbance values for endometriosis positive and negative samples.

6.6.0 - Ethical Considerations

When creating new medical devices, technologies, and treatments, an invention's impacts must be carefully identified and considered. As a result, the team examined the impacts this device may have on economics, the environment, society, politics, its ethical concerns, its healthy and safety concerns, its manufacturability, and its implications in sustainability.

6.6.1 - Economics

As previously described, endometriosis is a notoriously debilitating condition. Many of its commonly available diagnostic methods are largely inaccessible due to their invasiveness, the physical and mental discomfort they pose to a patient, and the high cost associated with pursuing a diagnosis and medical treatment. A small single use device consisting of several commonly available materials, 3D printed filament, cuvettes, magnets, amongst other previously discussed materials, should be relatively inexpensive to produce and distribute. As a result, this would ideally reduce the projected cost to healthcare providers, insurance providers, and patients, when

compared to more intensive methods such as laparoscopic surgery, transvaginal ultrasounds, and pelvic exams. For example, the gold standard, diagnostic laparoscopic surgery typically costs an insured patient 4,852 USD (Soliman, et al., 2015). For an MQP team at WPI, start up costs for developing all aspects of this device, especially for developing the novel sFlt-1 detection assay, were a costly initial investment, however to a large company capable of manufacturing all materials from sources in house, prices would shrink greatly, especially with a reliably maintained culture of sFlt-1 secreting cells.

A review from 2015 examined the cost of endometriosis posed to individual patients as well as nations. When examining direct and indirect costs, estimated societal annual costs for endometriosis were found to be: $1.26 billion in Denmark, $14.63 billion in Italy, and $78.05 billion in the USA (Soliman, et al., 2015). Bearing in mind these costs, it's clear that endometriosis poses a severe cost to individuals and to countries globally. Introducing a cheaper diagnostic method could be the first step in reducing the cost of care for individuals who suspect they have or do have endometriosis.

6.6.2 - Environmental Impact

With single use devices, like the one developed in this paper, waste and its environmental impact is a major concern. The main housing was 3D printed at WPI, and would likely continue to be made of plastic. In addition to the device housing, single use cuvettes were included and installed internally. The medical field has historically struggled with cutting back on single use plastics due to the strict requirements to maintain sterile environments with various equipment, such as syringes.

Additionally, this device relies on the utilization of picric acid, a highly volatile chemical. If stored improperly and left to oxidize, picric acid can become highly combustible. These chemicals must be properly disposed of following handling. Proper storage, handling, and disposal is needed for the components of the biomarker detection methods. Picric acid and NaOH solutions must be disposed of according to guidelines set by the workplace and governmental environment, health, and safety department. These protocols will not have to be new or developed in response to the introduction of this device, as most places handling testing will already have procedures and protocols for handling previously mentioned

chemicals.Samples containing any trace of patient urine must be disposed of in biohazardous waste.

6.6.3 - Societal Influence

Healthcare for individuals assigned female at birth has been historically underfunded and under researched, with many tools and methods having been around for centuries with little to no alterations made in recent years, such as speculums which resemble their early counterparts from the 1800s (Horwitz, 2019), despite the negative impact they pose to a patient's mental and physical health. In the USA alone, women were more likely to report healthcare access issues than men, with young women and black women specifically having higher rates of healthcare disparities (Daher, et al., 2021). More specifically, women under the age of 45 years cited abnormally high rates of delay in access to healthcare, inability to see a doctor due to cost, and cost-related medication non-adherence (Daher, et al., 2021). This issue is made even more concerning when considering that women reported higher rates of medical coverage when compared to their male counterparts (Daher, et al., 2021).

In early stages of developing this device, the team was able to speak with a wide range of individuals. One on one interviews and discussions with patients medically confirmed to have endometriosis expressed excitement at the potential of a fast, inexpensive, accessible, and non-invasive test to diagnose endometriosis via urinalysis. Talks with medical professionals led to offers of support to see this device through to completion by any means necessary, as professionals were excited by the prospect of a new objective method to diagnose endometriosis. Conversely, talks with a select few individuals highlighted the lack of knowledge surrounding healthcare for individuals assigned female at birth, asking why individuals should care if the research in the women's healthcare sector has been historically lacking. Having previously met with countless individuals of varying backgrounds voicing support of the device concept, the team ultimately felt that continuing the research and development of this device was not only necessary, but would be a disservice to the targeted audience if research halted.

6.6.4 - Political Ramifications

Endometriosis is a condition that impacts individuals globally. The creation, manufacturing, and distribution of this device could drastically shift a global approach to

diagnosing endometriosis, and in turn, a global approach to more comprehensive and accommodating healthcare for individuals who were assigned female at birth. Limiting barriers that impede access to treatment can be the first step in de-stigmatizing conversations surrounding pelvic health. By increasing access to a diagnosis of endometriosis, more individuals could finally have a reason for the debilitating pain and other symptoms they may experience. Doing this would grant these individuals access to the necessary resources and accommodations to improve their quality of life while also increasing their chance of encountering individuals who know of the condition and can empathize with them and their struggles. Following diagnosis and subsequent treatment, these individuals may begin to feel physically and mentally better, allowing them to enter/re-enter the workforce and other spaces, such as political ones, which could drastically change workplace environments and political policies with the inclusion of more assigned female at birth individuals. Cultural and societal views may alter and shift to be more inclusive of individuals struggling with chronic pain, “invisible illnesses”, individuals struggling with fertility, etc.

Reproductive, sexual, and pelvic health have traditionally been deeply stigmatized across many cultures, especially when addressing menstruation. For some cultures, this stigma is rooted in religious and cultural practices. For example, Nepali Hinduism prohibits menstruating women from entering a temple or a kitchen, from sharing a bed with their partner, or to touch a male relative (Crawford, et al., 2014). Although this is only one example, it provides insight to the potential struggles linked to cultural practices that may contribute to the stigmatization of menstruation and related pelvic health. Although some views and practices have since shifted in response to a rapidly changing society linked to industrialization and modernisation of daily lives and practices (Crawford, et al., 2014), their impacts can still be felt in traces when considering individual approaches to the topic of menstruation and sexual/reproductive health. In the US alone, education surrounding menstruation is severely lacking in schools (Sebert Kuhlmann, et al., 2022). A review of educational standards found that only three states required discussions on personal hygiene products relating to menstruation (Sebert Kuhlmann, et al., 2022). A survey in the same paper found that over 50% of respondents indicated a desire for more comprehensive education on menstruation and menstrual hygiene. More work must be done to further break down the stigmas surrounding the discussion of menstruation and pelvic health in schools, as

well as societally in order to incite further change that will encourage individuals to more comfortably voice concerns regarding their physical health.

6.6.5 - Ethical Concerns

Endometriosis is a notoriously painful condition that has been known to severely impact an individual's quality of life. Due to the severe pain caused by the buildup of scar tissue over time, patients with severe endometriosis are often left in crippling pain while going about their daily life. Early diagnosis is crucial in halting the development of endometriomas and the subsequent scar tissue. Implementing a non-invasive diagnostic method that is attractive to patients and healthcare providers for its low cost and objective nature would allow for a much shorter average diagnostic turnaround time, which is currently 6.7 years (Parasar, et al., 2017). Affording patients the chance to relate a name and condition to the group of symptoms they experience can be critical in improving their mental health, as they are longer left to question why they struggle to complete basic tasks in their daily life.

6.6.6 - Health and Safety Issues

As discussed previously in section 6.4.5, easier diagnosis means quicker access to treatment, which in turn improves a patient's quality of life. However, the creation, testing, and use of this device poses several short-term and long-term ethical concerns.

The team does not contain any trained diagnosticians, and as such is not capable of officially diagnosing endometriosis. Any preliminary testing of the device and its associated mechanisms should not be treated as such until solid data has been collected and analyzed following trials conducted hopefully in collaboration with a research department specializing in endometriosis or in the field of obstetrics and gynecology. In the event in which clinical testing begins, informed consent will be crucial in informing patients of their rights and how their personal and sensitive data will be handled in accordance with an Institutional Review Board's standards.

Following preliminary testing, work must be done to reduce the number of false positives and false negatives. Ideally, this test would be completely accurate in diagnosing endometriosis, but this potentially may not be feasible. In the event that not enough water was consumed prior to collection of a urine sample, creatinine levels may be too concentrated and provide a false

negative. Additionally, sFlt-1 has been found as a potential biomarker for other conditions, such as preeclampsia, which could lead to a potential false positive (Pant, et al., 2019). A false positive is a cause for concern as it may lead to treatment that is unnecessary or radical, especially in the case of a hysterectomy. The goal of the device was to reduce the invasiveness and obtrusiveness of traditional diagnostic methods, and so limiting the physical and mental distress posed to a patient in this way is also crucial when considering false positives. A false negative is a cause of concern as it may lead to a patient not receiving the care or medical attention that is necessary to their quality of life and holistic health.

Further work may be potentially done that could result in the redesigning of this device for consumer use, resembling the original concept of mirroring an over-the-counter pregnancy test. Although this method empowers a consumer to diagnose themselves and independently seek out treatment or medical intervention, it could potentially lead to misdiagnosis due to user error. Additionally, the test in its current form utilizes highly volatile materials that may not be suitable to sit for extended periods of time on a shelf in a non-temperature and non-humidity controlled environment, such as a grocery store or pharmacy.

6.6.7 - Manufacturability

The device in its current state was designed to be reproducible and easily manufactured. The device housing was affordably 3D printed with PLA and was designed to minimize use of excess material. Mass production efforts would likely use injection molding to allow for more precise tolerances. Its dimensions were designed to fit commonly available 3 mL cuvettes, which was beneficial for prototyping purposes. It should be noted that this feature may be altered in the future to allow for built-in reaction housing. Work done in synthesizing the novel sFlt-1 detection mechanism as well as in establishing a large protein stock of sFlt-1 were carefully documented and described in this report with the intent for this device to be eventually manufactured and distributed. The materials used for production are easily available for purchase through large and reputable suppliers of scientific materials, such as Thermo Fisher Scientific and Sigma-Aldrich.

6.6.8 - Sustainability

Manufacturing of this device and its cuvettes requires an input of energy. Energy used in factories and manufacturing sites can come from a variety of sources that vary from location to

location. In the USA, most commonly utilized sources of electricity included natural gas, nuclear energy, and coal as of 2020 (U.S. Department of Energy, 2020). Although steps have been made nationally to increase utilization of alternative, renewable sources, like wind, hydropower, solar power, biomass, wind, and geothermal energy, these sources combined comprise only 20% of the USA's produced electricity as of 2020 (U.S. Department of Energy, 2020). Further transport and shipping of this device would then occur via land, air, or sea, which may require the consumption of nonrenewable sources that may contribute further to carbon emissions. Further work and research should be done to compare how the usage of energy may compare to the costs associated with the maintenance and upkeep of doctor's offices, hospitals, and other facilities where more commonly available diagnostic methods (like laparoscopic surgery, transvaginal ultrasounds, and pelvic exams) may be performed.

Chapter 7: Discussion

7.1.0 - Detection Mechanisms

As discussed in the previous chapter, detection methods for both creatinine and sFlt-1 were developed and tested. A distinct gradient was observed when testing the creatinine detection method at different concentrations, implying that this detection method may be viable for use in the completed device. Despite reporting different absorbances, when the two detection methods were viewed in-line with one another, little-to-no visual change could be perceived. This shows that although the team could quantitatively determine the concentration of sFlt-1 in a urine sample utilizing their novel detection method when performed at a molar ratio of 1:100 sFlt-1 to AP, it would not be enough qualitatively for the current approach to testing. Further modifications and testing are needed to ensure that an appropriate level of saturation can be achieved via the sFlt-1 detection and quantification method in order to ensure the efficacy and validity of the proposed test. In the mechanisms' current states, they function as a proof of concept that sFlt-1 and creatinine can be quantifiably detected in trace amounts in urine in relation to one another, but this process could benefit from future refinements.

7.2.0 - Device Iterations

The device went through several iterations of concepts, which ultimately culminated in the creation of the urinalysis device detailed in this paper. The original thought was to detect and

quantify sFlt-1 in comparison to concentrations of creatinine in urine via fluorescence. This method was deemed not feasible due to time and budget constraints. The team then considered a urinalysis device that exploited two separate colorimetric assays to qualitatively compare the concentration of sFlt-1 in comparison to creatinine in a urine sample by way of a viewing window. This could then yield a diagnosis through two methods: a comparative color chart of known expected hues according to varying ratios indicative (or not) of endometriosis and a more objective device utilizing wavelength filters to remove the need for human opinion. Once again, due to time and budget constraints, the team pursued a device with a comparative color chart, but future work with wavelength filters could prove attractive in improving the diagnostic process. In order to be feasibly accomplished with the team's available resources, a urinalysis device with two colorimetric reactions to qualitatively compare concentrations of sFlt-1 and creatinine in urine with a comparative color chart is an attractive device form for non-invasively diagnosing endometriosis via urinalysis.

7.3.0 - sFlt-1 Protein Stock Production

To begin testing of the device on synthetic standards, the team needed a usable stock of the chosen biomarkers, sFlt-1 and creatinine. Creatinine was commercially available, while sFlt-1 and its associated gene were not. The team worked to establish a protein stock of sFlt-1 while genetically engineering commercially available hFlt-1. Further work is needed to refine the ligation process necessary to establish a usable and reliable stock of sFlt-1, specifically in the final step of ligation. In its current approach, the reaction kinetics are not favorable enough to guarantee a successful ligation that is crucial in establishing a stock of sFlt-1 for preliminary testing of the sFlt-1 detection mechanism.

Chapter 8: Conclusions and Recommendations

8.1.0 - Device Summary

The team successfully created a device that houses two colorimetric reactions, one that produces a blue pigment indicative of the concentration of sFlt-1 in urine and one that produces a yellow-orange pigment indicative of the concentration of creatinine in urine. This device has a window on the front which may be used to view the two backlit vials, in which one unified hue

may be viewed and then compared to a chart of colors representing known values of endometriosis positive and endometriosis negative urine.

8.1.1 - Creatinine Detection

Creatinine is an important biomarker in urine for diagnosing endometriosis, as Cho, et al., discovered in 2007 that it can be used in comparison to the concentration of sFlt-1 as a biomarker in urine for potentially diagnosing endometriosis non-invasively. Due to it being an indicator of kidney function (Eng, 2021), it is useful in quantifying how concentrated or dilute a urine sample is, which allows for the contextualization of the process of other proteins and molecules present in a urine sample.

As previously discussed, the detection and quantification of creatinine in urine is made possible by the Jaffe reaction, which forms a Janovsky complex. This reaction occurs when creatinine and picric acid interact in an alkaline environment, and causes the development of a yellow-orange pigment (Delanghe & Speeckaert, 2011). As seen previously in Chapter 6, the team created a standard curve of the Jaffe reaction that had discernible differences to the human eye as well as quantifiably when examined via spectroscopy.

In conclusion, creatinine can be reliably detected and quantified in human urine via the Jaffe reaction, and produces a difference in hue visible to the human eye. Thus, it can be used in the process of diagnosing endometriosis non-invasively when used in conjunction with sFlt-1.

8.1.2 - sFlt-1 Detection

sFlt-1's role as a regulator of angiogenesis makes it invaluable for non-invasively detecting endometriosis due to its expression in urine. In 2007, Cho, et al., found that the ratio of sFlt-1 to creatinine could be used as a biomarker for endometriosis. In general, endometriosis positive patients had a ratio that was approximately double the ratio found in endometriosis negative patients. Additionally, patients with minimal-mild endometriosis had a ratio nearly four times as high as endometriosis negative patients, likely due to its role in regulating the vascularization of endometriomas (Cho, et al., 2007).

The team created its own novel assay that utilized a novel "stack" of proteins that could reliably detect and quantify the concentration of sFlt-1 in a urine sample. The sFlt-1 acts as a final bridge that joins together two otherwise separate complexes, one being a stabilization

complex and the other being a blue pigment producing complex. When combined with the Jaffe reaction, these two colorimetric reactions create a hue indicative of the relative concentrations of each selected biomarker, thus providing a way for one to visualize the ratio.

When considering the results obtained from testing conducted with only AP, it is clear that the detection method must be refined in the future. As the proof of concept stands now, sFlt-1 is not able to be detected and quantified effectively when considering the turnaround time or the visible qualification of concentration of sFlt-1 in solution utilizing current methods. Proposed improvements will be discussed in detail in a later section, but in summary, refinements must be made to the ratio of AP to sFlt-1 in solution in order to ensure the production of a blue pigment that is plainly visible to the human eye.

Preliminary tests conducted on AP found that a 1:1 molar ratio of AP to sFlt-1 was not enough to produce a qualitative difference, let alone a quantitative difference. A 1:100 molar ratio of sFlt-1 to AP produced a qualitative difference as well as a quantitative one, but did not successfully perform when overlaid with a vial of the Jaffe reaction. As a result, it is clear that further adjustments must be made to the sFlt-1 detection process to increase the saturation of the produced hue in order to ensure the viability and success of a colorimetric assay to complement the Jaffe reaction.

8.1.3 - Device Results

As seen previously in Chapter 4, Figure 13, the proof of concept for the device and its dual colorimetric assay with a backlit window works in creating one unified hue. The proof of concept photos show a promising step in the right direction in showing that this novel device layout could produce a new standard in diagnosing via ratios. As previously mentioned in section 8.1.1, the Jaffe reaction is a method that works in producing qualitatively different hues dependent on the concentration of creatinine. As previously mentioned in 8.1.2, further steps must be taken to refine the colorimetric assay for quantifying the concentration of sFlt-1 in urine to ensure that the pigment produced is vibrant enough to produce a qualitative difference when viewed in tandem with the Jaffe reaction. Further improvements and steps to be taken will be discussed in detail below.

8.2.0 - Future Work and Recommendations

As it stands, the device produced by the research team is a proof of concept. It demonstrates that the device is capable of displaying two different colorimetric assays in line with one another that can be viewed through a window. When backlit and diffused, it produces one unified hue. The Jaffe reaction works as already intended in detecting and quantifying creatinine, but further steps must be taken to improve the detection of sFlt-1 as well as in further standardizing the test and device. Additionally, further testing steps and plans for this product will be discussed in detail below.

8.2.1 - Production of sFlt-1 Standards

As previously discussed, the team was unable to purchase sFlt-1 or its genes, and had to engineer it on their own from hFlt-1. The protein production process proved largely unsuccessful, which impacted the team's ability to test the novel sFlt-1 detection method in detail. Further steps should be taken in order to improve the chance of success when producing large quantities of sFlt-1 standards for use in testing the device with synthetic standards.

In order to improve the ligation process, the team will work in the future to reduce the sFlt-1 gene into smaller segments. By completing this, it improves the reaction kinetics, and would likely skew in favor of the segments successfully incorporating into the target cell. Previous work has shown that this approach of doing a multi-step ligation process with researchers introducing smaller portions of the overall gene can be effective in increasing the favorability of ligation (Revie, et al., 1988). With the team's current methods, the goal was to insert a 2kb segment into a 6.1kb cell. The size of the segment is large (over 800 bp) and with a similar vector size (6.1 kB), leads to a very kinetically unfavorable ligation. The reaction can potentially be repeated with newly-purchased T4 DNA ligase and buffer that has been proven to work as well.

8.2.2 - Improving Detection Methods

Although the team proved they could detect creatinine and sFlt-1 in urine in trace amounts, further steps must be taken to improve the results yielded from these tests. Currently, the blue hue produced by the novel colorimetric sFlt-1 detection assay is not saturated enough to produce a qualitative difference when overlaid with the yellow-orange hue produced by the Jaffe

reaction. Further work can also be done to improve the standardization of the test in an effort to make its results more objective, and less subjective.

Urine naturally takes on a yellow pigment due to the presence of urochrome. When utilizing the comparative color chart, this could impede the accuracy of provided results by falsely pushing the hue to take on more of a yellow tinge, thus producing a false negative in the event that a patient did not consume enough water before providing a urine sample. In the future, it would be beneficial to devise a way to either destroy urochrome in urine upon its addition to the test, or to find a way to filter out urochrome.

As previously discussed, the team considered the use of wavelength filters to help remove subjectivity from the results. These filters, in conjunction with a full spectrum LED placed behind the two cuvettes, would in theory only allow certain light to pass through based off of preselected wavelengths. During testing, the team found that the yellow orange hue produced by the Jaffe reaction had a wavelength of 483 nm while the blue hue produced by the sFlt-1 reaction had a wavelength of 490 nm. Urochrome in healthy urine has an absorbance wavelength of 190 -250 nm, according to Guminetsky, et al., 1999. With this in mind, a wavelength filter could be used to select exclusively for the predicted hue and wavelength produced by the combination of the Jaffe reaction and the sFlt-1 reaction, allowing for complete bypassing of urochrome's included hue. Additionally, this would remove human perception from the need to diagnose, as the filters would determine the observable hue for a viewer, and not a comparative color chart. This removes user opinion and error, and is a step in the direction to further improve the objectivity of the test.

In its current state, the novel detection method for sFlt-1 in urine needs further improvements to increase the diagnostic turnaround time, but also to improve the amplification of the blue pigment produced by the assay. The team needs to further refine the molar ratio of AP to sFlt-1 in the test. Original tests utilizing only AP found that a 1:1 ratio produced a blue hue that was not visible to the human eye, and was too close to the limit of detection of the spectrophotometer. A 1:100 ratio of sFlt-1 to AP produced a visible blue pigment, but this amount was still too low to produce a visible difference when overlaid with any vials produced by the Jaffe reaction, as detailed in Chapter 6. In addition to further changing the ratio of sFlt-1 to AP in testing, methods for improving the output include: increasing the number of AP conjugated to the detector complex or switching to a different detection method.

Another potential approach to improving the quantification of sFlt-1 present in a urine sample would be to change the signaling molecule or enzyme used to a different one capable of producing a more distinct signal. Colorimetric detection assays are very user friendly but also lack the specificity characteristic of other detection methods. For example, a fluorescence detection signal would produce a much more noticeable effect when comparing low signal. At the same time, the ease and diagnostic simplicity of a colorimetric test is lost. Additional testing should be performed in order to identify a signal molecule able to significantly enhance the signal.

Horseradish peroxidase (HRP) and chemiluminescence could be used in tandem with one another to improve the signaling of sFlt-1 detection. Luminescence is the radiation emitted by a molecule or atom upon their return to ground state from their excited state. This state of excitation comes from chemical reactions in chemiluminescence (Fereja, et al., 2013). This radiation can be exploited in chemiluminescence enzyme immunoassays, where an enzyme-labeled protein A/G or enzyme-labeled antibody can be catalyzed by HRP and ALP (Iranifam, 2013). In the context of a urinalysis device for non-invasively diagnosing endometriosis, HRP could be a signal molecule used to enhance the signaling of sFlt-1 by converting its substrates into fluorescent or luminescent pigments. This would improve the qualitative discernment of sFlt-1 levels in comparison to creatinine in urine. Chemiluminescence is a highly sensitive method with greatly varying dynamic ranges with ideal detection limits (Fereja, et al., 2013), making it a potentially attractive method for improving the detection of sFlt-1 in urine.

8.2.3 - Reduce Device Complexity

As it currently stands, the device can be further simplified to improve the manufacturing process. Due to time and budget constraints, the team opted to conjugate anti-sFlt-1 antibodies to magnetic beads coated with Protein A/G, held in place by a magnet at the base of the cuvette in the device. Ideally, the Protein A/G would be directly conjugated to the cuvette walls, rather than held in place by an intermediate (like the magnetic Dyna beads). This is because while the beads allow the detection method to stay connected to the physical device, there is a risk that using a magnet may impact the detection method's accuracy. In addition, reducing the complexity of the device lowers cost and reduces the number of failure points. In the current design, the magnet is

meant to rest at the bottom of the sample container. If the magnet is not strong enough, then some completed detection chains can be lost during a spill or rinse to remove urochrome. This loss of fully linked detection chain will lead to underreporting of the amount of sFlt-1 in the sample, causing a potential false negative reading because of (unknowingly decreased) sFlt-1 concentration. Conjugating Protein A/G directly to the device will prevent this. Because the stabilization complex is attached chemically to the device, it will not be prone to removal similar to a magnet design. This will decrease the potential to lose any fully linked detection chain and provide a more consistent and accurate reading of sFlt-1 concentration in more situations.

8.2.4 - Future Testing

Once the production of sFlt-1 standards and the method of detection for sFlt-1 is improved and the device is simplified, further testing will occur. Methods detailed in Section 4.4.5 for a four step plan in testing the detection of sFlt-1 will begin. In the first step, the testing of solely AP, the team will aim to refine the ratio of AP to sFlt-1 in the device. Testing will then proceed in the same piecewise plan as previously described, resulting in testing the full two part complex with the sFlt-1 protein stocks.

Following the refinement of sFlt-1 and the testing of the device mechanism on synthetic stocks, the team plans to move forward with testing the device on human urine. Work began during this project in contacting UMass Memorial's Obstetrics and Gynecology research department, with Dr. Kristen Matteson functioning as the team's main liaison. Foundational work in completing the necessary IRB forms (such as HIPAA Authorization and Informed Consent) as well as detailed procedures for the handling of confidential information as well as the biospecimens had been completed during this academic year.

The team hopes to collaborate with UMass Memorial to obtain samples from patients with a positive diagnosis of endometriosis confirmed medically via imaging and or biopsy, as well as from individuals who are not likely candidates for endometriosis. Testing would then proceed ensuring that positive samples reliably produce positive results, while negative samples would reliably produce negative results. This method is attractive as it would allow researchers to work backwards by having the device confirm information that is already known. From there, a rate of false positives and false negatives could be potentially produced, while also providing valuable insight into how the test may perform if a patient is undergoing treatment to manage

their symptoms (such as actively taking hormonal therapies or if they previously received a hysterectomy) and how this may impact their sFlt-1 levels. Another variable to examine would be to compare sFlt-1 levels to where a patient may be in their menstrual cycle at the time their urine sample is collected, as this may potentially impact the expression of sFlt-1 in urine.

8.2.5 - Future of the Device

The team has several plans for the future of this device. As of April 18th, the team officially had a patent on file with the U.S. patent office for a provisional patent covering a dual vial colorimetric assay based urinalysis device to non-invasively diagnose endometriosis. The team intends to move forward with filing a utility patent within the next calendar year. Under the advisement of a patent and intellectual property lawyer, this provisional patent will lead into three utility patents: one on the novel assay for detecting sFlt-1, one for the dual vial based device, and one on the concept of diagnosing endometriosis non-invasively through urinalysis.

An additional plan for this device and team is to form a company surrounding the device that will arise from the work detailed in this paper. This company will work to complete the improvements previously described in this section, and hopefully see this device through to market. Plans include either producing and distributing this device through the company, or by licensing out the rights to the patent to larger companies, or by selling the company to one of the aforementioned larger companies with the intent for them to have the sole rights to further research, manufacture, and distribute the device.

References

Agrawal, S., Tapmeier, T., Rahmioglu, N., Kirtley, S., Zondervan, K., & Becker, C. (2018a). Angiogenesis Diagram [Diagram]. http://www.mdpi.com/1422-0067/19/2/599

Agrawal, S., Tapmeier, T., Rahmioglu, N., Kirtley, S., Zondervan, K., & Becker, C. (2018b). The miRNA Mirage: How Close Are We to Finding a Non-Invasive Diagnostic Biomarker in Endometriosis? A Systematic Review. International Journal of Molecular Sciences, 19(2), 599. https://doi.org/10.3390/ijms19020599

Alimi, Y., Iwanaga, J., Loukas, M., & Tubbs, R. S. (2018). The Clinical Anatomy of Endometriosis: A Review. Cureus. https://doi.org/10.7759/cureus.3361

American Society for Reproductive. (1997). Revised American Society for Reproductive Medicine classification of endometriosis: 1996. Fertility and Sterility, 67(5), 817–821. https://doi.org/10.1016/S0015-0282(97)81391-X

Anjali, Ravinshu, & Arun. (2020). A Review on Different Optical Filters. https://doi.org/10.5281/ZENODO.3924499

Avrameas, S. (1969). Coupling of enzymes to proteins with glutaraldehyde. Immunochemistry, 6(1), 43–52. https://doi.org/10.1016/0019-2791(69)90177-3

Becker, C. M., Louis, G., Exarhopoulos, A., Mechsner, S., Ebert, A. D., Zurakowski, D., & Moses, M. A. (2010). Matrix metalloproteinases are elevated in the urine of patients with endometriosis. Fertility and Sterility, 94(6), 2343–2346. https://doi.org/10.1016/j.fertnstert.2010.02.040

Bjorkman, S., & Taylor, H. S. (2019). MicroRNAs in endometriosis: Biological function and emerging biomarker candidates†. Biology of Reproduction, 101(6), 1167–1178. https://doi.org/10.1093/biolre/ioz014

CD Bioparticles. (2022). A/G Coated Bead Diagram [Diagram]. https://www.cd-bioparticles.com/t/Protein-Isolation_48.html

Cho, S., Choi, Y. S., Yim, S. Y., Yang, H. I., Jeon, Y. E., Lee, K. E., Kim, H., Seo, S. K., & Lee, B. S. (2012). Urinary vitamin D-binding protein is elevated in patients with endometriosis. Human Reproduction, 27(2), 515–522. https://doi.org/10.1093/humrep/der345

Cho, S. H., Oh, Y. J., Nam, A., Kim, H. Y., Park, J. H., Kim, J. H., Park, K. H., Cho, D. J., & Lee, B. S. (2007). Evaluation of Serum and Urinary Angiogenic Factors in Patients with Endometriosis. American Journal of Reproductive Immunology, 58(6), 497–504. https://doi.org/10.1111/j.1600-0897.2007.00535.x

Crawford, M., Menger, L. M., & Kaufman, M. R. (2014). “This is a natural process”: Managing menstrual stigma in Nepal. Culture, Health & Sexuality, 16(3/4), 426–439. \

Daher, M., Al Rifai, M., Kherallah, R. Y., Rodriguez, F., Mahtta, D., Michos, E. D., Khan, S. U., Petersen, L. A., & Virani, S. S. (2021). Gender disparities in difficulty accessing

healthcare and cost-related medication non-adherence: The CDC behavioral risk factor surveillance system (BRFSS) survey. Preventive Medicine, 153, 106779. https://doi.org/10.1016/j.ypmed.2021.106779

Delanghe, J. R., & Speeckaert, M. M. (2011). Creatinine determination according to Jaffe—What does it stand for? Clinical Kidney Journal, 4(2), 83–86. https://doi.org/10.1093/ndtplus/sfq211

Eng, M. (2021, March 2). Urine Creatinine Test Normal Range + Low & High Levels—SelfDecode Labs. SelfDecode. https://labs.selfdecode.com/blog/creatinine-urine-test/

Fereja, T., Hymete, A., & Gunasekaran, T. (2013). A Recent Review on Chemiluminescence Reaction, Principle and Application on Pharmaceutical Analysis. 2013. https://doi.org/10.1155/2013/230858

Fernando, M., Ellery, S. J., Marquina, C., Lim, S., Naderpoor, N., & Mousa, A. (2020). Vitamin D-Binding Protein in Pregnancy and Reproductive Health. Nutrients, 12(5), 1489. https://doi.org/10.3390/nu12051489

Horwitz, R. (2019, October 31). Vaginal Speculum (after 1800) | The Embryo Project Encyclopedia. https://embryo.asu.edu/pages/vaginal-speculum-after-1800

Hwang, J.-H., Wang, T., Lee, K.-S., Joo, J.-K., & Lee, H.-G. (2013). Vitamin D binding protein plays an important role in the progression of endometriosis. International Journal of Molecular Medicine, 32(6), 1394–1400. https://doi.org/10.3892/ijmm.2013.1506

Ibraheem, N. A., Hasan, M. M., Khan, R. Z., & Mishra, P. K. (2012). Understanding Color Models: A Review. 2(3), 11.

International Organization for Standardization. (2019). ISO 20916:2019(en), In vitro diagnostic medical devices—Clinical performance studies using specimens from human subjects—Good study practice. International Organization for Standardization. https://www.iso.org/obp/ui/#iso:std:iso:20916:ed-1:v1:en

International Organization for Standardization. (2021). ISO 23118:2021(en), Molecular in vitro diagnostic examinations—Specifications for pre-examination processes in metabolomics in urine, venous blood serum and plasma. International Organization for Standardization. https://www.iso.org/obp/ui/#iso:std:iso:23118:ed-1:v1:en

Iranifam, M. (2013). Analytical applications of chemiluminescence-detection systems assisted by magnetic microparticles and nanoparticles—ScienceDirect. Science Direct, 51, 57–70. https://doi.org/10.1016/j.trac.2013.05.014

Jung, J.-J., Tiwari, A., Inamdar, S. M., Thomas, C. P., Goel, A., & Choudhury, A. (2012). Secretion of Soluble Vascular Endothelial Growth Factor Receptor 1 (sVEGFR1/sFlt1) Requires Arf1, Arf6, and Rab11 GTPases. PLoS ONE, 7(9), e44572. https://doi.org/10.1371/journal.pone.0044572

Kundu, S. K. (2014a). BCIP-AP Diagram [Diagram]. https://doi.org/10.13140/2.1.3444.5449

Kundu, S. K. (2014b). BiomedRecent Advances in Immunoassays. Amazon.com, Kindle Direct. https://doi.org/10.13140/2.1.3444.5449

Liu, Y., Liang, S., Yang, F., Sun, Y., Niu, L., Ren, Y., Wang, H., He, Y., Du, J., Yang, J., & Lin, J. (2020). Biological characteristics of endometriotic mesenchymal stem cells isolated from ectopic lesions of patients with endometriosis. Stem Cell Research & Therapy, 11(1), 346. https://doi.org/10.1186/s13287-020-01856-8

Markovic-Mueller, S., Stuttfeld, E., Asthana, M., Weinert, T., Bliven, S., Goldie, K. N., Kisko, K., Capitani, G., & Ballmer-Hofer, K. (2017). Structure of the Full-length VEGFR-1 Extracellular Domain in Complex with VEGF-A. Structure, 25(2), 341–352. https://doi.org/10.1016/j.str.2016.12.012

Mason, B. R., Chatterjee, D., Menias, C. O., Thaker, P. H., Siegel, C. L., & Yano, M. (2020). Encyclopedia of endometriosis: A pictorial rad-path review. Abdominal Radiology, 45(6), 1587–1607. https://doi.org/10.1007/s00261-019-02381-w

Matsushiro, N., & Ohta, N. (2003). Theoretical analysis of subtractive color mixture characteristics. Color Research & Application, 28(3), 175–181. https://doi.org/10.1002/col.10143

Mayo Clinic. (2021). Endometriosis—Diagnosis and treatment—Mayo Clinic. https://www.mayoclinic.org/diseases-conditions/endometriosis/diagnosis-treatment/drc-20354661

Mayo Clinic. (2022a). Pelvic Exam Diagram [Diagram]. https://www.mayoclinic.org/diseases-conditions/endometriosis/diagnosis-treatment/drc-20354661

Mayo Clinic. (2022b). Transvaginal Ultrasound Diagram [Diagram]. https://www.mayoclinic.org/diseases-conditions/endometriosis/diagnosis-treatment/drc-20354661

Migneault, I., Dartiguenave, C., Bertrand, M. J., & Waldron, K. C. (2004). Glutaraldehyde: Behavior in aqueous solution, reaction with proteins, and application to enzyme crosslinking. BioTechniques, 37(5), 790–802. https://doi.org/10.2144/04375RV01

Mount Sinai. (2022). Creatinine urine test Information | Mount Sinai—New York. https://www.mountsinai.org/health-library/tests/creatinine-urine-test

NCBI. (n.d.). Sandwich ELISA Diagram [Diagram]. Retrieved April 27, 2022, from https://www.ncbi.nlm.nih.gov/books/NBK92434/figure/immunometh.F1/

Parasar, P., Ozcan, P., & Terry, K. L. (2017). Endometriosis: Epidemiology, Diagnosis and Clinical Management. Current Obstetrics and Gynecology Reports, 6(1), 34–41. https://doi.org/10.1007/s13669-017-0187-1

Pelvic Rehabilitation Medicine. (2022). Laparoscopy Diagram [Diagram]. https://www.pelvicrehabilitation.com/services/endometriosis-surgery/

Posen, S. (1967). Alkaline Phosphatase. Annals of Internal Medicine, 67(1), 183. https://doi.org/10.7326/0003-4819-67-1-183

Raikwar, N. S., Liu, K. Z., & Thomas, C. P. (2014). N-Terminal Cleavage and Release of the Ectodomain of Flt1 Is Mediated via ADAM10 and ADAM 17 and Regulated by VEGFR2 and the Flt1 Intracellular Domain. PLoS ONE, 9(11), e112794. https://doi.org/10.1371/journal.pone.0112794

Reichardt, W., Overbeck, J., & Steubing, L. (1967). Free Dissolved Enzymes in Lake Waters. Nature, 216(5122), 1345–1347. https://doi.org/10.1038/2161345a0

Revie, D., Smith, D. W., & Yee, T. W. (1988). Kinetic analysis for optimization of DNA ligation reactions. - PMC. PMID: 2848221

Rossini, E. L., Milani, M. I., Carrilho, E., Pezza, L., & Pezza, H. R. (2018). Jaffe Reaction Diagram [Diagram]. https://linkinghub.elsevier.com/retrieve/pii/S0003267017311777

Sandström, A., Bixo, M., Johansson, M., Bäckström, T., & Turkmen, S. (2020). Effect of hysterectomy on pain in women with endometriosis: A population‐based registry study. BJOG: An International Journal of Obstetrics & Gynaecology, 127(13), 1628–1635. https://doi.org/10.1111/1471-0528.16328

Sebert Kuhlmann, A., Hunter, E., Wall, L. L., Boyko, M., & Teni, M. T. (2022). State Standards for Menstrual Hygiene Education in U.S. Schools. Journal of School Health, 92(4), 418–420. https://doi.org/10.1111/josh.13135

Serdar Bulun. (2004). Aromatase and Endometriosis. Seminars in Reproductive Medicine, 22(1), 45–50. https://doi.org/10.1055/s-2004-823026

Sigma-Aldrich. (2014). Sigma-Aldrich Alkaline Phosphatase Blue Microwell Substrate Product Information. https://www.sigmaaldrich.com/deepweb/assets/sigmaaldrich/product/documents/325/404/ab0200dat.pdf

Simonot, L., & Hébert, M. (2014). Between additive and subtractive color mixings: Intermediate mixing models. Journal of the Optical Society of America A, 31(1), 58. https://doi.org/10.1364/JOSAA.31.000058

Soliman, A. M., Yang, H., Du, E. X., Kelley, C., & Winkel, C. (2016). The direct and indirect costs associated with endometriosis: A systematic literature review. Human Reproduction, 31(4), 712–722. https://doi.org/10.1093/humrep/dev335

Tanbo, T., & Fedorcsak, P. (2017). Endometriosis-associated infertility: Aspects of pathophysiological mechanisms and treatment options. Acta Obstetricia et Gynecologica Scandinavica, 96(6), 659–667. https://doi.org/10.1111/aogs.13082

ThorLabs. (2022). Bandpass Filter Tutorial. ThorLabs. https://www.thorlabs.com/newgrouppage9.cfm?objectgroup_id=10772

Toora, B. D., & Rajagopal, G. (2002). Measurement of creatinine by Jaffe's reaction—Determination of concentration of sodium hydroxide required for maximum color development in standard, urine and protein free filtrate of serum. Indian Journal of Experimental Biology, 40(3), 352–354. PMID: 12635710.

Tremblay, K., Tran, A., Marko, J., & Inger, E. (2019). Endometriosis Detection Device via Urine Sampling. Internal WPI BME report. Unpublished

UCSF Health. (n.d.). Endometriosis Diagnosis | UCSF Health. Retrieved April 25, 2022, from https://www.ucsfhealth.org/conditions/endometriosis/diagnosis

U.S. Department of Energy. (2020). Alternative Fuels Data Center: Electricity Production and Distribution. https://afdc.energy.gov/fuels/electricity_production.html

Wee-Stekly, W.-W., Kew, C. C. Y., & Chern, B. S. M. (2015). Endometriosis: A review of the diagnosis and pain management. Gynecology and Minimally Invasive Therapy, 4(4), 106–109. https://doi.org/10.1016/j.gmit.2015.06.005

Wisdom, G. B. (2005). Conjugation of Antibodies to Alkaline Phosphatase. In R. Burns (Ed.), Immunochemical Protocols (pp. 123–126). Humana Press. https://doi.org/10.1385/1-59259-873-0:123

Zhai, Y., Lui, Y., Qi, Y., Long, X., Gao, J., Yao, X., Chen, Y., Wang, X., Lu, S., & Zhao, Z. (2020). The soluble VEGF receptor sFlt-1 contributes to endothelial dysfunction in IgA nephropathy. 15(8). https://doi.org/10.1371/journal.pone.0234492

Appendix

Appendix A

A scannable QR code that will lead to a PDF read-only version of the original BME3300 report in its entirety.

Appendix B

A sequence of hFlt-1.

Data gathered from Uniprot.org (identifier: P17948-1)

```
   1 mvsywdtgvl lcallsclll tgssgsklk dpelslkgtq himqagqtlh lqcrgeaahk
  61 wslpemvske serlsitksa cgrngkqfcs tltlntaqan htgfysckyl avptskkket
 121 esaiyifisd tgrpfvemys eipeiihmte grelvipcrv tspnitvtlk kfpldtlipd
 181 gkriiwdsrk gfiisnatyk eiglltceat vnghlyktny lthrqtntii dvqistprpv
 241 kllrghtlvl nctattplnt rvqmtwsypd eknkrasvrr ridqsnshan ifysvltidk
 301 mqnkdkglyt crvrsgpsfk svntsvhiyd kafitvkhrk qqvletvagk rsyrlsmkvk
 361 afpspevvwl kdglpateks aryltrgysl iikdvteeda gnytillsik qsnvfknlta
 421 tlivnvkpqi yekavssfpd palyplgsrq iltctaygip qptikwfwhp cnhnhsearc
 481 dfcsnneess ildadsnmgn riesitqrma iiegknkmas tlvvadsris giyiciasnk
 541 vgtvgrnisf yitdvpngfh vnlekmpteg edlklsctvn kflyrdvtwi llrtvnnrtm
 601 hysiskqkma itkehsitln ltimnvslqd sgtyacrarn vytgeeilqk keitirdqea
 661 pyllrnlsdh tvaisssttl dchangvpep qitwfknnhk iqqepgiilg pgsstlfier
 721 vteedegvyh ckatnqkgsv essayltvqg tsdksnleli tltctcvaat lfwllltlfi
 781 rkmkrsssei ktdylsiimd pdevpldeqc erlpydaskw efarerlklg kslgrgafgk
 841 vvqasafgik ksptcrtvav kmlkegatas eykalmtelk ilthighhln vvnllgactk
 901 qggplmvive yckygnlsny lkskrdlffl nkdaalhmep kkekmepgle qgkkprldsv
 961 tssesfassg fqedkslsdv eeeedsdgfy kepitmedli sysfqvargm eflssrkcih
1021 rdlaarnill sennvvkicd fglardiykn pdyvrkgdtr lplkwmapes ifdkiystks
1081 dvwsygvllw eifslggspy pgvqmdedfc srlregmrmr apeystpeiy qimldcwhrd
1141 pkerprfael veklgdllqa nvqqdgkdyi pinailtgns gftystpafs edffkesisa
1201 pkfnsgssdd vryvnafkfm sleriktfee llpnatsmfd dyqgdsstll aspmlkrftw
1261 tdskpkaslk idlrvtsksk esglsdvsrp sfchsscghv segkrrftyd haelerkiac
1321 cspppdynsv vlystppi
```

Sequence highlighted in red contains the transmembrane and intracellular portions of hFlt-1.

Appendix C

A sequence of sFlt-1.

Data gathered from Uniprot.org (identifier: P17948-2)

MVSYWDTGVLLCALLSCLLLTGSSSGSKLKDPELSLKGTQHIMQAGQTLHLQCRGEAA
HKWSLPEMVSKESERLSITKSACGRNGKQFCSTLTLNTAQANHTGFYSCKYLAVPTSKK
KETESAIYIFISDTGRPFVEMYSEIPEIIHMTEGRELVIPCRVTSPNITVTLKKFPLDTLIPD
GKRIIWDSRKGFIISNATYKEIGLLTCEATVNGHLYKTNYLTHRQTNTIIDVQISTPRPV
KLLRGHTLVLNCTATTPLNTRVQMTWSYPDEKNKRASVRRRIDQSNSHANIFYSVLTIDK
MQNKDKGLYTCRVRSGPSFKSVNTSVHIYDKAFITVKHRKQQVLETVAGKRSYRLSMK
VKAFPSPEVVWLKDGLPATEKSARYLTRGYSLIIKDVTEEDAGNYTILLSIKQSNVFKNLT
ATLIVNVKPQIYEKAVSSFPDPALYPLGSRQILTCTAYGIPQPTIKWFWHPCNHNHSEARC
DFCSNNEESFILDADSNMGNRIESITQRMAIIEGKNKMASTLVVADSRISGIYICIASNK
VGTVGRNISFYITDVPNGFHVNLEKMPTEGEDLKLSCTVNKFLYRDVTWILLRTVNNRT
MHYSISKQKMAITKEHSITLNLTIMNVSLQDSGTYACRARNVYTGEEILQKKEITIRGEHC
NKKAVFSRISKFKSTRNDCTTQSNVKH

Sequence highlighted in green is the novel 31 amino acid sequence that replaces the transmembrane and intracellular portion of hFlt-1 to convert hFlt-1 into sFlt-1.

Appendix D

The team's original proposed timeline of work and research for the academic year.

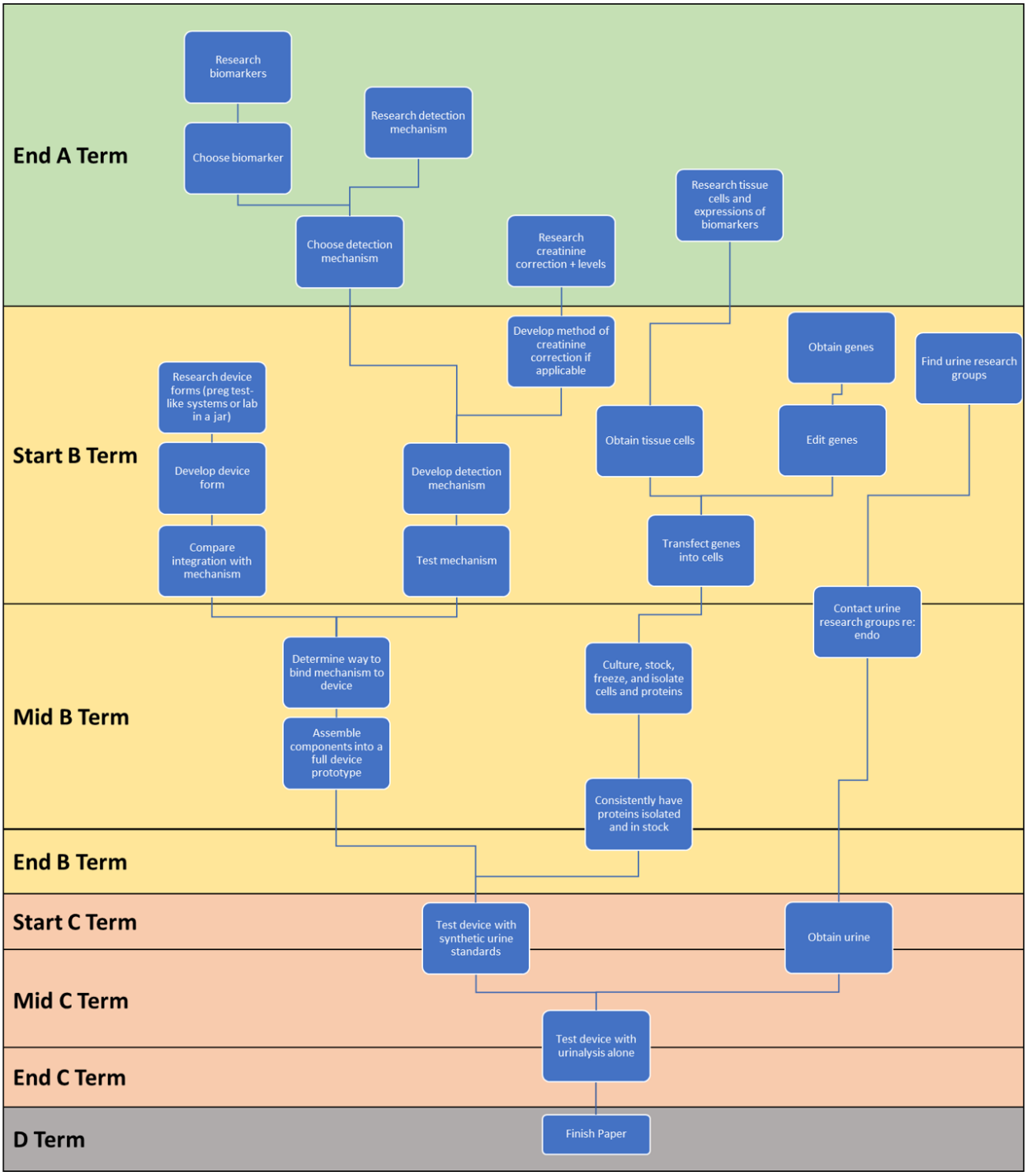

Appendix E

Protocol for Promega PureYield Plasmid Miniprep kit and system.

PureYield™ Plasmid Miniprep System

INSTRUCTIONS FOR USE OF PRODUCTS A1220, A1221, A1222 AND A1223

Quick PROTOCOL

Solution Preparation

Before lysing cells and purifying DNA, prepare the Column Wash Solution by adding ethanol. Cap tightly after addition. See Technical Bulletin #TB374 for detailed instructions.

DNA Purification by Centrifugation

Prepare Lysate

1. Add 600µl of bacterial culture to a 1.5ml microcentrifuge tube.
   Note: For higher yields and purity use the alternative protocol below to harvest and process up to 3ml of bacterial culture.
2. Add 100µl of Cell Lysis Buffer (Blue), and mix by inverting the tube 6 times.
3. Add 350µl of cold (4–8°C) Neutralization Solution, and mix thoroughly by inverting.
4. Centrifuge at maximum speed in a microcentrifuge for 3 minutes.
5. Transfer the supernatant (~900µl) to a PureYield™ Minicolumn without disturbing the cell debris pellet.
6. Place the minicolumn into a Collection Tube, and centrifuge at maximum speed in a microcentrifuge for 15 seconds.
7. Discard the flowthrough, and place the minicolumn into the same Collection Tube.

Wash

8. Add 200µl of Endotoxin Removal Wash (ERB) to the minicolumn. Centrifuge at maximum speed in a microcentrifuge for 15 seconds.
9. Add 400µl of Column Wash Solution (CWC) to the minicolumn. Centrifuge at maximum speed in a microcentrifuge for 30 seconds.

Elute

10. Transfer the minicolumn to a clean 1.5ml microcentrifuge tube, then add 30µl of Elution Buffer or nuclease-free water directly to the minicolumn matrix. Let stand for 1 minute at room temperature.
11. Centrifuge for 15 seconds to elute the plasmid DNA. Cap the microcentrifuge tube, and store eluted plasmid DNA at –20°C.

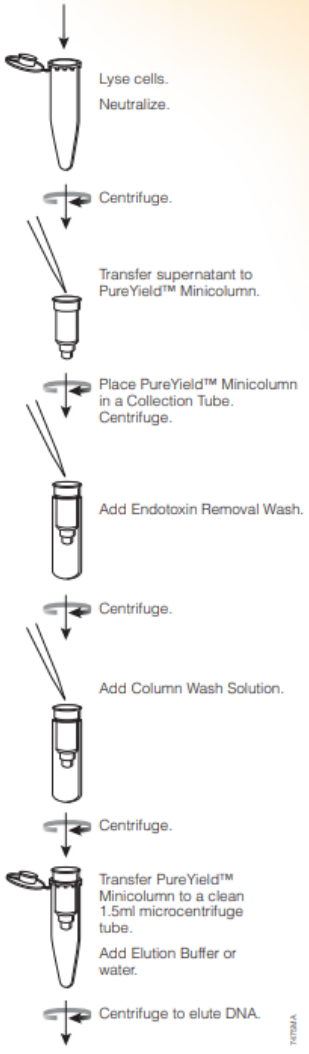

Alternative Protocol for Larger Culture Volumes

1. Centrifuge 1.5ml of bacterial culture for 30 seconds at maximum speed in a microcentrifuge. Discard the supernatant.
2. Add an additional 1.5ml of bacterial culture to the same tube and repeat Step 1.
3. Add 600µl of TE buffer or water to the cell pellet, and resuspend completely.
4. Proceed to Step 2 of the standard protocol above.

For complete protocol information see Technical Bulletin #TB374, available at: **www.promega.com/tbs**

ORDERING/TECHNICAL INFORMATION:
www.promega.com • Phone 608-274-4330 or 800-356-9526 • Fax 608-277-2601

Promega

Printed in USA. Revised 8/09
Part #9FB093

PureYield™ Plasmid Miniprep System

INSTRUCTIONS FOR USE OF PRODUCTS A1220, A1221, A1222 AND A1223

Quick PROTOCOL

DNA Purification by Vacuum

Prepare Lysate

1. Transfer 1.5ml of culture to a 1.5ml microcentrifuge tube
   Note: If you wish to process larger volumes of bacterial culture (up to 3ml) use the alternative protocol provided below.
2. Centrifuge at maximum speed in a microcentrifuge for 1 minute.
3. Remove and discard medium.
4. Resuspend the cell pellet in 600µl of TE buffer or water.
5. Add 100µl of Cell Lysis Buffer (Blue), and mix by inverting the tube 6 times.
6. Add 350µl of cold (4–8°C) Neutralization Solution, and mix thoroughly by inverting.
7. Centrifuge at maximum speed in a microcentrifuge for 3 minutes. Place a PureYield™ minicolumn on a Luer-Lok® adapter of a VacMan® or VacMan® Jr Laboratory Vacuum manifold
8. Transfer the supernatant (~900µl) into a PureYield™ Minicolumn.
9. Apply vacuum pulling the lysate through the column.

Wash

10. Add 200µl of Endotoxin Removal Wash (ERB) to the minicolumn. Allow the vacuum to pull the solution through the column.
11. Add 400µl of Column Wash Solution (CWC) to the minicolumn. Allow the vacuum to pull the solution through the column. Release the vacuum, and remove the PureYield™ Minicolumn.

Elute

12. Place the column in a 2ml collection tube, and centrifuge at maximum speed in a microcentrifuge for 1 minute.
13. Transfer the minicolumn into a clean 1.5ml microcentrifuge tube, then add 30µl of Elution Buffer or nuclease-free water directly to the minicolumn matrix. Let stand for 1 minute at room temperature.
14. Centrifuge for 15 seconds to elute the plasmid DNA. Cap the microcentrifuge tube, and store eluted plasmid DNA at –20°C.

For complete protocol information see Technical Bulletin #TB374, available at: **www.promega.com/tbs**

Alternative Protocol for Larger Culture Volumes

1. Centrifuge 1.5ml of bacterial culture for 30 seconds at maximum speed in a microcentrifuge.
2. Discard the supernatant.
3. Add an additional 1.5ml of bacterial culture to the same tube. Repeat Steps 1 and 2.
4. Add 600µl of TE buffer or water to the cell pellet, and resuspend completely.
5. Proceed to Step 5 of the standard protocol above.

ORDERING/TECHNICAL INFORMATION:
www.promega.com • Phone 608-274-4330 or 800-356-9526 • Fax 608-277-2601

Promega
Printed in USA. Revised 8/09
Part #9FB093

Appendix F

Protocol for the Promega Wizard PCR and Gel Cleaning Kit. The team only used the centrifuge method for both PCR cleaning and gel cleaning.

Wizard® SV Gel and PCR Clean-Up System

INSTRUCTIONS FOR USE OF PRODUCTS A9280, A9281, A9282, AND A9285.

Quick PROTOCOL

DNA Purification by Centrifugation

Gel Slice and PCR Product Preparation

A. Dissolving the Gel Slice

1. Following electrophoresis, excise DNA band from gel and place gel slice in a 1.5ml microcentrifuge tube.
2. Add 10µl Membrane Binding Solution per 10mg of gel slice. Vortex and incubate at 50–65°C until gel slice is completely dissolved.

B. Processing PCR Amplifications

1. Add an equal volume of Membrane Binding Solution to the PCR amplification.

Binding of DNA

1. Insert SV Minicolumn into Collection Tube.
2. Transfer dissolved gel mixture or prepared PCR product to the Minicolumn assembly. Incubate at room temperature for 1 minute.
3. Centrifuge at 16,000 × *g* for 1 minute. Discard flowthrough and reinsert Minicolumn into Collection Tube.

Washing

4. Add 700µl Membrane Wash Solution (ethanol added). Centrifuge at 16,000 × *g* for 1 minute. Discard flowthrough and reinsert Minicolumn into Collection Tube.
5. Repeat Step 4 with 500µl Membrane Wash Solution. Centrifuge at 16,000 × *g* for 5 minutes.
6. Empty the Collection Tube and recentrifuge the column assembly for 1 minute with the microcentrifuge lid open (or off) to allow evaporation of any residual ethanol.

Elution

7. Carefully transfer Minicolumn to a clean 1.5ml microcentrifuge tube.
8. Add 50µl of Nuclease-Free Water to the Minicolumn. Incubate at room temperature for 1 minute. Centrifuge at 16,000 × *g* for 1 minute.
9. Discard Minicolumn and store DNA at 4°C or –20°C.

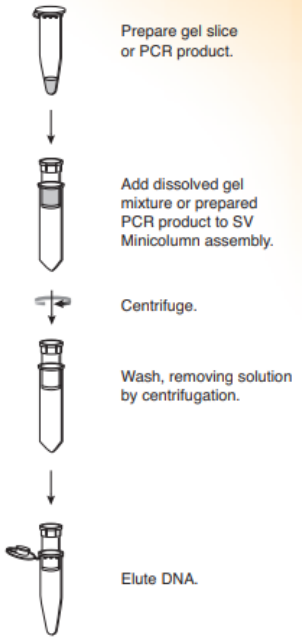

3760MA07_2A

Additional protocol information is available in Technical Bulletin #TB308, available online at:
www.promega.com

ORDERING/TECHNICAL INFORMATION:
www.promega.com • Phone 608-274-4330 or 800-356-9526 • Fax 608-277-2601

Promega

Printed in USA. Revised 11/09
Part #9FB072

Appendix G

The plasmid map of pcDNA from SnapGene.